GDF15 as a Potential Target for Overcoming Cancer-Associated Fibroblast Mediated Treatment Resistance in Esophageal Adenocarcinoma

Inaugural Dissertation

Zur

Erlangung des Doktorgrades
Dr. nat. med.

der Medizinischen Fakultät
und
der Mathematisch-Naturwissenschaftlichen Fakultät
der Universität zu Köln

vorgelegt von

Ningbo Fan

aus Sichuan, China

Druck-King, Köln

2024

Betreuerin:	Prof. Dr. Christiane J. Bruns
Referent/in:	Prof. Dr. Axel Hillmer Prof. Dr. Thomas Langer Prof. Dr. Jürgen Wolf
Datum der mündlichen Prüfung:	12.12.2023

Zusammenfassung

Durch eine umfassende Literaturanalyse konnte die nach aktuellen Richtlinien empfohlene neoadjuvante Radiochemotherapie (NCRT), gefolgt von einer Operation, als optimale Behandlungsstrategie von Patienten mit lokal fortgeschrittenem Ösophaguskarzinom bestätigt werden. Weiterhin fokussierten wir uns auf molekulare Mechanismen, die zur Behandlungsresistenz gegenüber Chemo- und Strahlentherapie in Ösophagus-Adenokarzinom (EAC)-Zellen führen. Wir generierten erfolgreich tumorassoziierte Fibroblasten (CAFs) und patienten-abgeleitete Organoidmodelle (PDOs) aus Primärgewebe von EAC-Patienten und setzten diese in einem *ex vivo* Ko-Kultursystem ein. EAC-CAFs spielten eine entscheidende Rolle bei der Förderung der Behandlungsresistenz von EAC-Tumorzellen in verschiedenen Tumor-CAF-Ko-Kultursystemen. Zudem verbesserten EAC-CAFs die mitochondriale Funktion in EAC-Zellen. Weiterhin identifizierten wir GDF15 aus unserer Tumor-CAF-Ko-Kultur durch transkriptomische Analysen. GDF15 ist teilweise an der CAF-vermittelten Behandlungsresistenz beteiligt. Die Depletion von GDF15 führte weiterhin zu Behandlungssensibilisierung und beeinträchtigter mitochondrialer Funktion in EAC-Zellen. Zusätzlich beobachteten wir, dass EAC-CAFs die Progression von EAC-Zellen, teilweise durch Aktivierung des AKT-Signalwegs, förderten, während die Depletion von GDF15 die Aktivierung des AKT-Signalwegs in EAC-Zellen abschwächte. Des Weiteren zeigten wir eine signifikante Zunahme des Serum-GDF15-Spiegels nach der CROSS-Behandlung bei EAC-Patienten, welcher einen unabhängigen Risikofaktor für ein schlechteres Gesamtüberleben darstellt. Die externe Validierung mithilfe öffentlicher Datenbanken bestätigte sowohl eine signifikant höhere GDF15-Expression in Tumorgewebe, im Vergleich zu normalem Ösophagus-Gewebe, als auch einen Zusammenhang zwischen einer hohen GDF15-Expression und einem schlechteren Gesamtüberleben bei EAC-Patienten.

Summary

We corroborated current guidelines recommending neoadjuvant chemoradiotherapy (NCRT) followed by surgery as the optimal treatment approach for managing patients with locally advanced esophageal cancer (EC) through the comprehensive analysis of existing literature. We further focused on the molecular mechanisms regarding treatment resistance to chemotherapy and radiotherapy in esophageal adenocarcinoma (EAC) cells. We successfully generated cancer-associated fibroblasts (CAFs) and tumor patient-derived organoids (PDOs) from the primary tumor tissues of EAC patients. We found that EAC CAFs played a crucial role in promoting EAC tumor cell treatment resistance using both 2D and 3D tumor-CAFs co-culture systems. Besides, EAC CAFs enhanced the mitochondrial function in EAC cells. To the best of our knowledge, we are the first group describing the methodology and performing functional experiments utilizing EAC PDOs and paired EAC CAFs for *ex vivo* co-culture. We further identified GDF15 from tumor-CAFs co-culture setup through transcriptomic analysis. We found that GDF15 was involved in both EAC tumor and EAC CAFs-mediated treatment resistance. The depletion of GDF15 led to treatment sensitization and impaired mitochondrial function in EAC cells. Moreover, we observed that EAC CAFs promoted EAC cell progression, partly by activating the AKT pathway, whereas the depletion of GDF15 attenuated AKT pathway activation in EAC cells. Furthermore, we observed a significant increase in serum GDF15 levels after the CROSS treatment in EAC patients. High serum GDF15 after the CROSS treatment, but not at the diagnosis stage, was an independent risk factor for predicting poor overall survival (OS) in EAC patients. The external validation using public databases showed that GDF15 expression was significantly higher in tumor tissues compared to normal tissues in EC and was higher in EAC patients compared to esophageal squamous cell carcinoma (ESCC) patients. High GDF15 expression was significantly associated with poorer OS in EAC patients.

Content

Abstract

Background: Esophageal cancer (EC) ranks as the 7th most common cancer and 6th leading cause of cancer-related deaths worldwide. The standard treatment for locally advanced EC involves neoadjuvant chemoradiotherapy (NCRT)/neoadjuvant chemotherapy (NT) followed by surgery. Cancer-associated fibroblasts (CAFs) play a pivotal role and contribute to various aspects of tumor initiation and progression within the tumor microenvironment (TME). We aim to compare the effectiveness of NCRT and NCT in treating EC patients and to explore the molecular mechanisms underlying treatment resistance in esophageal adenocarcinoma (EAC), with a specific focus on the involvement of CAFs.

Methods: A network meta-analysis was performed to compare the effectiveness of NCRT, NCT, and surgery alone in randomized control trials (RCTs) published up to September 2021. EAC CAFs and EAC patient-derived organoids (PDOs) were established from primary patient tissues. Transcriptomic analysis was used to identify potential factors that were involved in CAF-tumor interaction. Lentiviral transduction was conducted to establish stable GDF15 knockdown EAC cells and CAFs. *In vitro* cell viability assays and apoptosis analysis were performed to assess the sensitivity of EAC cells to chemotherapy and radiotherapy. GDF15 concentration was determined using ELISA. To validate CAF-mediated EAC tumor progression, we utilized EAC PDOs and paired CAFs as an *ex vivo* preclinical model. The prognostic value of GDF15 was assessed using our in-house data and externally validated through public databases.

Results: 25 RCTs with 4563 EC patients were included in the network meta-analysis. NCRT improved overall survival (OS) compared to NCT (HR: 0.83, 95%CrI: 0.69-0.99) and surgery alone (HR: 0.72, 95%CrI: 0.63-0.82). *In vitro* studies demonstrated that CAFs promoted EAC chemotherapy resistance and

radiotherapy resistance. Transcriptomic analysis revealed the enrichment of GDF15 in the EAC tumor-CAF transwell co-culture system, showing opposite expression patterns between tumor and CAF cells. GDF15 concentration was significantly elevated in the co-culture medium. Knockdown of GDF15 in OE33 and OE19 cells restored treatment sensitivity against chemotherapy and radiotherapy. Similar results were obtained when OE33 and OE19 cells were co-cultured with GDF15-depleted CAFs. In the 3D EAC PDO model, enhanced chemoresistance was observed when PDOs were co-cultured with paired CAFs or cultured in a medium containing human GDF15 recombinant protein. Downstream exploration revealed that GDF15 was involved in AKT pathway activation and mitochondrial oxidative phosphorylation in EAC cells. Moreover, GDF15 expression was significantly higher in the tumor tissue than in adjacent normal tissue in EAC patients (p=0.0056). Low GDF15 mRNA expression was associated with better OS in EAC patients (p=0.025). Notably, GDF15 serum concentration was significantly higher after the CROSS treatment (p<0.0001), and a high serum concentration after the CROSS was an independent risk factor for a poor OS in EAC patients (HR: 3.100, 95%CI: 1.092-8.799, p=0.034). Conclusion: NCRT followed by surgery represents the optimal treatment strategy for managing locally advanced EC patients. The co-culture system of EAC PDOs with paired CAFs offers a viable approach for studying tumor-stroma interactions. CAFs play a crucial role in modulating EAC treatment resistance, with GDF15 partly linking CAFs and EAC communications within the tumor microenvironment. GDF15 exhibits a regulatory role in EAC mitochondrial function and therapy resistance. Moreover, the predictive value of GDF15 serum concentration highlights its potential as a prognostic biomarker in EAC patients.

Keywords: esophageal adenocarcinoma, tumor microenvironment, cancer-associated fibroblasts, GDF15, organoids, therapy resistance

Introduction

1. The epidemiology of esophageal cancer

Esophageal cancer (EC) represents a significant global health burden, with approximately 604,100 new cases and 544,076 cancer-related deaths in 2020 according to the global cancer statistics[1]. It ranks as the 7th most common cancer and the 6th leading cause of cancer-related mortality worldwide. Approximately 70% of EC cases occur in males, highlighting a gender disparity in its prevalence[1–3]. Among the various regions, Eastern Asia stands out as the region with the highest incidence rates of esophageal cancer globally, followed by Southern Africa, Eastern Africa, Northern Europe, and South Central Asia[1,3]. Moreover, the geographical differences are also reflected in the distribution of the two main subtypes of EC: esophageal squamous cell carcinoma (ESCC) and esophageal adenocarcinoma (EAC)[3,4]. In the year 2020, it was estimated that there were approximately 512,500 cases of ESCC, 85,700 cases of EAC, and additional 6,000 other histologic subtypes diagnosed globally[3]. EAC is more prevalent in developed countries, including those in northern and western Europe, the United States, Canada, and Australia. In contrast, ESCC predominantly affects developing countries, such as eastern and south-central Asia, as well as south Africa[1,3,4]. An increasing trend in EAC incidence, accompanied by a decrease in ESCC incidence, has been observed in western countries over the past decades. However, in eastern countries such as China, Japan, and South Korea, ESCC continues to exhibit a significantly higher incidence compared to EAC[4,5].

In addition to the distinct epidemiological patterns, the risk factors associated with the development of EAC and ESCC are also different. Barrett's esophagus (BE), characterized by the replacement of the normal squamous epithelium in the distal esophagus with specialized columnar epithelium containing goblet cells, is the identified precursor to EAC[6,7]. Approximately 10-15% of patients

with BE exhibit symptoms of gastroesophageal reflux disease (GERD)[7], and frequent GERD symptoms are one of the earliest recognized non-genetic risk factors for EAC development[8]. Other EAC risk factors include obesity, tobacco smoking, low vegetables/fruits dietary style, and family history[4,5,8]. Alcohol consumption is a widely recognized risk factor for many types of cancer, however, population-based studies have indicated no significant correlation between alcohol consumption and an increased risk of EAC[9–11]. In contrast, several studies have strongly supported a significant relationship between alcohol consumption and the development of ESCC[11–13]. Besides, tobacco smoking is another prominent risk factor for ESCC, exhibiting a dose-dependent increase in risk and a synergistic effect when combined with alcohol consumption[13,14]. Furthermore, low socioeconomic status, a diet lacking in sufficient vegetables and fruits, consumption of hot beverages/food, betel quid chewing, and family history are additional well-recognized factors associated with ESCC[4,5,13].

2. Multidisciplinary management of esophageal cancer

The standard treatment for EC patients involves a multidisciplinary approach that combines endoscopic treatment, chemotherapy, radiotherapy, surgery, targeted therapy, and immunotherapy[15].

For pre-neoplastic tissues (e.g. Barrett's esophagus) and early-stage disease (e.g. pathological carcinoma in situ (pTis), pT1a, and selected superficial pT1b without lymphovascular invasion), endoscopic therapy such as endoscopic mucosal/submucosal dissection and/or ablation is preferred to achieve complete removal of the disease with minimal procedural risks[15,16].

For locally advanced EC, surgery-based neoadjuvant chemotherapy (NCT) or neoadjuvant chemoradiotherapy (NCRT) are standard treatment strategies worldwide[15]. Several important clinical trials have demonstrated the advantages of NCRT over surgery alone in EC patients. The large-scale,

national-based Dutch Chemoradiotherapy for Oesophageal Cancer followed by Surgery Study (CROSS) has shown a significant long-term survival benefit of NCRT compared to surgery alone in both EAC and ESCC patients with a median follow-up time of 12.25 years[17,18]. Since its initial release in 2012, the CROSS regimen has gained widespread acceptance and is now considered one of the standard treatment approaches for patients with esophageal cancer[18]. In addition to the EAC-dominant CROSS trial, the multicenter NEOCRTEC5010 trial, which included 451 ESCC patients, provided compelling evidence for the efficacy of NCRT in treating ESCC[19,20]. These findings further strengthen the application of NCRT in the comprehensive treatment of esophageal cancer. As to NCT, NCT followed by surgery has emerged as the standard of care in the management of locally advanced ESCC in Japan[21,22]. This standard has been established based on the findings of the JCOG9024 and JCOG9907 trials, which compared NCT with adjuvant chemotherapy after surgery and surgery alone[23,24]. Moreover, the recently reported JCOG1109 trial with optimized NCT regimen involving preoperative docetaxel, cisplatin and fluorouracil (5-FU), has further strengthened the efficacy of NCT in improving outcomes for ESCC patients[25]. Regarding EAC patients, only one randomized controlled trial has specifically compared NCT with surgery in the EAC subpopulation, showing a slight advantage of NCT over surgery but without statistical significance[26]. Perioperative chemotherapy, a well-established strategy to treat gastric cancer, has been employed to treat EAC patients in some western centers[27]. Several landmark clinical trials focusing on gastric cancer have included a subset of patients with EAC or adenocarcinoma of the gastroesophageal junction (AGEJ) and have reported promising survival benefits associated with perioperative chemotherapy[28–30]. However, it should be noted that the findings from these clinical trials conducted in the context of gastric cancer may not be directly applicable or sufficient to guide the treatment of EAC. A recent retrospective study from our center has compared the

outcomes of perioperative chemotherapy (FLOT regimen) with NCRT (CROSS regimen) in 578 EAC patients and showed no difference between NCRT and perioperative chemotherapy regarding overall survival (OS)[31]. Here, ongoing randomized controlled trials (RCTs) are expected to offer more robust evidence regarding the efficacy of perioperative chemotherapy in treating EAC patients[32,33].

For advanced EC patients with recurrence or metastasis, systemic therapy involving either one or in combination of chemoradiation, chemotherapy, and targeted therapy plays a crucial role in palliative care, improving survival outcomes, and enhancing overall quality of life[15]. Limited targeted therapy options are available for EC patients, where one well-established approach is the use of trastuzumab in combination with chemotherapy as the first-line treatment for advanced EAC patients with positive human epidermal growth factor receptor 2 (HER2) overexpression[34,35]. In recent years, immunotherapy has emerged as an effective treatment strategy in the management of EC. Nivolumab, a human monoclonal anti-programmed death 1 (PD-1) antibody, has shown significant improvements in OS and progression-free survival (PFS) when used in combination with chemotherapy as the first-line treatment for both advanced EAC and ESCC patients as compared to chemotherapy alone[36,37]. Additionally, as the second-line treatment, nivolumab has shown significant OS benefits in advanced ESCC patients after the prior fluoropyrimidine- and platinum-based chemotherapy[38]. Similar favorable prognosis outcomes have been observed with another anti-PD-1 antibody pembrolizumab when used as either first or second-line treatments in the management of advanced EC patients[39–43]. Furthermore, in patients with locally advanced EC who underwent NCRT followed by surgery, the utilization of nivolumab as an adjuvant therapy approach significantly improved disease-free survival (DFS) in both ESCC and EAC patients irrespective of PD-L1 expression levels[44], further broadening the therapeutic landscape of immunotherapy in EC clinical practice.

However, despite the increasing advancements in the multidisciplinary management of EC patients, the prognosis of esophageal cancer remains poor, with a 5-year survival rate of around 20%[2,4,5]. In EAC, the 5-year survival rate for patients diagnosed with pathological stage I stands at approximately 80%, which subsequently diminishes to 45%, 18%, and 2% as the disease progresses to stages II, III, and IV, respectively[8]. The unfavorable prognosis of EAC mandates a deeper comprehension of tumor progression and the formulation of advanced therapeutic strategies.

3. Cancer-associated fibroblasts and esophageal cancer treatment resistance

Since the description of the 'seed and soil' theory by Stephen Paget in 1889[45], the tumor microenvironment (TME), comprising immune cells, cancer-associated fibroblasts (CAFs), endothelial cells, pericytes, and other components, has been widely acknowledged as a crucial factor dynamically regulating tumor growth and progression[46,47]. TME shields tumor cells from multi-treatment stress by providing a physical barrier and a supportive niche, exerting paracrine effects, inducing tumor cell quiescence, enriching cancer stemness, and modulating metabolism and immune profiles[48–50]. As the main components within the TME, CAFs play a crucial role in reorganizing the TME under intrinsic and extrinsic stresses, thereby facilitating tumor metastasis, therapeutic resistance, tumor dormancy, and reactivation[51–53]. Mechanistically, CAFs play a pivotal role in mediating the interactions among cancer cells, stromal cells, and the extracellular matrix (ECM) through physical interactions as well as the secretion of growth factors, cytokines, and chemokines[51,52,54]. Besides, CAFs contribute to ECM remodeling, tumor immunology modulation, and angiogenesis, thus influencing multiple aspects of tumor development[54–57]. The comprehensive function of CAFs within the gastrointestinal (GI) cancer TME was summarized in Figure 1 by Kobayashi H et al[52].

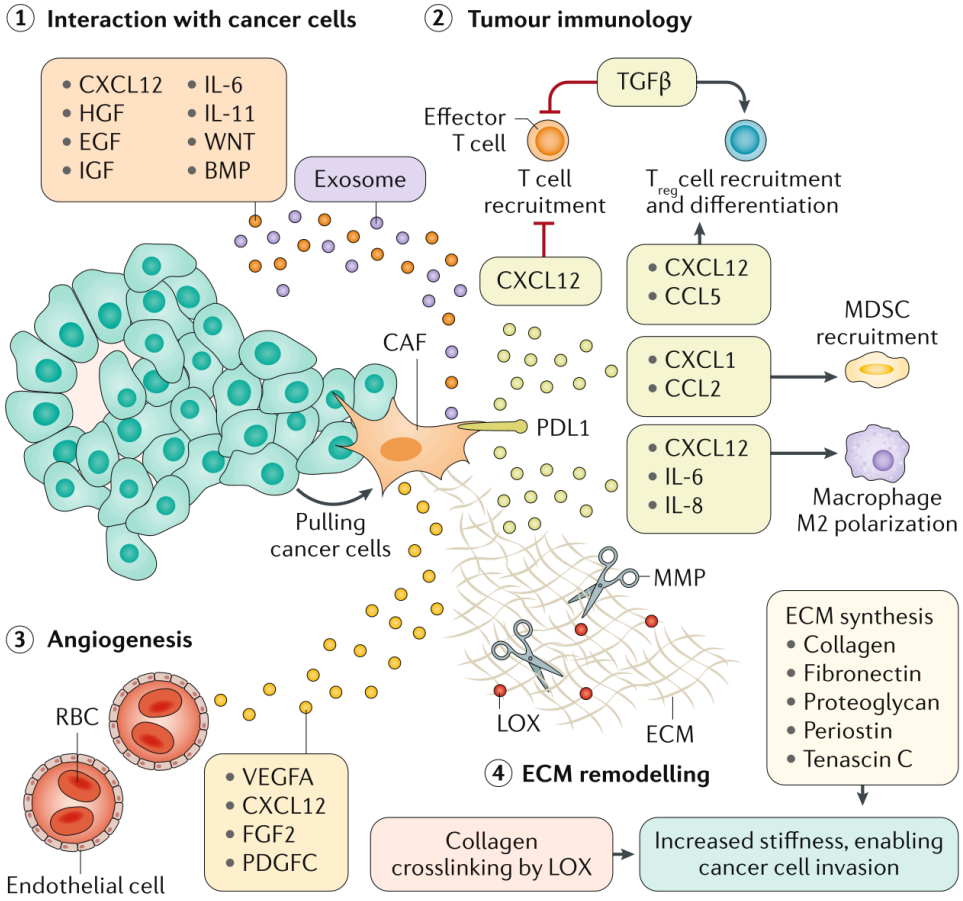

Figure 1. The comprehensive function of CAFs within the TME.

Note. Adapted from "Cancer-associated fibroblasts in gastrointestinal cancer" by Kobayashi H, 2019, Nat Rev Gastroenterol Hepatol; 16(5):282-295[52]. Copyright 2019 Springer Nature, reprinted with permission.

The contribution of CAFs to tumor treatment resistance is a key role of their tumor-supportive functions in the tumor microenviroment[58,59]. In pancreatic cancer, CAFs have been implicated in the induction of chemotherapy resistance through various mechanisms, including interference with drug delivery and intracellular activation of anti-cancer drugs[60–62], modulation of apoptosis- and proliferation-related signaling pathways in cancer cells[63–65], and elicitation of stromal pro-tumorigenic responses to chemotherapy[66,67]. Similarly, CAF-mediated tumor resistances to radiotherapy, targeted therapy, and immunotherapy have been reported in various GI cancers, including pancreatic cancer[68,69], gastric cancer[70–72], colorectal cancer[73,74], and esophageal cancer[75,76].

In ESCC, single-cell and spatial transcriptomic analyses of different stages of esophageal lesions have revealed that the gradual loss of ANXA1 levels in esophageal epithelial cells during ESCC development activates ESCC CAFs, which further promotes ESCC progression[77,78]. Besides, ESCC cancer cells secrete fibroblast growth factor-2 (FGF2) to recruit FGFR2+ fibrocytes to the tumor sites through the CXCL12/CXCR4 axis, promoting their differentiation into functional CAFs[79]. ESCC cells can also recruit CAFs through the secretion of CC motif chemokine ligand 5 (CCL5), establishing a positive feedback loop that promotes tumor cell proliferation[80]. ESCC-derived exosomes can activate normal fibroblasts into CAFs, secreting interleukin 6 (IL-6) that promotes cell proliferation and cisplatin resistance[81]. Notably, cisplatin treatment has been found to in turn stimulate ESCC CAFs to secrete plasminogen activator inhibitor-1 (PAI-1), which further dampens the efficacy of cisplatin by activating the AKT and ERK1/2 signaling pathways, inhibiting caspase-3 activity, and reducing reactive oxygen species accumulation[82]. The activated state of CAFs in ESCC confers chemoresistance and radioresistance through various mechanisms, including the generation of monocytic myeloid-derived suppressor cells[83], activation of TGF-β1/FOXO1 signaling[84], CXCL1-mediated DNA damage repair with the activation of the Mek/Erk signaling pathway[85], and upregulation of long noncoding RNAs (lncRNA) DNM3OS[86]. In addition, several studies have reported the suppressive function of ESCC CAFs in immunotherapy. The secretion of FGF2 by ESCC CAFs upregulated Sprouty RTK signaling antagonist 1 (SPRY1) expression, establishing the dysfunctional state of CD8+ T cells and promoting ESCC tumor growth[87]. ESCC CAFs mediated T-cell exhaustion through the secretion of transforming growth factor-β1 (TGF-β1), including laminin γ2 (Ln-γ2) expression to structure a protective barrier for tumors to restrict T-cell infiltration into tumor nests, and attenuate response to anti-PD-1 blockade therapy[88]. Moreover, CAFs-derived Wingless-type MMTV integration site family member 2 (WNT2) suppressed dendritic cell

(DC) differentiation and impaired DC-mediated antitumor T-cell responses through the SOCS3/p-JAK2/p-STAT3 signaling cascades[89].

As to EAC cells, IL-6 is a well-studied communication molecule between EAC cells and activated EAC CAFs[90]. Through IL-6 signaling and induction of epithelial-mesenchymal transition (EMT), EAC CAFs promote EAC treatment resistance to both chemotherapy and radiation *in vitro*[91]. It has been reported that targeting activated EAC CAFs with phosphodiesterase type 5 inhibitors (PDE5i) can reverse CAF-mediated chemotherapy resistance in EAC cells, suggesting a potential clinical application for CAF-directed targeted therapy in EAC patients[92]. Given the limited research conducted on tumor-stromal interactions in EAC, further investigation is warranted to better understand the complexities of CAF-mediated EAC tumor resistance.

4. Growth differentiation factor 15 (GDF15) in gastrointestinal cancers

Growth differentiation factor 15 (GDF15), also known as macrophage inhibitory cytokine 1 (MIC-1) and non-steroidal anti-inflammatory drug-activated gene-1 (NAG-1), is a divergent member of the TGF-β superfamily[93,94]. Similar to other peptide hormones, GDF15 is synthesized as a precursor protein, generating a ~40 kDa pro-peptide-GDF15 in the cytoplasm that subsequently undergoes proteolytic cleavage in the endoplasmic reticulum to release a ~25 kDa mature dimeric protein[95,96]. To date, the glial cell line–derived neurotrophic factor receptor alpha (GFRα)-like (GFRAL) receptor is the only known receptor for GDF15. GFRAL is predominantly expressed in the central nervous system (CNS), specifically in the area postrema and nucleus of the solitary tract, and small adjacent regions in the hindbrain of both humans and mice. Limited evidence suggests the presence of GFRAL in other regions[95–97]. Therefore, the GDF15-GFRAL axis is primarily implicated in metabolic and inflammatory diseases including obesity, diabetes, atherosclerosis, liver fibrosis, and cancer-related cachexia[96–98]. Pre-clinical and clinical studies have specifically focused

on the therapeutic potential of targeting GDF15 in the management of obesity and anorexia/cachexia syndromes[99,100].

In addition to the role of GDF15 in energy homeostasis, the GDF15 function in cancer research has also garnered significant attention. GDF15 has been widely recognized as a valuable biomarker in various types of cancers. It has been reported that elevated GDF15 serum concentrations independently predict all-cause mortality in patients with various diseases, including solid tumors[101,102]. In gastrointestinal cancers, a meta-analysis of 17 studies involving 3996 patients demonstrated the potential of GDF15 as both a diagnostic biomarker (with a sensitivity of 0.74, specificity of 0.83, and area under the curve (AUC) of 0.84) and a prognostic biomarker (with a hazard ratio (HR) of 2.34 and 95% confidence interval (CI) of 2.03-2.70 for OS)[103]. Similar meta-analysis in gastric cancer (GC) patients, which extracted data from the literature as well as the Gene Expression Omnibus (GEO) and The Cancer Genome Atlas (TCGA) databases, showed the diagnostic potential of GDF15 with a combined sensitivity of 0.69, a specificity of 0.90, and an AUC of 0.90[104]. For distinguishing early-stage GC patients, GDF15 showed a better diagnostic performance when compared with other serum biomarkers such as CA-199, CA72-4, and PG1/PG2[105]. A prospective case-control study comprising 618 colorectal carcinoma (CRC) case patients and 950 matched control subjects revealed that an elevated pre-diagnostic serum GDF15 concentration was an independent risk factor for the incidence of CRC[106]. Serum concentrations of GDF15 were found to be elevated in patients with adenomas and CRC patients as compared to those with no or hyperplastic polyps, while showing a subsequent decrease following polypectomy treatment, suggesting a potential role for GDF15 in the detection of colonic neoplasia[107]. By comparing the serum GDF15 in 258 healthy controls, 135 patients with colonic polyps, and 58 CRC patients, significantly elevated levels of GDF15 were observed in CRC patients compared to colonic polyps, and in patients with colonic polyps compared to

healthy controls[108]. In a cohort of 224 CRC patients, increased levels of GDF15 were found to be associated with advanced TNM tumor stage, particularly in relation to metastasis status. And high GDF15 serum levels were significantly associated with worse OS and DFS[108]. Similar results were obtained from several large-scale studies showing that high serum levels of GDF15 in CRC patients were associated with worse OS[109,110]. Besides, tissue microarrays form 320 CRC patients revealed a significant correlation between a higher intensity of GDF15 expression and an increased recurrence rate[111]. These findings were supported by another study, which identified higher GDF15 concentrations in metastatic CRC patients as compared to non-metastatic CRC patients and healthy controls[112]. It should be noted that serial measurements of serum GDF15 in 623 CRC patients revealed a contrasting role of GDF15 in CRC. Initially, GDF15 concentrations increased with NSAID treatment and were positively associated with the non-steroidal anti-inflammatory drugs (NSAIDs)-mediated preventive effects on colonic neoplasia. However, once polyps were present, GDF15 was found to be a predictor of adenomatous polyp burden and adenoma recurrence[113]. Regarding esophageal cancer, by comparing serum GDF15 concentrations in 286 ESCC patients with 250 healthy controls, serum GDF15 was significantly higher in ESCC. In those ESCC patients, higher serum GDF15 was significantly associated with tumor invasion and lymph node metastasis and was correlated with worse OS and DFS[114]. Besides, higher GDF15 expression was also detected in tumor tissues compared to adjacent normal tissues at protein level[114]. And the high expression of GDF15 in tumor tissue was related to poor OS and DFS in ESCC patients[115]. In advanced ESCC patients, increased serum GDF15 concentrations were observed in patients with >5% weight loss before chemotherapy as compared with patients without weight loss, and high GDF15 concentration was significantly related to worse OS (12.0 months vs. 18.5 months, p= 0.047)[116]. As to EAC patients, tissue GDF15 expression was significantly elevated in patients with EAC compared to

those with BE and healthy controls[117]. Similar to the ESCC population, high serum GDF15 levels were significantly associated with poor prognosis in EAC patients[117]. Besides, consistent results were reported by other studies indicating that serum GDF15 was increased in EAC patients as compared to healthy control, and high GDF15 concentration was associated with poor survival of patients with EAC and AGEJ[118,119]. Collectively, these consistent findings across various GI studies underscore the potential role of GDF15 as a valuable biomarker in the management of EC patients.

Mechanism studies have revealed the multifaceted role of GDF15 in tumor biology and its involvement in various aspects of cancer progression[120–122]. In gastric cancer, GDF15 exhibited proapoptotic activity upon NSAIDs treatment independent of COX-2 expression[123–125]. GDF15 activated the AKT and ERK-1/2 pathways through ErbB2 transactivation in both breast and gastric cancer cells[126]. By activating MAP2K and STAT3 pathways and incusing EMT, GDF15 enhanced gastric cancer cell proliferation, migration, and invasion abilities[127,128]. It was reported that GDF15 overexpression promoted cancer stemness in GC cells[129]. Besides, upon 5-FU treatment, hypoxia-inducible factor 1α (HIF1α) was activated and resulted in the accumulation of M2-type tumor-associated macrophages (TAMs), which promoted chemoresistance by producing GDF15 to exacerbate the fatty acid β-oxidation in GC cells[130]. In colorectal cancer, by comparing three paired acquired 5-FU resistant CRC cell lines with their respective control cells, GDF15 expression was found to be markedly upregulated in the acquired 5-FU resistant CRC cell lines[131]. GDF15 induced chemoresistance in CRC cells through the activation of the AKT pathway, while GDF15 depletion in p53 wild-type but not p53-null or mutant CRC cells showed restored sensitivity to different chemotherapeutic drug treatments[132]. The functional role of GDF15 was also reported within the tumor microenvironment. Macrophage-derived GDF15 was involved in macrophage-mediated invasion and migration ability in CRC cells through the activation of c-Fos from Lamin

A/C[133]. The stimulation of the GDF15 on mouse fibroblast cells showed enhanced fibroblast cell proliferation and upregulated expression of extracellular matrix genes[134]. Senescent fibroblasts, which were found to be significantly enriched in CRC tissues, were detected to secrete GDF15 thereby promoting cell proliferation, migration, and invasion in CRC cells via the activation of the MAPK and PI3K signaling pathways[135].

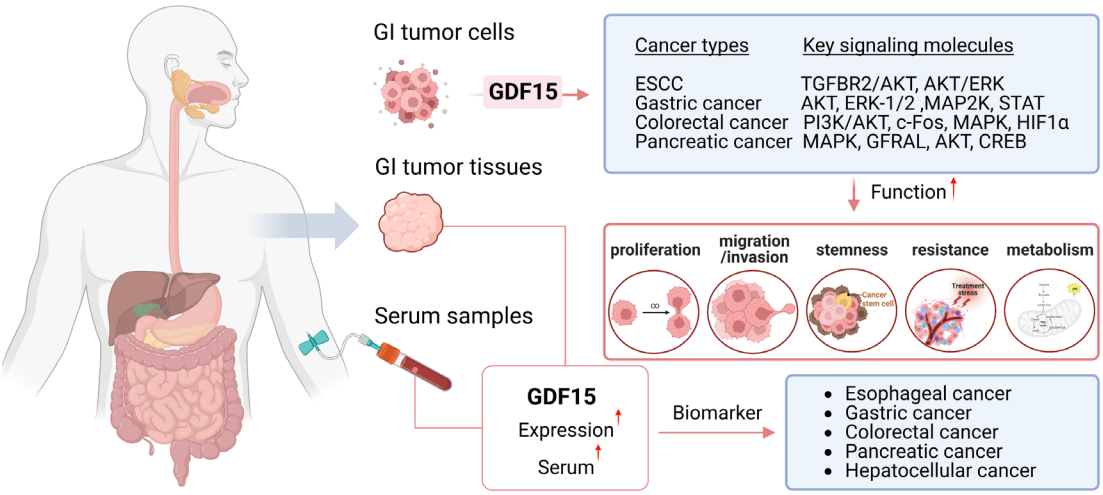

Figure 2. The role of GDF15 in gastrointestinal cancers.
GDF15 exhibits elevated levels in both GI tumor tissues and sera, showing a correlation with aggressive disease status and poor prognosis. Through diverse signaling pathways, GDF15 mediates tumor proliferation, metabolism, stemness, metastasis, and treatment resistance in GI cancers.

In esophageal cancer, by using recombinant GDF15 protein (rGDF15), the study revealed that GDF15 enhanced the ESCC cell proliferation, migration, and invasion through TGF-β type II receptor activation[136]. ESCC patients with high levels of GDF15 expression exhibited an inferior response to chemotherapy, and the administration of rGDF15 induced resistance of ESCC cells to cisplatin treatment through the activation of the TGFBR2-AKT pathway[137]. Regarding the tumor microenvironment, ESCC-derived conditional medium activated macrophage cells with an increased secretion of GDF15, and administration of rGDF15 promoted ESCC cell proliferation through the activation of the AKT/ERK pathway[115].

In conclusion, GDF15 plays an independent or interactive role in the progression of GI cancers, particularly in its interaction with the tumor microenvironment (Figure 2). However, there is limited literature discussing the molecular functions of GDF15 in EAC patients, and its specific role in the interaction between CAFs and EAC remains unknown.

5. Patients-derived organoids (PDOs) model in esophageal cancer

Patient-derived organoids (PDOs) are primary cells cultured in a three-dimensional (3D) system that closely mimics human development and organ regeneration *in vitro*[138,139]. The early attempts at *in vitro* organism regeneration can be traced back to the first decade of the 20th century when researchers began to culture tissue fragments. H. V. Wilson reported a method of regenerating dissociated small masses of undifferentiated sponge tissues into a new sponge[140]. Ross Harrison isolated fragments of embryonic tissue from frog embryos and cultured them in a drop of frog lymph, through which he observed the growth and development of living nerve fibers[141]. Until the end of the first decade of the 21st century, landmark studies that reported the successful generation of self-organized cerebral cortex tissue from embryonic stem cells (ESCs) using 3D aggregation cultures, as well as the generation of "mini-guts" from a single leucine-rich repeat-containing G protein-coupled receptor 5 (Lgr5)-positive stem cell in an extracellular matrix (ECM) gel, have propelled the field of 3D culture organoids system to a new level[142,143]. Since then, there has been a dramatic increase in the number of published studies focusing on the organoids model[144,145]. PDOs have been successfully established from a wide range of organs, encompassing the gut[146–148], stomach[149,150], pancreas[151–153], liver[153,154], kidney[155,156], breast[157,158], lung[159–161], thyroid[162,163], brain[164,165], and notably, the esophagus[166–168], which is of particular interest in our study. Compared to classic two-dimensional (2D) culture systems, 3D PDOs derived from primary tissues recapitulate

transcriptome and proteome profiles, metabolic functions, and microscale tissue architecture of the original organs[138]. This advanced model provides valuable insights for drug development and personalized cancer treatment, offering a more accurate representation of organ biology and enhancing our understanding of disease mechanisms[169,170]. Besides, the utilization of PDO models holds great promise in reducing the reliance on animal experimentations owing to their potential in recreating complex *in vitro* tumor microenvironments and accelerating the development of anticancer therapeutics[171–173]. To date, the subcutaneous tumor xenograft mouse model has remained the predominant choice for *in vivo* preclinical research in esophageal cancer, primarily attributed to their cost-effectiveness, technical feasibility, and ethical advantages over other model systems such as orthotopic EC xenograft mouse model and patient-derived xenograft mouse model[174,175]. However, the inherent limitations of subcutaneous models in recapitulating the complex human tumor microenvironment underline the importance of developing novel preclinical models to enhance our understanding of EC. In this regard, EC PDOs have demonstrated a great potential.

EC PDOs can be generated from both ESCC and EAC patients and are standardly described for various applications, including growth monitoring, histology characterization, and drug screening[167,176]. Karakasheva TA et al. generated four EAC PDOs from treatment-naive patient biopsies and found that these PDOs showed similar response patterns to chemotherapy and γ-irradiation *in vitro* as compared to the paired patients' clinical response to chemoradiotherapy, suggesting the potential of PDOs in predicting the clinical response to novel therapeutic strategies in EAC patients[177]. The comprehensive comparisons of histological and genomic features in five endoscopic biopsy-derived EAC PDOs and paired biopsy tissues have demonstrated that EAC PDOs closely recapitulate the corresponding tumors, with an approximate overlap of 60% in single nucleotide variants (SNVs)[178].

Besides, the response of the EAC PDOs to chemotherapy and HER-2 targeted therapy showed concordance with the response of the patients, indicating the potential utility of EAC PDOs in predicting therapeutic outcomes[178]. In a comparative analysis involving ten cases of EAC PDOs and their paired tumor tissues obtained from esophagectomy, EAC PDOs demonstrated remarkable similarities in histopathological features and genomic landscape to the primary tumors, and they preserved the intra-tumor heterogeneity and clonal dynamics that were observed in the original tumor samples, making them a valuable tool for medium throughput drug sensitivity screenings *in vitro*[179]. Using the EAC PDO model, Dings MPG et al. evaluated radiotherapy sensitivities of EAC tumors and explored the synergy landscape with potential targeted therapeutic drugs to identify drug efficacy[180]. Scott SJ et al. validated 2D cell results that the presence of specific mitotic defects led to impaired attachment of chromosomes to the microtubules of the mitotic spindle, providing valuable insights into the mechanisms underlying polyploidy formation in EAC[181]. As to the ESCC PDO model, ESCC PDOs recapitulated the histopathology of the corresponding ESCC tumor tissues, and their successful application in assessing the response to 5-FU treatment *in vitro* demonstrated the efficacy of ESCC PDOs as a valuable preclinical platform for investigating mechanisms of cancer therapy resistance[182]. Besides, the utilization of both ESCC cell line-derived and patient-derived organoid models have revealed the association between alcohol metabolism and the enrichment of cancer stem cells (CSCs) in ESCC[183].

In addition to tumor PDOs, organoids derived from human and mouse esophageal epithelial cells have provided valuable insights into the regulatory mechanisms governing squamous epithelial homeostasis and the genetic determinants driving the initiation of ESCC[184–186]. Besides, the successful generation of PDOs from normal gastroesophageal junction (GEJ) tissue has enabled the investigation of oncogenic mechanisms involved in the

development of EAC through the application of the CRISPR-Cas9 gene editing system[166]. Moreover, PDOs generated form Barrett's esophagus were utilized to study the origin and malignant transition of BE[187,188]. By exposing BE-derived PDOs to acid and bile salts treatments to simulate the conditions of BE with GERD *in vitro*, Zhang Q et al. observed an EMT process and the development of subsquamous intestinal metaplasia in BE PDOs [189,190]. Furthermore, studies have reported the successful establishment of human esophageal organoids from human pluripotent stem cells through a sequential differentiation approach[168,191]. The manipulation of organoid formation in these studies has revealed crucial genes and pathways involved in esophageal specification and development, providing valuable insights for modeling human pathologies and advancing tissue engineering approaches[168,191].

Taken together, EC PDOs provide a valuable tool for translational studies in esophageal cancer. In the scope of my doctoral study, we aim to establish EAC PDOs and their paired EAC CAFs, enabling the investigation of tumor-stroma interactions within the dynamic tumor microenvironment.

In summary, esophageal cancer remains a significant global public health challenge. The optimal neoadjuvant treatment for locally advanced EC is still unclear. The poor prognosis of EAC highlights the exigency for an in-depth investigation of tumor progression. Overcoming treatment resistance is a major barrier to EAC management. Further investigation is warranted to elucidate the role of CAFs in contributing to the development of treatment resistance in EAC. The molecular functions of GDF15 in EAC patients, particularly its interactions with CAFs and their role in the disease process, remain elusive. Moreover, the exploration of tumor-CAF interactions through the utilization of EAC PDO models is a promising area that requires further study.

Aim of the study

1. To compare the treatment efficacy between neoadjuvant chemoradiotherapy and neoadjuvant chemotherapy followed by surgery in patients with locally advanced esophageal cancer.
2. To establish patient-derived CAFs from EAC primary tissues and investigate tumor-stroma interaction *in vitro*.
3. To explore the molecular mechanisms involved in CAF-mediated EAC tumor progression and identify potential therapeutic targets or biomarkers for the clinical management of EAC patients.
4. To investigate the molecular function and underlying mechanisms of GDF15 in the crosstalk between EAC tumors and EAC CAFs.
5. To establish EAC PDOs and assess the feasibility of using EAC PDOs with paired EAC CAFs as an *ex vivo* model for validating the tumor-stroma interactions observed in 2D cell culture.
6. To evaluate the clinical significance of GDF15 in EAC patients.

Methods

1. Network meta-analysis

Our study followed the PRISMA extension statement for reporting network meta-analysis[192] and has been registered at PROSPERO since February 2020 (registration number: CRD42020170619). A comprehensive description of the detailed network meta-analysis methods can be found in our publication[193].

Briefly, an extensive search was conducted in major online databases, including MEDLINE, Embase, and Cochrane Central Register of Controlled Trials, to identify relevant RCTs published until September 2021. We included prospective RCTs that enrolled patients with confirmed ESCC or EAC. These trials aimed to compare different treatment arms, including neoadjuvant chemoradiotherapy followed by surgery, neoadjuvant chemotherapy followed by surgery, or surgery alone, and provided end-point information with OS or DFS in the intention-to-treat population. Only peer-reviewed articles published in English were considered, while studies exhibiting high bias that was judged by the revised Cochrane risk-of-bias tool (RoB2 tool) for randomized trials[194], comparing perioperative chemotherapy, representing former versions of the same trials with updated survival data available, or lacking full-text availability were excluded from our analysis.

We extracted HRs with 95% CIs from included studies and utilized the HR calculations spreadsheet[195] to calculate the natural logarithm of the hazard ratios (lnHR) and standard errors for data preparation. For pairwise meta-analysis, we used ‘meta’ package in R software (version 3.5.3) to compare different treatment approaches and report direct evidence regarding OS by providing HR with 95% CI. The Q test and I^2 statistic were used to evaluate study heterogeneity, where an I^2>50% or a p<0.05 indicates significant heterogeneity among studies[196]. For network meta-analysis, we used Stata (version 14.0) to generate network plots illustrating the network geometry for

comparing different treatment arms. The R package 'gemtc' was utilized to conduct network meta-analysis within the Bayesian framework[197], where HRs with corresponding 95% credible intervals (CrIs) were calculated to report the synthesized direct and indirect evidence for OS.

2. Establishment of EAC CAFs

To establish EAC CAFs, EAC patients' primary tissues from either endoscopic biopsy or operation were collected, washed, and minced into small fragments. The six-well plates were pre-coated with 1:20 diluted collagen type I (Corning, Bedford, MA, USA, product number: 354249) for one hour. The tissue pieces were then seeded onto the collagen-coated plates and cultured in a CAF culture medium.

The CAF culture medium was supplemented with extra 0.6% amphotericin B (R&D Systems, Flowery Branch, GA, USA, product number: B23192) and 0.2% normocin (InvivoGen, San Diego, CA, USA, product number: ant-nr-2) in the first week. A half medium change was performed after 4-5 days from seeding, and the medium was refreshed every 3-5 days once fibroblasts emerged from the tissue pieces. The fibroblasts were then expanded and stored for further use.

3. Cell culture

Human esophageal adenocarcinoma cell lines OE33 and OE19 were purchased from the Sigma Cell Line Bank (Sigma, 96070808 and 96071721, respectively). EAC CAFs TBE60, TBE63, TBO1657, CAF2304, and CAF2765 were established as previously described in the surgical laboratory of the University Hospital of Cologne. Wnt-3a cell line was kindly donated by Hans Cleaver group. Cultrex HA-R-Spondin 1-Fc 293T cell line was purchased from R&D Systems (3710-001-01).

EAC cell lines were cultured in RPMI 1640 medium (Gibco, Paisley, UK,

product number: 61870-010) supplemented with 10% fetal bovine serum (FBS) (Capricorn Scientific, Ebsdorfergrund, Germany, product number: FBS-12A) and 1% penicillin/streptomycin (P/S) (Gibco, Grand Island, NY, USA, product number: 15140-122). EAC CAFs were cultured in advanced DMEM/F-12 medium (Gibco, Grand Island, NY, USA, product number: 12634-010) supplemented with 10% FBS, 1% P/S, and 1% L-Glutamine (Gibco, Paisley, UK, product number: 25030-024). Cells were maintained in a humidified atmosphere with 5% CO_2 at 37°C.

Cell lines were routinely screened for mycoplasma contamination using MycoStrip (InvivoGen, San Diego, CA, USA, product number: rep-mys-50) according to the manufacturer's instructions to ensure a mycoplasma-free culture. The utilization of patients' materials from the Department of General, Visceral, Tumor, and Transplant Surgery at the University Hospital of Cologne was conducted under the approval of BIOMASOTA, as granted by the Ethics Committee of the University of Cologne (ID: 13-091).

4. Establishment and maintenance of EAC PDOs

Fresh human EAC primary tissue samples were obtained from surgical resection at the University Hospital of Cologne. The tissues underwent a series of steps to prepare the single-cell suspensions. Initially, the tissues were washed with DPBS (Gibco, Paisley, UK, product number: 14190-094) and mechanically minced into small fragments. These fragments were then enzymatically dissociated using a digestion buffer mix comprising 5U Dispase (Stem cell, Vancouver, BC, Canada, product number: 07913), 3600U Collagenase IV (GENAXXON bioscience, Ulm, Germany, product number: c4310), and 0.6% amphotericin B. Subsequently, the resulting fragments were further dissociated using 0.25% trypsin EDTA (Gibco, Paisley, UK, product number: 25200056). After the dissociation, the remaining fragments were filtered through a 100-µm strainer to obtain single-cell suspensions. These

suspensions were then seeded into the Matrigel matrix (Corning, Tewksbury, UK, product number: 354230) and supplemented with an EAC PDO culture medium comprising Wnt-3a conditioned medium, R-Spondin1 conditioned medium and different growth factors. The detailed composition of the EAC PDO culture medium was provided in Table 1. EAC PDO culture medium was refreshed every 4-6 days. Following the emergence of EAC PDOs from single cells, they were further passaged, expanded, and cryopreserved for future use.

Table 1. EAC PDO medium preparation

	Volume		**Final concentration**
Basal medium	**50**	**ml**	
Advanced DMEM/F-12	48.2	ml	
HEPES (1 M)	500	µl	10 mM
Amphotericin B	300	µl	0.6%
P/S (100X)	500	µl	1X
L-Glutamine (100X)	500	µl	1X
Gentamicin (10 mg/mL)	25	µl	5 µg/ml
EAC PDO medium	**50**	**ml**	
Basal medium	22.9	ml	
Wnt-3a conditioned medium*	12	ml	
R-Spondin1 conditioned medium#	12	ml	
N-2 (100×)	500	µl	1X
B-27 (50×)	1	ml	1X
N-Acetyl-L-cysteine (0.5 M)	100	µl	1 mM
CHIR-99021 (5 mM)	5	µl	0.5 µM
Recombinant human epidermal growth factor (EGF) (100 µg/mL)	125	µl	250 ng/ml
A83-01 (25 mM)	1	µl	0.5 µM
SB202190 (10 mM)	5	µl	1 µM
Gastrin I (1 mM)	5	µl	0.5 µM
Nicotinamide (1 M)	1	ml	20 µM
Gentamicin (10 mg/mL)	25	µl	10 µM
Normocin (50 mg/mL)	100	µl	100 µg/ml
P/S (100x)	276	µl	1X
Add freshly into wells:			
Noggin (100 µg/mL)	1:1000		100 ng/ml
Y-27632 (10 mM)	1:1000		10 µM
Fibroblast Growth Factor 10 (FGF-10) (100 µg/mL)	1:1000		100 ng/ml

*produced from Wnt-3a cells

#produced from Cultrex HA-R-Spondin 1-Fc 293T cells

In our recently published visual protocol, we have described two different routine methods for subculture and cryopreservation of EAC PDOs: with and without single-cell digestion[198]. Once EAC PDOs reach confluency, PDOs can be maintained with and without single-cell digestion. A workflow of the EAC PDOs subculture process was shown in Figure 3.

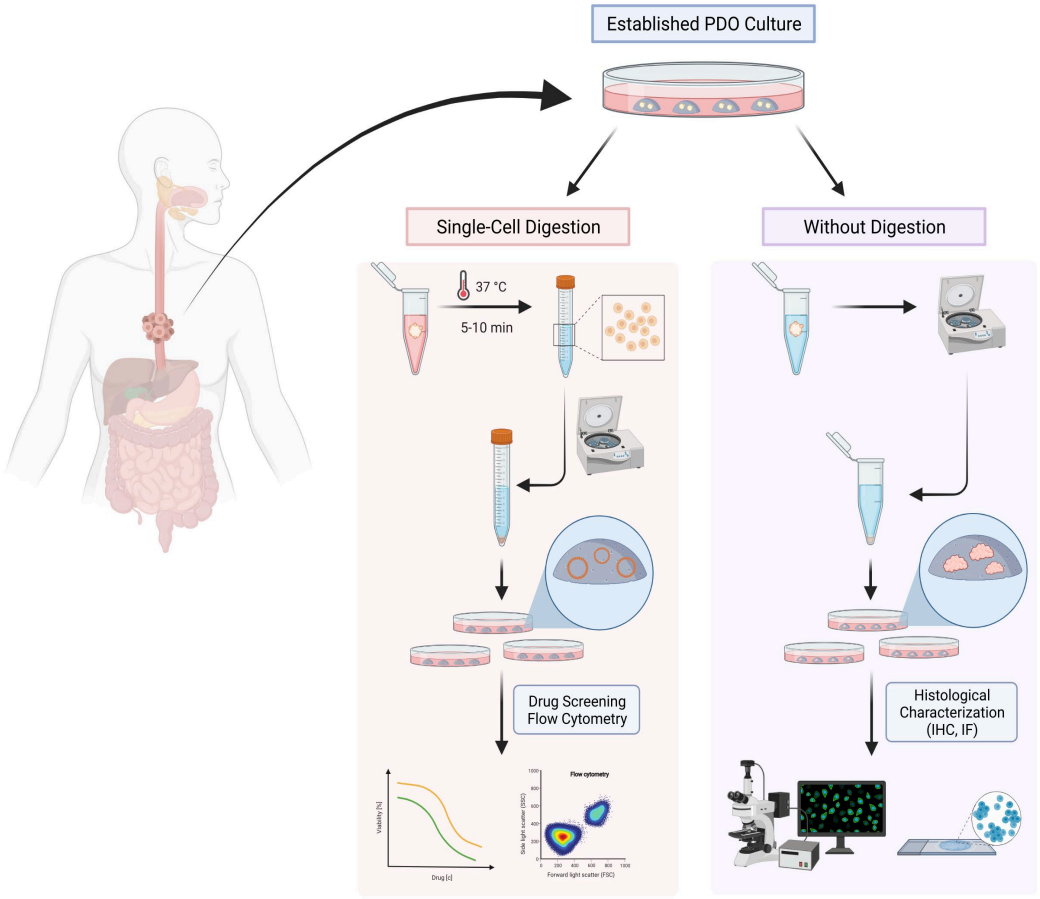

Figure 3. A workflow of EAC PDOs subculture processes with and without single-cell digestion[198].

Well-growing EAC PDOs were harvested and pelleted at 4°C. For single-cell digestion, PDOs underwent enzymatic digestion with 0.25% trypsin for 5-10 minutes to obtain single cells, which were further seeded into a fresh Matrigel matrix. These single cells exhibited a tendency to form hollow structures, which facilitated experiments requiring control of cell numbers, similar density, and size measuring. Alternatively, the undigested subculture involved splitting PDOs without enzymatic disruption, resulting in a tendency of growing into

compact structures, which were suitable for histological analyses, rapid expansion, and efficient recovery from cryopreservation.

5. Cell proliferation assay

Cells were seeded in 24-well plates and incubated overnight. The medium was replaced the next day, with subsequent medium refreshment every 2-4 days. The plates were fixed with 4% ROTIHistofix (Carl Roth, Karlsruhe, Germany, product number: P807) on days 0, 2, 4, and 6. After fixation, the plates were stained with 0.05% crystal violet solution (Sigma-Aldrich, Taufkirchen, Germany, product number: V5265) and imaged for visual results. To quantify the staining, the crystal violet particles were dissolved in an equal volume of 10% acetic acid (Sigma-Aldrich, Taufkirchen, Germany, product number: A-6283). Subsequently, 100µl of each dissolved crystal violet solution was transferred to a 96-well plate, and absorbance was measured at 570nm. All assays were performed in triplicate. Relative cell proliferation was calculated by normalizing the measurements to the day 0 values using GraphPad Prism (GraphPad Software, Boston, MA, USA, version 9.5.0).

6. Cell viability assay

To evaluate cell drug sensitivity and viability, the MTT assay was performed for 2D cell lines, while the luminescent cell viability assay was employed for EAC PDOs.

In the MTT assay, cells were seeded overnight in a 96-well plate at a consistent density. Subsequently, the cells were exposed to increasing concentrations of chemotherapeutic drugs for 48 hours. After the treatment, the cells were incubated with 5mg/ml MTT solution (Sigma-Aldrich, Taufkirchen, Germany, product number: 475989) at 37°C for 3.5-4 hours. Following incubation, the MTT solution was discarded, and MTT solvent was added to each well to dissolve the MTT formazan crystals. Absorbance at 570nm was measured, and

the collected data were subjected to analysis.

For luminescent cell viability analysis, EAC PDOs were harvested and enzymatically digested into single cells. The single cells were subsequently mixed with 1:10 dilution of Matrigel matrix and PDO medium, and evenly distributed into a 96-well plate. When small PDO spheres emerged after 3-5 days of seeding, increasing concentrations of chemotherapeutic drugs were introduced to the plates. Following a 48-hour incubation period, cell viability was assessed using the CellTiter-Glo reagent (Promega, Madison, WI, USA, product number: G7570) in accordance with the manufacturer's instructions. Luminescence signals were recorded for data analysis.

Data analysis was performed using GraphPad Prism. Each assay was conducted in triplicate.

7. Apoptosis analysis

The cells were treated either with cisplatin or exposed to ionizing radiation using a gamma irradiation device (BIOBEAM GM, Gamma Service Medical GmbH, Leipzig, Germany). After 48 hours, the cells were harvested and suspended in Annexin V binding buffer containing Annexin V APC (ImmunoTools, Friesoythe, Germany, product number: 31490016) and DAPI staining dye. The suspension was incubated at room temperature for 20 minutes. Subsequently, flow cytometry analysis was performed using the Attune™ NxT Flow Cytometer (Life Technologies, Carlsbad, USA), and the data were analyzed using FlowJo v10.4 software (BD Life Sciences, Ashland, USA).

8. Quantitative Real-time PCR (qPCR) analysis

Cultured cells or EAC tissue samples were subjected to RNA extraction using TRI reagent (Sigma-Aldrich, Taufkirchen, Germany, product number: T9424). The High-Capacity cDNA Reverse Transcription Kit (Thermo Fisher Scientific Baltics UAB, Vilnius, Lithuania, product number: 4368814) was employed for

reverse transcription following the manufacturer's instructions. The relative expression levels of target mRNAs were determined using the Fast SYBR green master mix (Thermo Fisher Scientific Baltics UAB, Vilnius, Lithuania, product number: 4385617) and measured by the QuantStudio 7 Flex Real-Time PCR System (Life Technologies, Carlsbad, CA, USA, product number: 4485701). Relative gene expression from qPCR experiments was analyzed using the $2^{-\Delta\Delta Ct}$ method. The primers utilized in this study are listed in Table 2.

Table 2. List of primers for qPCR.

Gene	Sequence (5' to 3')
GAPDH-for	GAAGGTGAAGGTCGGAGTC
GAPDH-rev	GAAGATGGTGATGGGATTTC
18s rRNA-for	GCTTAATTTGACTCAACACGGGA
18s rRNA-rev	AGCTATCAATCTGTCAATCCTGT
β-actin-for	AGAGCTACGAGCTGCCTGAC
β-actin-rev	AGCACTGTGTTGGCGTACAG
αSMA-for	TACATAGTGGTGCCCCCTGA
αSMA-rev	TTGCCTGATGGGCAAGTGAT
IL6-for	CCTGAACCTTCCAAAGATGGC
IL6-rev	TTCACCAGGCAAGTCTCCTCA
PDGFRα-for	TGGCAGTACCCCATGTCTGAA
PDGFRα-rev	CCAAGACCGTCACAAAAAGGC
Vimentin-for	ACGTCTTGACCTTGAACGCA
Vimentin-rev	CGTGAGGTCAGGCTTGGAAA
GDF15-for	GACCCTCAGAGTTGCACTCC
GDF15-rev	GCCTGGTTAGCAGGTCCTC

9. Western blot for protein analysis and applied antibodies

For protein extraction, cells were harvested and lysed on ice using RIPA buffer (Cell Signaling Technology, Danvers, MA, USA, product number: 9806). The lysates were subjected to the Bioruptor Pico sonication system (Diagenode, Denville, NJ, USA) for 10 cycles at 4°C to facilitate protein degradation. Protein samples were collected by centrifugation at 12,000×g for 10 minutes at 4°C to remove cell debris. Protein concentrations were determined using the BCA protein assay (Thermo Fisher Scientific, Rockford, IL, USA, product number:

2161296). The protein samples were then prepared and denatured in NuPAGE LDS sample buffer (Life Technologies Corporation, Carlsbad, CA, USA, product number: NP0007) and heated at 70°C for 10 minutes.

Twenty micrograms of protein were loaded onto SDS-PAGE gel and subsequently transferred to a PVDF membrane (MACHEREY-NAGEL, Düren, Germany, product number: 741260) using the Trans-Blot Turbo transfer system (Bio-Rad Laboratories, Hercules, CA, USA). The transferred membranes were blocked in 1x Roti-Block (Carl Roth, Karlsruhe, Germany, product number: A151) for 1 hour at room temperature. Following the blocking step, the membranes were incubated overnight at 4°C with specific primary antibodies. After thorough washing, the blots were probed with secondary antibodies specific to the primary antibodies for 1 hour at room temperature. Protein bands were visualized using the SuperSignal West Pico PLUS Chemiluminescent Substrate (Life Technologies, Carlsbad, CA, USA, product number: 34577) and detected using the ChemoStar ECL Imager (INTAS Science Imaging, Göttingen, Germany). The antibodies utilized in this study are listed in Table 3.

Table 3. List of antibodies for western blot.

Antibodies	Host	Class	Manufacturer	Product No.
First antibodies				
α-Tubulin	Mouse	Monoclonal	Cell Signaling Technology, Danvers, MA, USA	3873
GAPDH	Mouse	Monoclonal	Proteintech group, Rosemont, IL, USA	60004-1-Ig
GDF15	Mouse	Monoclonal	Sigma-Aldrich, Taufkirchen, Germany	AMAB90687
phospho-AKT (Ser473)	Rabbit	Monoclonal	Cell Signaling Technology, Danvers, MA, USA	4058
phospho-AKT (Thr308)	Rabbit	Monoclonal	Cell Signaling Technology, Danvers, MA, USA	13038
AKT (pan)	Rabbit	Monoclonal	Cell Signaling Technology, Danvers, MA, USA	4685
HRP-conjugated secondary antibodies				
anti-Rabbit	Goat	Polyclonal	Invitrogen, Rockford, IL, USA	31460
anti-Mouse	Goat	Polyclonal	Invitrogen, Rockford, IL, USA	31430

10. Immunofluorescence staining and immunohistochemistry staining

For immunofluorescence (IF) staining, cells were fixed with 4% ROTIHistofix for 15 minutes at room temperature, followed by permeabilization with 0.2% Triton X-100 (EuroClone, Pero, Italy, product number: EMR237500) in DPBS for 15 minutes. To block non-specific binding, cells were incubated with normal serum block (BioLegend, Dedham, MA, USA, product number: 927503) for 40 minutes. Subsequently, the cells were incubated overnight at 4°C with primary antibodies. After washing with DPBS, the cells were incubated with fluorochrome-conjugated secondary antibodies for 1 hour at room temperature. Nuclei were counterstained with DAPI, and fluorescence images were captured using the Olympus IX83 inverted microscope (Evident Corporation, Tokyo, Japan).

As to immunohistochemistry (IHC) staining, paraffin-embedded EAC PDO slides were deparaffinized by incubating at 60°C for 1 hour, followed by sequential washes with xylene (Sigma-Aldrich, Taufkirchen, Germany, product number: X2377) and graded ethanol solutions (Carl Roth, Karlsruhe, Germany, product number: 9065). Antigen retrieval was performed by heating the slides in a pH 6.0 citrate buffer (Carl Roth, Karlsruhe, Germany, product number: 5110.3) using the PT-Module (Thermo Shandon Limited, Runcorn, Cheshire, UK). After cooling, endogenous peroxidase was inactivated by incubating the sections with 0.3% hydrogen peroxide solution (Th. Geyer, Renningen, Germany, product number: 452.2511) in methanol (Carl Roth, Karlsruhe, Germany, product number: 8388.5) for 20 minutes. Subsequently, the slides were incubated overnight at 4°C with primary antibodies diluted in antibody diluent reagent solution (Life Technologies, Frederick, MD, USA, product number: 003218). After washing with 1X TBS buffer (Thermo Fisher Scientific, Rockford, IL, USA, product number: 28358), the slides were incubated with a secondary antibody conjugated to horseradish peroxidase (HRP) for 45 minutes at room temperature. Detection of the antibody signal was achieved

using EnVision system-HRP (Dako North America, Carpinteria, CA, USA, product numbers: K4009 and K4005, for anti-Rabbit and anti-Mouse, respectively). Finally, the slides were counterstained with Mayer's hematoxylin solution (Panreac Quimica, Barcelona, Spain, product number: 254766), followed by dehydration and coverslipping. The stained slides were visualized using an inverted light microscope.

11. Enzyme-linked immunosorbent assay (ELISA)

ELISA was conducted to quantify the concentration of GDF15 in patient serum samples and cell culture media using the human GDF-15 Quantikine ELISA Kit (R&D Systems, Minneapolis, MN, USA, product number: DGD150) following the manufacturer's instructions. Initially, samples were centrifuged and filtered to eliminate particulates, and then diluted with calibrator diluent at a ratio of 1/4 or 1/5. The samples and standards were added to the wells and allowed to incubate for two hours at room temperature. Following the incubation, the wells were washed and the GDF15 conjugate was introduced for an additional incubation of one hour. After another washing step, the substrate solution was added to initiate a color reaction, which was stopped using the stop solution after 30 minutes. The absorbance of each well was measured using a microplate reader at 450nm. GDF15 concentration was calculated using a linear regression fit based on the standard curve. Three replicates were measured for each cell culture media.

12. Plasmid construction and lentiviral transduction

For RNA interference, plasmids expressing the short hairpin RNA (shRNA) targeting GDF15 were constructed using the pLKO.1 puro vector (Addgene plasmid #8453). The shRNA sequences targeting GDF15 (5'-GCTCCAGACCTATGATGACTT-3', and 5'-CCGGATACTCACGCCAGAAGT-3') were designed using the genetic perturbation platform (Broad Institute,

Cambridge). For non-target control, the shRNA target sequence (5'-AGGTAGTGTAATCGCCTTGTT-3') was used. The forward and reverse oligonucleotides containing the shRNA sequences were synthesized (Thermo Fisher Scientific, Rockford, IL, USA) and annealed. The pLKO.1 puro vector was linearized, and the annealed shRNA oligonucleotides were ligated into the vector through AgeI and EcoRI. The resulting ligation mixtures were transformed into competent cells, and positive colonies were selected by ampicillin (Carl Roth, Karlsruhe, Germany, product number: HP62.2) and confirmed by DNA sequencing.

Stable cell lines expressing the shRNA sequence were generated through lentiviral transduction. HEK293T cells were transfected with transfer plasmid using a 2nd generation packaging system (packaging plasmid psPAX2 and envelop plasmid pMD2.G, Addgene plasmid #1226 and #12259, respectively) through polyethylenimine (PEI) (Sigma-Aldrich, Taufkirchen, Germany, product number: 408727) in a mass ratio of 1:3 DNA/PEI. The medium was replaced 24 hours post-transfection, and the supernatant containing the virus was collected and filtered through a 0.45 µm strainer at 48 hours and 72 hours. The virus-containing supernatant was mixed in a 1:1 ratio with fresh medium supplemented with 8 µg/ml polybrene (MedChemExpress, Monmouth Junction, NJ, USA, product number: HY-112735) and used for cell transduction. Puromycin (InvivoGen, San Diego, CA, USA, product number: ant-pr-1) selection was initiated 48-72 hours post-transduction, and the selective medium was refreshed every 2-3 days and maintained for 1 week.

13. Mitochondrial stress test

Cell mitochondrial stress test was performed using the Agilent Seahorse XF Cell Mito Stress Test Kit (Agilent Technologies, Wilmington, DE, USA, product number: 103015) following the manufacturer's instructions. Cells were seeded in XF cell culture plates and incubated until reaching the desired confluency.

The assay medium was prepared by supplementing the XF DMEM medium with 10mM glucose, 1mM pyruvate, and 2mM glutamine. The cells were washed and incubated with assay medium in a non-CO_2 incubator at 37°C for 1 hour prior to assay. The assay plate was prepared by adding injection solutions including oligomycin, carbonyl cyanide-p-trifluoromethoxy phenylhydrazone (FCCP), and rotenone/antimycin A (Rot/AA). The assay plate was then inserted into the Seahorse XFe96 Analyzer (Agilent Technologies, Wilmington, DE, USA), and the instrument sequentially injected 2.5μM oligomycin, 1μM FCCP, and 0.5μM Rot/AA while simultaneously measuring the real-time oxygen consumption rate (OCR) and extracellular acidification rate (ECAR) of the cells. Four to six replicates were measured for each sample. Data were analyzed by Wave software (version 2.6.1.53) (Agilent Technologies, Wilmington, DE, USA) and visualized using GraphPad Prism.

14. Next-generation RNA sequencing (RNA-seq) sample preparation and data analysis

The EAC cell line OE33 was subjected to a transwell co-culture with two CAF cell lines, TBE60 and TBE63, for a duration of seven days. Parallel culturing of OE33, TBE60, and TBE63 was also performed as a control. Triplicate samples from each experimental group were subjected to RNA extraction using the previously described method. Following the previous study from our collaborate group[199], mRNA-seq libraries were prepared for sequencing using the QuantSeq 3' mRNA-Seq Library Prep Kit FWD for Illumina (Lexogen GmbH, Vienna, Austria) according to the low-input protocol. Subsequently, constructed libraries were sequenced on the HiSeq 4000 system (Illumina, Hayward, CA, USA) by 1x50 bases.

To analyze the data, STAR software (version 2.6)[200] was used to align the high-throughput reads to the human genome (Homo sapiens GRCh38). The aligned reads were then counted with HTSeq, and differential gene expression analysis

was performed using the 'DESeq2' R package (version 1.22.2)[201] in R software (version 3.5.3). Differential gene expression was determined based on a significance threshold of adjusted *p*-value less than 0.05 and a minimum log2 fold change of 1.

15. Proteomics sample preparation and data analysis

OE33 sh-GDF15 cell line was supplemented with 50 ng/ml human recombinant GDF15 protein (rGDF15) (PeproTech, Cranbury, NJ, USA, product number: 120-28C) for seven days, along with parallel culturing of OE33 sh-NT and OE33 sh-GDF15 cell lines. Protein samples were prepared according to the instructions from Proteomics Core Facility Cologne with materials provided (www.proteomics.cecad-labs.uni-koeln.de). Cells were lysed with 8M urea/50mM triethylammonium bicarbonate (TEAB) buffer and subjected to the Bioruptor Pico sonication system (Diagenode, Denville, NJ, USA) for chromatin degradation. Protein concentrations were measured using the BCA method and 50µg protein per sample was collected. Samples were subsequently incubated with 5mM dithiothreitol (DTT) for one hour, followed by 40mM chloroacetamide (CAA) in the dark for 30 minutes, and then incubated with Lysyl endopeptidase (Lys-C) at a ratio of 1/75 for 4 hours. After the incubation, the samples were diluted with 50mM TEAB to achieve a final urea concentration of less than 2M and incubated with trypsin at a 1/75 enzyme-to-substrate ratio overnight. Enzymatic digestion was stopped by acidifying the samples with formic acid to a final concentration of 1%, and samples were further purified using SDB-RP StageTips prior to measurement. Samples were analyzed by LC-MS/MS on a Q-Exactive Plus mass spectrometer coupled to an Easy nanoLC 1000 system (Thermo Fisher Scientific, Rockford, IL, USA). The raw data were processed by MaxQuant (version 2.2)[202] using standard settings with label-free quantification (LFQ) activated. The match-between-runs function was enabled between replicates. Protein analysis was performed and visualized based on LFQ using

the R package ‘DEP’ in R software (version 3.5.3).

16. Public database

Public databases were utilized for data extraction and analysis to assess the correlation between GDF15 expression and clinical significance in EAC patients. The TCGA (Esophageal Adenocarcinoma, PanCancer Atlas) database was accessed and downloaded from cBioPortal[203]. A total of 182 patients’ mRNA expression data with matched clinical information were extracted, including 95 patients with ESCC and 87 patients with EAC. The GSE26886 and GSE92396 datasets were obtained from the NCBI GEO database[204] for gene expression analysis. GSE26886 database provides gene expression profiling of 20 Barrett's esophagus patients, 21 EAC patients, nine ESCC patients, and 19 patients with normal esophageal squamous epithelium[205]. GSE92396 database contains nine paired samples of EAC tumor and adjacent normal tissue. The websites of the databases utilized in this study were listed in Table 4.

Table 4. List of the public databases.

Name of database	Website
The TCGA database	https://www.cbioportal.org/study/summary?id=esca_tcga_pan_can_atlas_2018
GSE26886	https://www.ncbi.nlm.nih.gov/geo/query/acc.cgi?acc=GSE26886
GSE92396	https://www.ncbi.nlm.nih.gov/geo/query/acc.cgi?acc=GSE92396

17. Other reagents

Additional reagents used in this study were summarized in Table 5.

Table 5. List of other reagents.

Reagents	Manufacturer	Product No.
Cisplatin	Hexal AG, Holzkirchen, Germany	hH8716

Oxaliplatin	Accord Healthcare, Utrecht, Netherlands	gy0776
AKT inhibitor VIII	MedChemExpress, Monmouth Junction, NJ, USA	HY-10355
HEPES 1M	Life Technologies Corporation, Grand Island, NY, USA	15630080
Gentamicin	Life Technologies Corporation, Grand Island, NY, USA	15710064
N-2 supplement	Life Technologies Corporation, Grand Island, NY, USA	17502048
B-27 supplement	Life Technologies Corporation, Grand Island, NY, USA	17504001
N-Acetyl-L-cysteine	Sigma-Aldrich, Taufkirchen, Germany	A9165
CHIR-99021	MedChemExpress, Monmouth Junction, NJ, USA	HY-10182
Recombinant Human EGF	PeproTech, Cranbury, NJ, USA	AF-100-15
A83-01	Tocris Bioscience, Bristol, UK	2939
SB202190	MedChemExpress, Monmouth Junction, NJ, USA	HY-10295
[Leu^{15}] Gastrin I human	Sigma-Aldrich, Taufkirchen, Germany	G9145
Nicotinamide	Sigma-Aldrich, Taufkirchen, Germany	N0636
Recombinant Human Noggin	PeproTech, Cranbury, NJ, USA	120-10C
Y-27632	Sigma-Aldrich, Taufkirchen, Germany	Y0503
Recombinant Human FGF-10	PeproTech, Cranbury, NJ, USA	100-26

18. Statistics

The experiments were performed at least in triplicate to ensure reproducibility. Data are presented as mean ± standard deviation (SD). Statistical comparisons between groups were conducted using unpaired or paired Student's t-test, or one-way analysis of variance (ANOVA) as appropriate. Survival analysis was performed using the Kaplan-Meier method, and statistical differences were evaluated using the log-rank test. Univariate and multivariate Cox regression analyses were performed to identify risk factors associated with OS in EAC patients. A two-sided p-value<0.05 was considered statistically significant. Data were analyzed using GraphPad Prism software (version 9.5.0) and IBM SPSS Statistics software (version 25, IBM Corporation, Armonk, NY, USA).

Results

1. Network meta-analysis addresses the advantage of neoadjuvant chemoradiotherapy in treating patients with locally advanced esophageal cancer[193] (Published as the first author)

Neoadjuvant chemoradiotherapy and neoadjuvant chemotherapy followed by surgery constitute standard clinical approaches for managing patients with locally advanced esophageal cancer[15,206]. When it comes to the comparisons between NCRT and NCT, to date, only four RCTs have directly compared these two neoadjuvant management[207–210]. However, the small sample sizes and conflicting conclusions of these studies have left uncertainties regarding the superiority of one approach over the other. Network meta-analysis is a well-established statistical method to integrate both direct and indirect evidence and produce comprehensive results across a network of RCTs[211]. As there are multiple RCTs comparing NCRT or NCT with surgery alone, the surgery treatment can be utilized as a bridge to establish indirect evidence for comparing NCRT and NCT. Therefore, we performed a network meta-analysis to evaluate the relative effectiveness of NCRT and NCT in the management of locally advanced esophageal cancer patients[193].

1.1. Study selection

We thoroughly searched MEDLINE, Embase, CENTRAL, and conferences for RCTs published up to September 2021 that were comparing two or more treatment strategies including NCRT, NCT, and surgery. A total of 1264 publications were identified at the first screening. After removing duplicates and unmatched records based on title and abstract screening, 56 studies went through full-text assessments, and 25 studies were included in our final analysis. The detailed study selection procedure was shown in Figure 4a, and the detailed included studies can be found in Fan et al[193]. The analysis included

4563 patients in total. Out of 25 included studies, only four studies directly compared NCRT with NCT, while 13 studies compared NCRT with surgery alone, and eight studies compared NCT with surgery alone. OS is the main outcome of interest and was reported in all included studies.

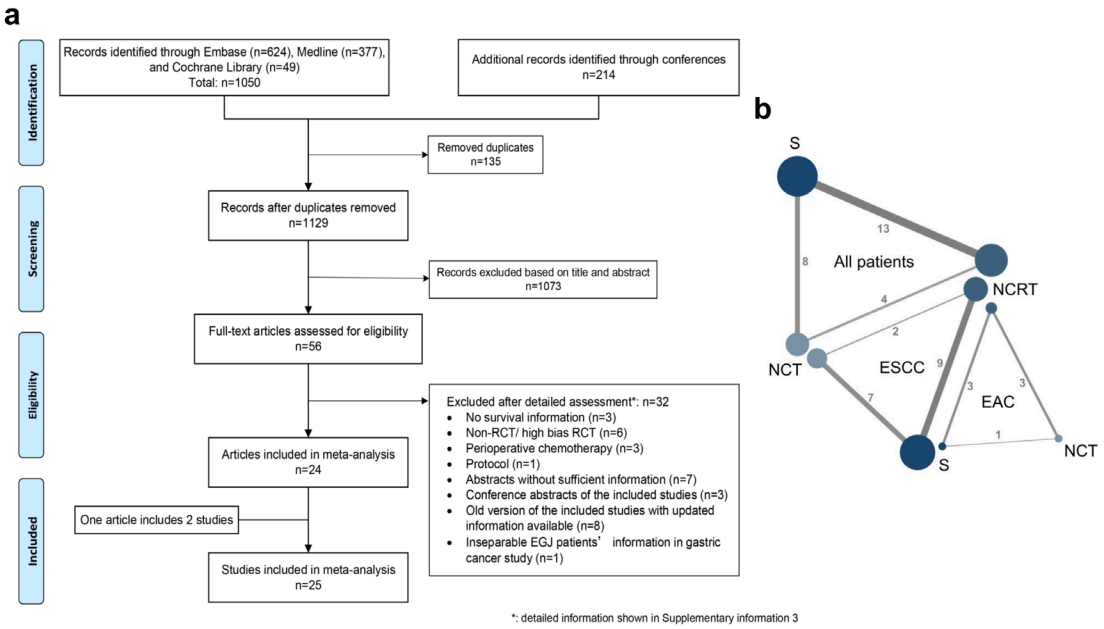

Figure 4. The flow chart of study selection[193].

a. The flow chart of study selection.

b. Network diagrams of treatment comparisons on overall survival in all included EC patients and ESCC and EAC subpopulations. The numbers reflect the trials that compared the connecting treatments.

1.2. Pairwise comparison and network analysis on OS in EC patients

The network diagrams of the comparisons among three treatment strategies in terms of OS were shown in Figure 4b. Pairwise comparison as well as network meta-analysis were performed to compare each treatment arm. In pairwise comparison (Figure 5a), both NCRT and NCT showed better OS than surgery alone (HR: 0.76, 95%CI: 0.68-0.85 and HR: 0.88, 95%CI: 0.78-0.98, respectively) while there was no difference between NCRT and NCT (HR: 0.82, 95%CI: 0.64-1.04). The corresponding network meta-analysis revealed a superior prognosis with NCRT compared to NCT (HR: 0.83, 95%CrI: 0.69-0.99) and surgery alone (HR: 0.72, 95%CrI: 0.63-0.82), but found comparable OS

between NCT and surgery (HR: 0.87, 95%CrI: 0.74-1.02) after synthesizing the direct and indirect evidence (Figure 5b).

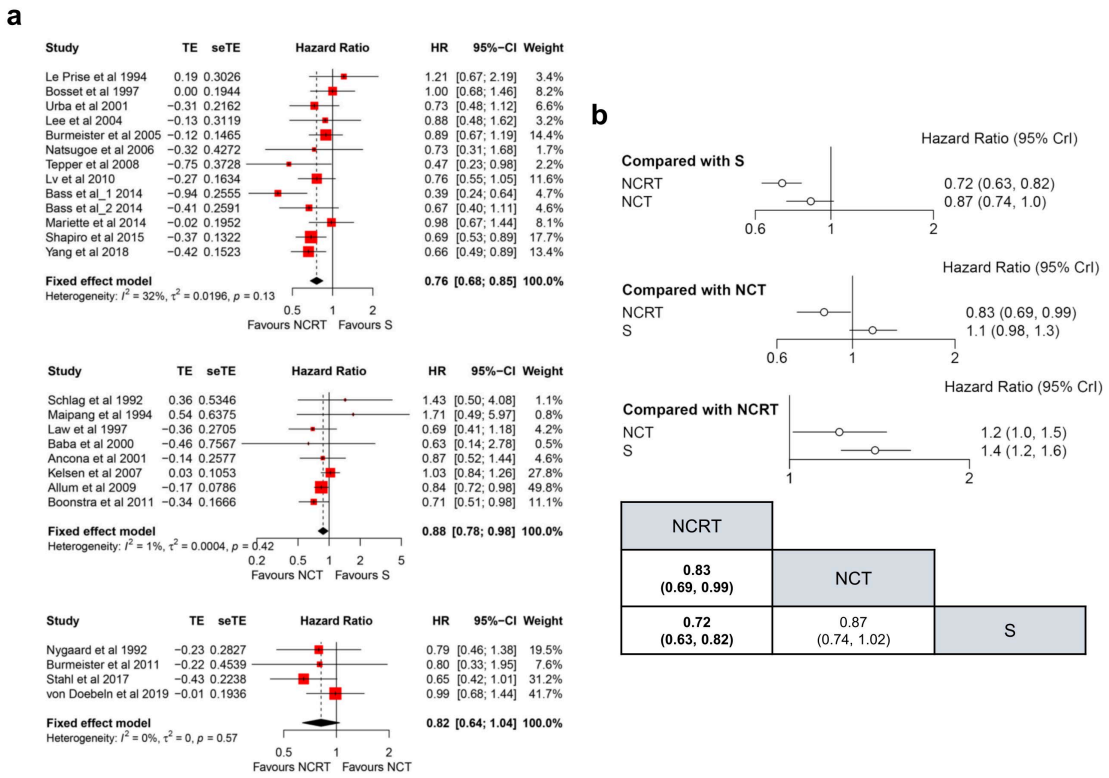

Figure 5. Pairwise comparison and network meta-analysis on overall survival in esophageal cancer patients[193].

a. Pairwise comparisons of NCRT and surgery, NCT and surgery, and NCRT and NCT on OS.

b. Network meta-analysis of NCRT and surgery, NCT and surgery, and NCRT and NCT on OS. Bold text indicates a statistically significant difference.

In summary, our analysis highlights the significance of neoadjuvant chemoradiotherapy in managing esophageal cancer patients. Therefore, understanding the molecular mechanisms of chemotherapy/radiotherapy resistance is crucial and may provide valuable pre-clinical insights that could ultimately benefit patients. The comprehensive network meta-analysis, encompassing comparisons of disease-free survival (DFS), subgroup analyses within the ESCC and EAC subpopulations, evaluations of short-term outcomes, and sensitivity analyses involving literature published after the year 2000, has been presented in detail in our publication[193]. Due to the limited availability of

RCTs for EAC data extraction and the high heterogeneity observed in the comparison arms of NCRT versus surgery alone (I^2=80%, p<0.01) in the EAC subgroup, treatment recommendations specific to EAC were not formulated. Nevertheless, we strongly advocate the need for additional RCTs to explore different therapeutic strategies in EAC patients.

2. Generation and validation of EAC CAFs derived from primary tumor samples of EAC patients

CAFs are the key components within the tumor microenvironment and are involved in tumorigenesis and tumor progression in various types of cancers including EC[54,212,213]. CAFs have been identified as key players in conferring treatment resistance to EC cells[90,91]. Therefore, we established EAC CAFs from EAC primary patient tissues to investigate the crosstalk between CAFs and EAC cells. We aim to gain insights into the molecular mechanisms underlying CAF-mediated resistance to multiple treatments in EAC.

Table 6. Characteristics of the EAC patients for EAC CAFs included in this study.

	TBE60	TBE63	TBO1657	CAF2304	CAF2765
Age	50	57	57	81	70
Gender	Female	Male	Male	Male	Female
Sample source	Biopsy	Biopsy	Operation	Operation	Operation
Pathology	EAC	EAC	EAC	EAC	EAC
Treatment status at sample collection	Untreated	Untreated	After neoadjuvant treatment	Untreated	Untreated
Treatment strategy	CROSS+surgery	CROSS+surgery	FLOT+surgery	Surgery	Surgery
Neoadjuvant therapy response	Minor	Major	Minor	-	-
TNM stage	ypT3N2M0	ypT3N1M0	ypT4aN3M0	pT2N1M0	pT3N2M0

We took both biopsy samples from endoscopy and samples after the operation to generate EAC CAFs. More than 30 CAFs were established during my study period and five CAFs were used for quality evaluation in this study, with TBE63 and TBE60 derived from endoscopic biopsies, while TBO1657, CAF2304, and CAF2765 were obtained during surgical procedures. Of these, only TBO1657

had received neoadjuvant FLOT treatment before surgical resection, while the rest were untreated prior to surgery. The clinical information of EAC patients for EAC CAFs included in this study were summarized in Table 6.

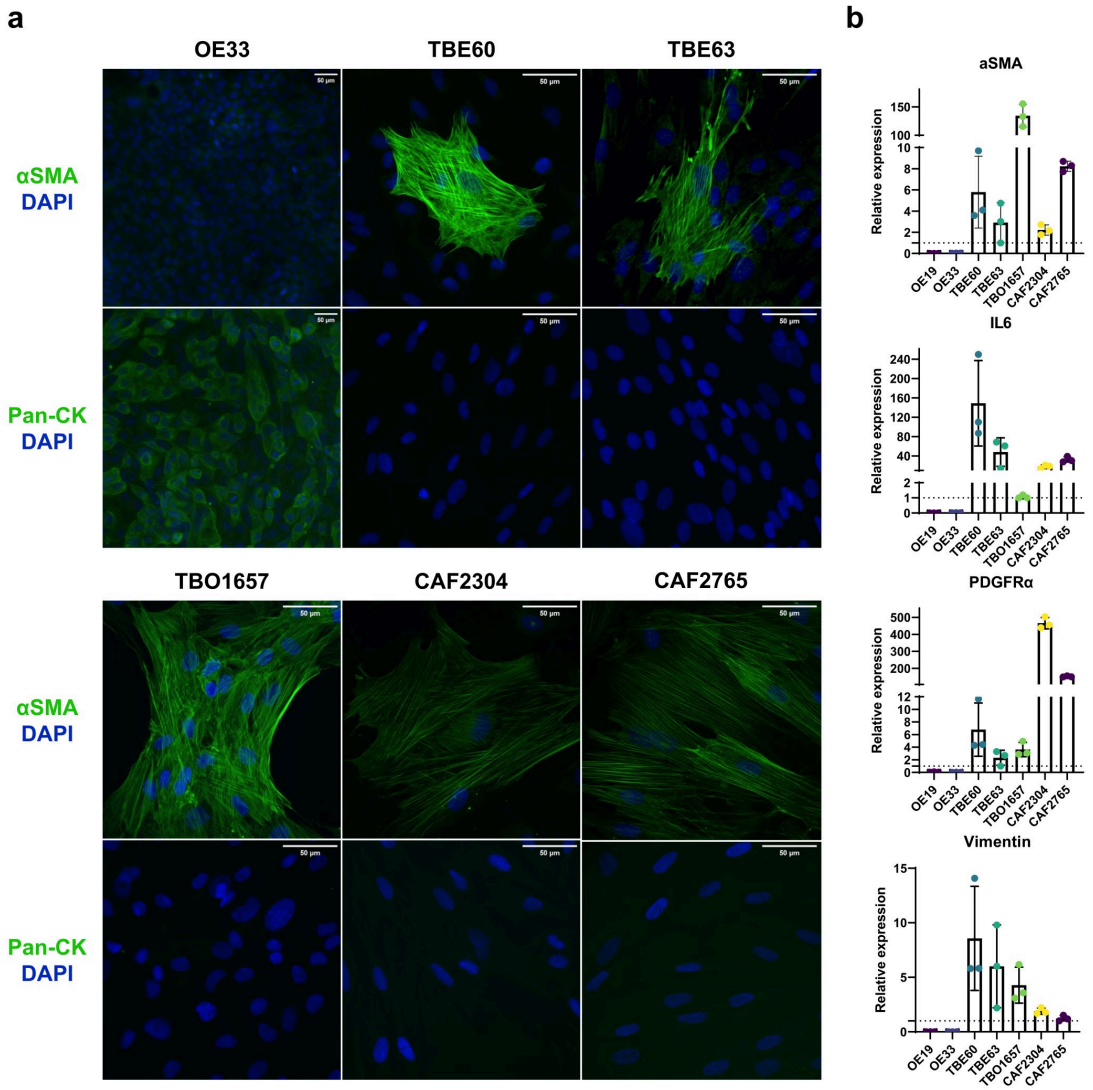

Figure 6. Validation of EAC CAFs.

a. The IF staining of epithelial marker Pan-CK, fibroblast marker αSMA, and DAPI in EAC cell line OE33 and different EAC CAFs TBE60, TBE63, TBO1657, CAF2304, and CAF2765. OE33 is positively expressed of Pan-CK but negatively expressed of αSMA, while all the CAFs are positively expressed of αSMA but not Pan-CK. Scale bar: 50μm.

b. Relative mRNA expression of fibroblast markers αSMA, IL-6, PDGFRα and Vimentin in EAC cell lines OE19 and OE33 and EAC CAFs TBE60, TBE63, TBO1657, CAF2304 and CAF2765. Data are represented as mean ± SD.

We validated EAC CAFs using fibroblast-related markers αSMA, IL-6, PDGFRα, and vimentin as well as epithelial marker Pan-CK. The IF staining showed that

all five CAFs were αSMA positive but Pan-CK negative whereas EAC tumor cell line OE33 served as a control that was positively expressed of Pan-CK but negatively expressed of αSMA (Figure 6a). Besides, we compared the mRNA expression levels of fibroblast-related markers in our CAFs and EAC tumor cell lines OE33 and OE19, and the results showed that αSMA, IL-6, PDGFRα, and vimentin were expressed diversely in CAF cell lines but not expressed in OE33 and OE19 (Figure 6b).

Taken together, we successfully established EAC CAFs from different EAC patients. The distinct expression profiles indicated a notable heterogeneity among EAC CAFs.

3. EAC CAFs promote EAC cell proliferation and treatment resistance *in vitro*

3.1. EAC CAFs promote EAC cell proliferation *in vitro*

To explore the interaction between EAC cells and EAC CAFs in tumor microenvironments *in vitro*, a transwell co-culture set-up was used (Figure 7a). CAFs were seeded into the 6-well plate whereas EAC cells were seeded on the 0.4μm pore size transwell insert to create a physical barrier between the two cell types. Following a seven-day co-culture period, EAC cells were collected and subsequently subjected to functional analyses.

EAC cells OE33 and OE19 showed enhanced cell proliferation ability as compared to the control after co-cultured with two different EAC CAFs (TBE60 and TBE63) in the shared medium for seven days (Figure 7b). The mean relative cell proliferation on day 6 compared to day 0 exhibited values of 28.90 ± 4.23 for OE33, 43.47 ± 8.84 for OE33 co-cultured with TBE63, and 47.59 ± 0.41 for OE33 co-cultured with TEB60. Similarly, the mean relative cell proliferation on day 6 compared to day 0 recorded values of 11.64 ± 2.03 for OE19, 33.12 ± 8.92 for OE19 co-cultured with TBE63 and 21.50 ± 3.56 for OE19 co-cultured with TEB60.

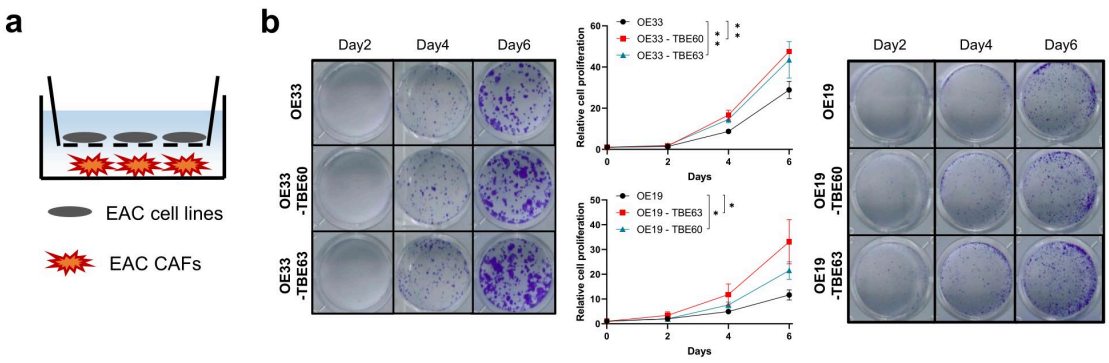

Figure 7. EAC CAFs promote EAC cell proliferation *in vitro*.

a. Transwell co-culture setup of co-culturing EAC cell lines with EAC CAFs.

b. Cell proliferation assay shows that both EAC CAFs TBE60 and TBE63 promote OE33 and OE19 cells cell proliferation *in vitro*. Data are represented as mean ± SD. Paired t-test, **p*<0.05, ***p*<0.01.

3.2. ECA CAFs promote EAC chemoresistance *in vitro*

Cisplatin and Oxaliplatin are two key chemotherapeutic drugs that are wildly used to treat esophageal cancer patients. Using the same transwell co-culture setup, we found that OE33 and OE19 were more resistant to cisplatin and oxaliplatin treatment *in vitro* after co-culture with TBE60 and TBE63 for seven days (Figure 8a, 8b). The IC50 values after 48 hours of cisplatin treatment were as follows: 1.9μM for OE33, 2.4μM for OE33 after co-culture with TBE63, 3.1μM for OE33 after co-culture with TBE60, 11.3μM for OE19, 22.7μM for OE19 after co-culture with TBE63, and 17.3μM for OE19 after co-culture with TBE60. Similarly, oxaliplatin treatment resulted in IC50 values of 8.1μM for OE33, 14.0μM for OE33 after co-culture with TBE63, 14.2μM for OE33 after co-culture with TBE60, 39.3μM for OE19, 54.1μM for OE19 after co-culture with TBE63, and 63.4μM for OE19 after co-culture with TBE60.

We further validated enhanced EAC cell chemoresistance using apoptosis assay. Consistently, OE33 and OE19 showed significantly lower percentages of apoptotic cell populations after co-culture with EAC CAFs when exposed to cisplatin treatment (3μM and 30μM, respectively) for 48 hours (Figure 8c, 8d). The average apoptotic cell percentages were as follows: 56.57% ± 5.09% for OE33, 46.46% ± 2.26% for OE33 co-cultured with TBE63, and 26.69% ± 1.34%

for OE33 co-cultured with TEB60, following 48 hours of 3μM cisplatin treatment. Similarly, after 48 hours of 30μM cisplatin treatment, the mean apoptotic cell percentages were 16.90% ± 0.21% for OE19, 13.78% ± 0.92% for OE19 co-cultured with TBE63, and 14.86% ± 0.69% for OE19 co-cultured with TEB60.

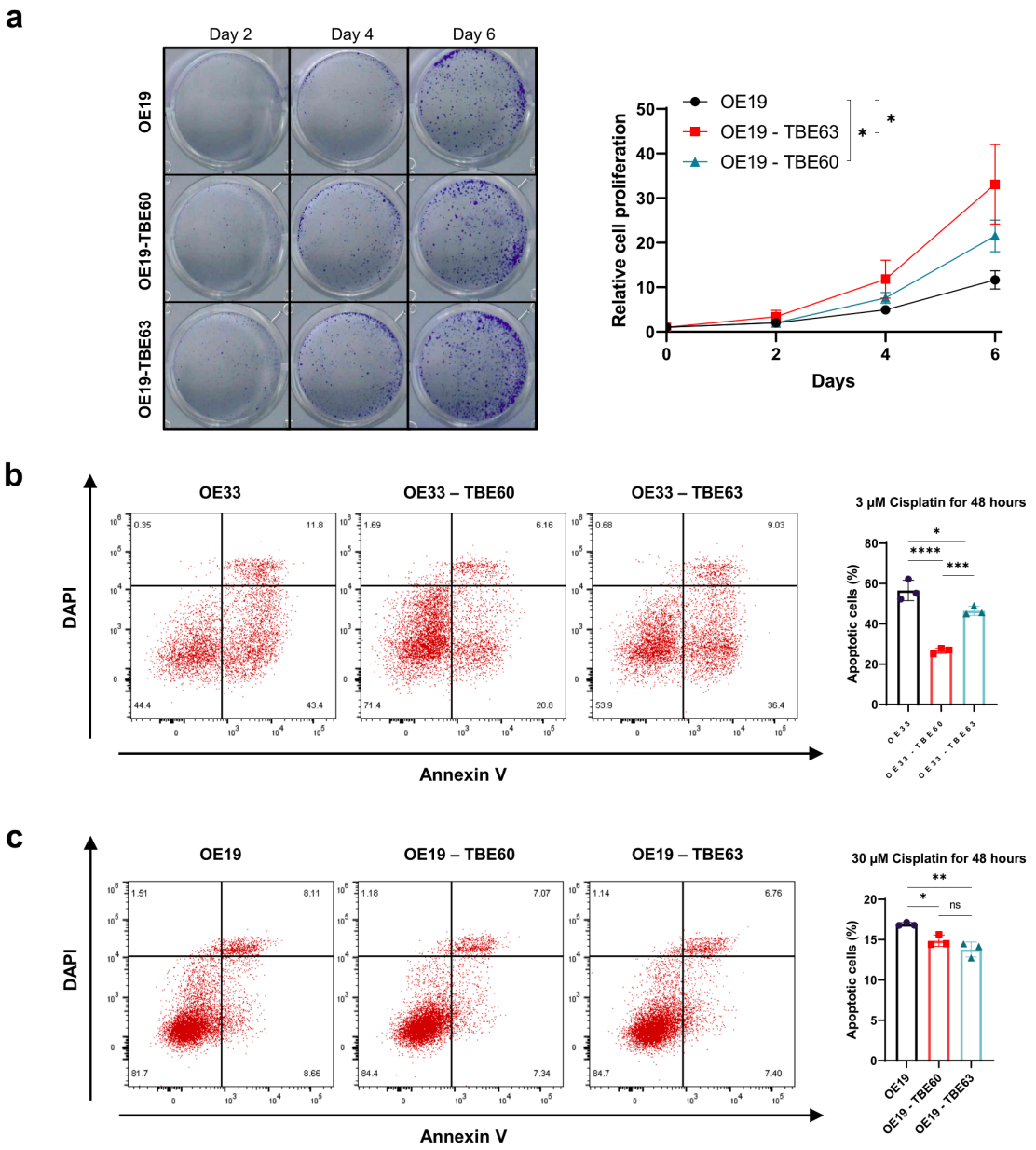

Figure 8. EAC CAFs promote EAC chemoresistance *in vitro*.

a. Cell viability assay shows that OE33 is more resistant to cisplatin and oxaliplatin treatment *in vitro* after co-culture with two different EAC CAFs TBE60 and TBE63. Data are represented as mean ± SD.

b. Cell viability assay shows that OE19 is more resistant to cisplatin and oxaliplatin treatment *in vitro* after co-culture with two different EAC CAFs TBE60 and TBE63. Data are represented as mean ± SD.

c. Apoptosis assay shows that after co-culture with two different EAC CAFs TBE60 and TBE63, OE33 has fewer apoptotic populations after 48 hours of 3μM cisplatin treatment *in vitro*. Data are represented as mean ± SD. Unpaired t-test, **p*<0.05, ****p*<0.001, *****p*<0.0001.

d. Apoptosis assay shows that after co-culture with two different EAC CAFs TBE60 and TBE63, OE19 has fewer apoptotic populations after 48 hours of 30μM cisplatin treatment *in vitro*. Data are represented as mean ± SD. Unpaired t-test, ns: *p*>0.05, **p*<0.05, ***p*<0.01.

3.3. EAC CAFs promote EAC radioresistance *in vitro*

To explore the radiotherapy sensitivity of OE33 and OE19 with and without co-culture with TBE60 and TBE63, cells were exposed to ionizing radiation *in vitro* and apoptosis analyses were performed 48 hours after the radiation. The results showed enhanced resistance to ionizing radiation of EAC cells after co-culture with EAC CAFs with significantly fewer apoptotic cell populations in the co-culture groups as compared to the control groups (Figure 9a, 9b).

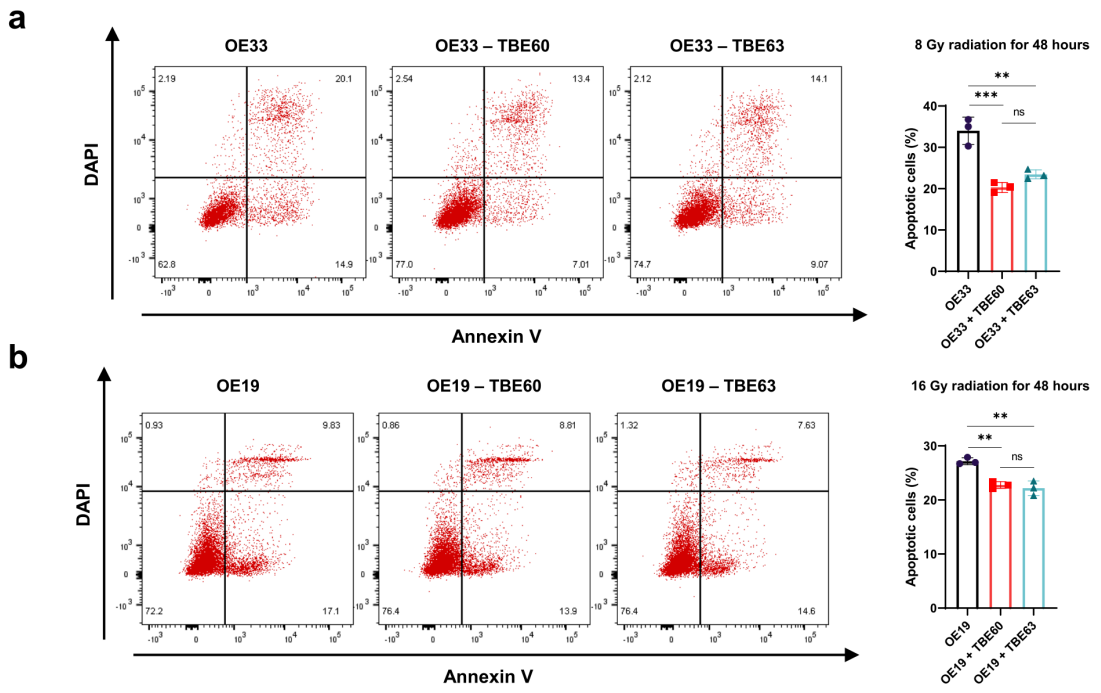

Figure 9. EAC CAFs promote EAC radiotherapy resistance *in vitro*.

a. Apoptosis assay shows that after co-culture with two different EAC CAFs TBE60 and TBE63, OE33 has fewer apoptotic populations 48 hours after exposure to 8Gy ionizing radiation *in vitro*. Data are represented as mean ± SD. Unpaired t-test, ns: *p*>0.05, ***p*<0.01, ****p*<0.001.

b. Apoptosis assay shows that after co-culture with two different EAC CAFs TBE60 and TBE63, OE19 has fewer apoptotic populations 48 hours after exposure to 16Gy

ionizing radiation *in vitro*. Data are represented as mean ± SD. Unpaired t-test, ns: $p>0.05$, $^{**}p<0.01$.

In OE33, 48 hours after exposure to 8 Gy ionizing radiation, the average apoptotic cell percentages were as follows: 34.00% ± 3.32% for OE33, 23.46% ± 1.09% for OE33 co-cultured with TBE63, and 20.31% ± 1.21% for OE33 co-cultured with TEB60. Similarly, 48 hours after exposure to 16 Gy ionizing radiation in OE19, the mean apoptotic cell percentages were 27.17% ± 0.63% for OE19, 22.18% ± 1.34% for OE19 co-cultured with TBE63, and 22.76% ± 0.62% for OE19 co-cultured with TEB60.

In summary, these data suggest that EAC CAFs promote EAC cell proliferation and treatment resistance *in vitro*.

4. GDF15 is involved in the crosstalk between EAC cells and EAC CAFs, and higher expression of GDF15 predicts poor prognosis of EAC patients

4.1. Transcriptomic analysis identifies GDF15 as a potential functional factor in the tumor-stroma interaction

To further understand the potential molecular mechanism of the crosstalk between EAC cells and EAC CAFs, we performed a transcriptomic analysis of the co-culture setup.

OE33 were co-cultured with TBE60 and TBE63 for seven days, and both cells with and without co-culture were subjected to high-throughput RNA sequencing (Figure 10a). Transcriptomic analysis identified several dysregulated genes, among which GDF15 stood out due to its opposite expression pattern in OE33 and two CAF cell lines after co-culture. GDF15 was upregulated in CAFs but downregulated in OE33, suggesting a possible dynamic interaction between CAFs and tumor cells (Figure 10b). We further analyzed GDF15 expression at the single-cell level in four EAC patients from our hospital. The results showed

that GDF15 was highly expressed in both CAFs and EAC tumor cells, highlighting its potential role in the CAF-mediated tumor microenvironment (Figure 10c).

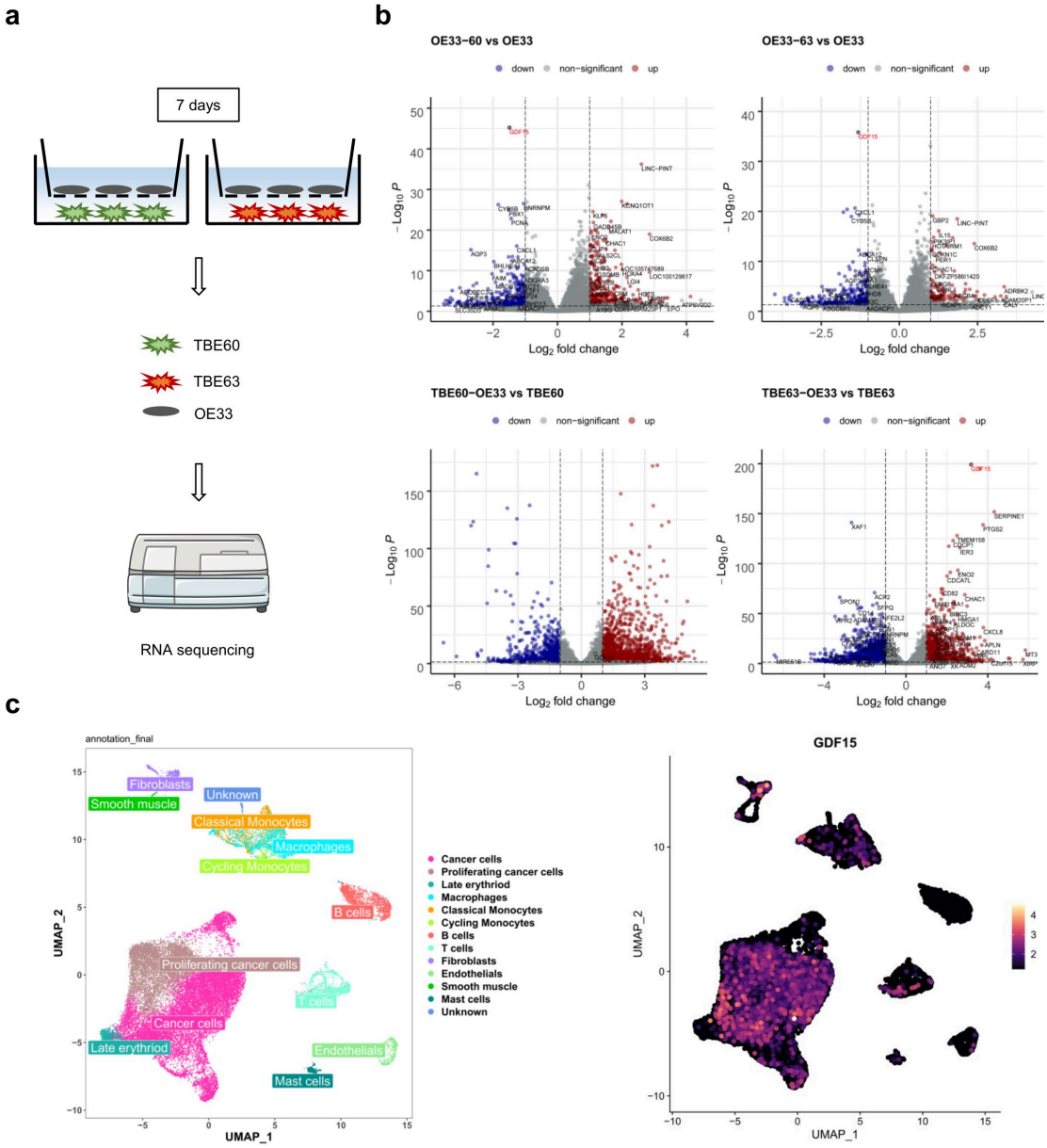

Figure 10. GDF15 is involved in the crosstalk between EAC cells and EAC CAFs.

a. The workflow for RNA sequencing of transwell co-cultured cells.

b. Volcano plots showing dysregulated genes in OE33, TBE60, and TBE63 after the seven days of transwell co-culture. The plots display the log2 fold change (x-axis) versus the -log10 adjusted *p*-value (y-axis) for each gene. Genes upregulated and downregulated are denoted in red and blue, respectively, while non-significant genes are represented in gray. The dashed lines represent the thresholds for statistical significance. The plot highlights several dysregulated genes, including GDF15, with an

opposite expression pattern in OE33 cells and CAFs.

c. UMAP plots depicting the major cell types identified by single-cell RNA sequencing of tissues from four EAC patients. GDF15 is highly expressed in both cancer cells and fibroblasts.

4.2. Clinical relevance of GDF15 expression in EAC patients

Next, we explored the clinical significance of GDF15 in patients with esophageal cancer using publicly available databases. Analysis of the GSE26886 database showed that GDF15 expressions were significantly higher in EAC tissues as compared to ESCC, Barrett's esophagus, and squamous epithelium (Figure 11a). Similarly, analysis of the TCGA database revealed the higher expression levels of GDF15 in EAC patients compared to ESCC patients (Figure 11b). Besides, we examined GDF15 expressions in individual patient samples. We found that GDF15 expressions were significantly higher in EAC tumor tissues than in adjacent normal tissues in the GSE92396 database (Figure 11c). Similar results were obtained from our in-house analysis of 25 paired EAC tumor and normal tissues at the University Hospital of Cologne (Figure 11d).

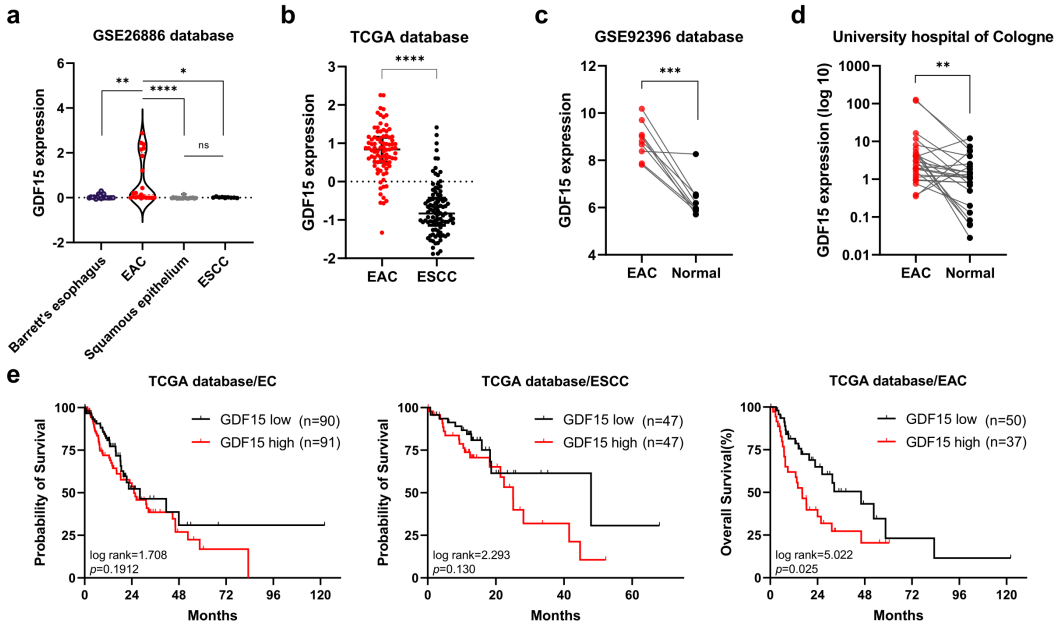

Figure 11. Clinical significance of GDF15 in esophageal cancer.

a. GDF15 expression is significantly higher in EAC tissues as compared to ESCC, Barrett's esophagus, and squamous epithelium in the GSE26886 database. Unpaired

t-test, ns: $p>0.05$, *$p<0.05$, **$p<0.01$, ****$p<0.0001$.

b. GDF15 expression is significantly higher in EAC patients as compared to ESCC patients in the TCGA database. Unpaired t-test, ****$p<0.0001$.
c. GDF15 expression is significantly higher in EAC tumor tissues as compared to adjacent normal tissues in the GSE92396 database. Paired t-test, ***$p<0.001$.
d. GDF15 expression is significantly higher in EAC tumor tissues as compared to adjacent normal tissues in 25 paired EAC tumor and normal tissues from the University Hospital of Cologne. Paired t-test, **$p<0.01$.
e. High levels of GDF15 expression are associated with a trend towards poor prognosis in both EC patients and the ESCC subpopulation from the TCGA database, but without statistical significance (Log rank=1.708, $p=0.1912$ for EC patients, and log rank=2.293, $p=0.130$ for ESCC subpopulation). High levels of GDF15 expression are significantly associated with reduced overall survival in EAC patients from the TCGA database (Log rank=5.022, $p=0.025$).

We further investigated the association of GDF15 expression with the prognosis of EC patients using the TCGA database. As shown in Figure 11e, high levels of GDF15 expression were observed to be associated with a trend towards poor prognosis in both EC patients and the ESCC subpopulation but without statistical significance (Log rank=1.708, $p=0.1912$, and log rank=2.293, $p=0.130$, respectively). In the EAC subpopulation, high levels of GDF15 expression were significantly associated with reduced overall survival (Log rank=5.022, $p=0.025$), suggesting a potential role for GDF15 as a prognostic biomarker in EAC.

In summary, we identified GDF15 from *in vitro* EAC tumor-stroma crosstalk using transcriptomic analysis, which showed the opposite expression patterns between EAC cells and EAC CAFs after the transwell co-culture. We further addressed the clinical significance of GDF15 in EAC patients.

5. GDF15 depletion in EAC tumor cells reduces treatment resistance *in vitro*

To understand the role of GDF15 in the interaction of EAC and CAFs, we first examined the GDF15 concentration in our transwell co-culture system. In a total of 3ml culture medium system, the supernatants were collected 48 hours after

the co-culture for GDF15 detection. GDF15 concentrations were significantly higher in OE19-TBE60 (514.76 ± 64.38 pg/ml, p=0.0004) and OE19-TBE63 (1063.04 ± 41.19 pg/ml, p<0.0001) co-cultured supernatants when compared with control (75.22 ± 21.17 pg/ml). Similarly, GDF15 concentrations were significantly higher in OE33-TBE60 (1395.37 ± 126.68 pg/ml, p=0.0011) and OE33-TBE63 (2265.35 ± 187.86 pg/ml, p=0.0002) as compared to control (766.63 ± 24.00 pg/ml) (Figure 12a).

We then knocked down GDF15 in OE19 and OE33 cells using the short hairpin RNA system (Figure 12b). There were no significant differences regarding cell proliferation ability after GDF15 depletion in both OE33 and OE19 cells (Figure 12c). However, GDF15 depletion showed increased sensitivity towards cisplatin and oxaliplatin treatment in both OE33 and OE19 cells (Figure 12d). The IC50 values for cisplatin treatment decreased from 34.9μM to 23.3μM in OE19 and from 2.2μM to 1.5μM in OE33 following GDF15 knockdown. The IC50 values for oxaliplatin treatment decreased from 31.2μM to 14.4μM in OE19 and from 8.9μM to 6.1μM in OE33 after GDF15 knockdown. Similarly, OE19 and OE33 sh-GDF15 groups showed significantly higher percentages of apoptotic cell populations when exposed to cisplatin treatment (30μM and 3μM, respectively) for 48 hours, indicating a decreased treatment resistance to chemotherapy (Figure 12e). The populations of apoptotic cells exhibited an increase from 25.33% ± 0.68% to 30.97% ± 2.27% in OE19 and from 18.69% ± 1.66% to 30.40% ± 2.50% in OE33 upon GDF15 knockdown.

Moreover, depletion of GDF15 resulted in increased sensitivity to ionizing radiation *in vitro*, as evidenced by significantly higher apoptotic cell populations 48 hours post-radiation compared with sh-NT groups (Figure 12f). The populations of apoptotic cells increased from 26.59% ± 2.70% to 38.43% ± 2.27% in OE19 cells following exposure to 16 Gy ionizing radiation, and from 22.58% ± 6.11% to 33.90% ± 3.27% in OE33 cells after exposure to 8 Gy ionizing radiation upon GDF15 knockdown.

Taken together, GDF15 depletion resulted in reduced treatment resistance in EAC tumor cells.

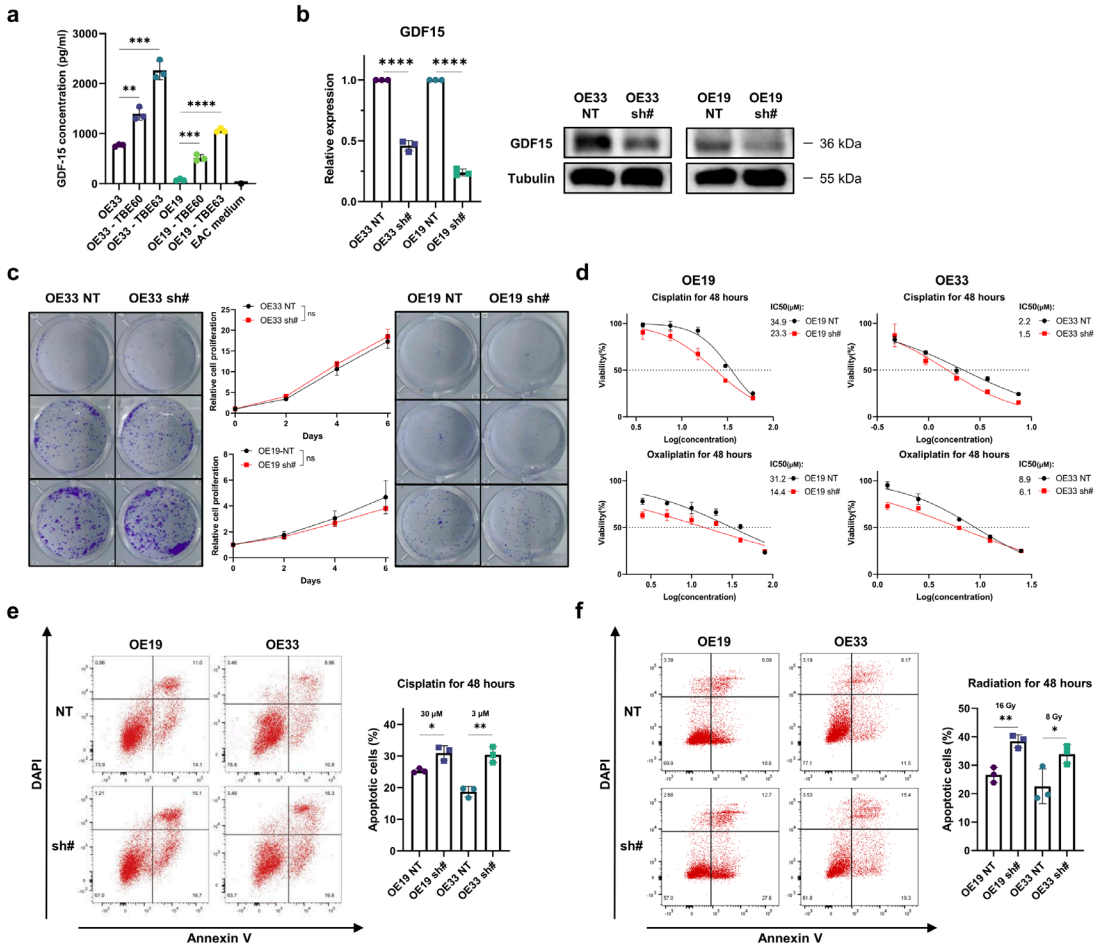

Figure 12. GDF15 depletion results in reduced treatment resistance in EAC cells.

a. GDF15 concentrations are significantly higher in the co-culture medium in both OE33 and OE19 cells. Data are represented as mean ± SD. Unpaired t-test, **p<0.01, ***p<0.001, ****p<0.0001.

b. Validation of GDF15 knockdown (sh#) and control (NT) tumor cells in qPCR and western blot. Relative expressions of GDF15 in knockdown and control cells are presented in three different passages using control as the baseline. Unpaired t-test, ****p<0.0001.

c. Cell proliferation assay shows no proliferation difference after GDF15 knockdown in both OE33 and OE19 cells. Data are represented as mean ± SD. Paired t-test, ns: p>0.05.

d. Cell viability assay shows increased sensitivity to cisplatin and oxaliplatin treatment after GDF15 knockdown in OE33 and OE19 cells. Data are represented as mean ± SD.

e. Apoptosis assay shows increased apoptotic populations in OE19 and OE33 GDF15 knockdown cells after 48 hours of cisplatin treatment (30μM and 3μM, respectively). Data are represented as mean ± SD. Unpaired t-test, *p<0.05, **p<0.01.

f. Apoptosis assay shows increased apoptotic populations in OE19 and OE33 GDF15 knockdown cells 48 hours after exposure to ionizing radiation (16 Gy and 8 Gy, respectively). Data are represented as mean ± SD. Unpaired t-test, *p<0.05, **p<0.01.

6. GDF15 depletion in EAC CAFs restores CAF-mediated EAC treatment resistance *in vitro*

To explore the function of GDF15 in CAF-mediated treatment resistance, we established a stable GDF15 knockdown CAF cell line TBE63 (Figure 13a).

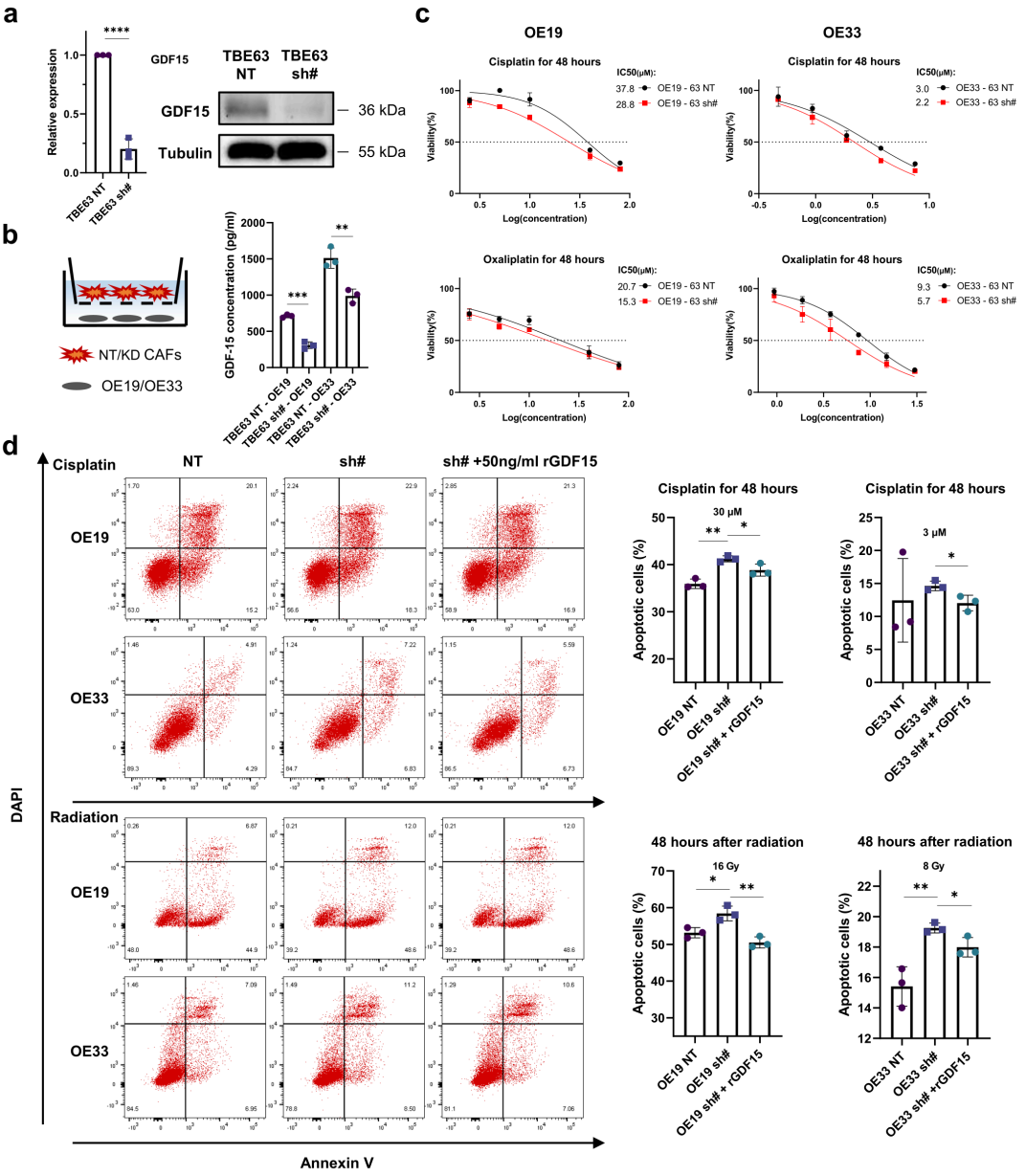

Figure 13. GDF15 depletion results in reduced EAC CAF-mediated treatment resistance in the tumor microenvironment.

a. Validation of GDF15 knockdown and control CAF cell TBE63 in qPCR and western blot. Relative expressions of GDF15 in knockdown and control cells are presented in three different passages using control as the baseline. Unpaired t-test, ****p<0.0001.
b. Transwell co-culture setup of co-culturing EAC cell lines with GDF15-depleted/control TBE63 cells. GDF15 concentrations are significantly decreased in OE19/OE33-TBE63 GDF15 knockdown co-culture medium. Data are represented as mean ± SD. Unpaired t-test, **p<0.01, ***p<0.001.
c. Cell viability assay shows increased sensitivities to cisplatin and oxaliplatin treatment in OE33 and OE19 cells after co-culture with GDF15-depleted TBE63. Data are represented as mean ± SD.
d. Rescue assays show that adding human rGDF15 in GDF15 depletion cells further restores the cell resistance to chemotherapy and ionizing radiation that has been reduced by GDF15 knockdown in OE19 and OE33 cells. The apoptosis assay is performed to determine cell sensitivity by calculating the apoptotic cell populations after the treatment. Data are represented as mean ± SD. Unpaired t-test, *p<0.05, **p<0.01.

We transwell co-cultured both OE19 and OE33 with TBE63 GDF15 depletion cells and control cells (Figure 13b). As expected, GDF15 concentrations were significantly decreased in the OE19-TBE63 sh-GDF15 co-culture medium (308.62 ± 46.88 pg/ml, p=0.0002) and OE33-TBE63 sh-GDF15 co-culture medium (989.68 ± 94.34 pg/ml, p=0.0059) as compared to OE19/OE33-TBE63 sh-NT groups (711.68 ± 21.30 pg/ml and 1512.12 ± 140.97 pg/ml, respectively) (Figure 13b). In addition, we observed increased chemotherapy sensitivities in OE19 and OE33 cells after co-cultured with GDF15-depleted TBE63, as shown by decreased cell viabilities for cisplatin and oxaliplatin treatment when compared with control (Figure 13c). Furthermore, we performed the rescue assays by adding 50 ng/ml human rGDF15 in GDF15-depleted EAC cell culture medium and continuously cultured them for seven days. The results revealed that adding rGDF15 further restored the cell resistance to chemotherapy and ionizing radiation that had been reduced by GDF15 knockdown in both OE19 and OE33 cells (Figure 13d).

Taken together, GDF15 depletion resulted in reduced EAC CAF-mediated treatment resistance in the tumor microenvironment.

7. Generation and validation of patient-derived tumor organoids from EAC primary tissue[198] (Published one part of this result as the first author)

Patient-derived tumor organoids have emerged as a promising preclinical model that represents key histopathological, genetic, and phenotypic features of the parent tumor *in vitro*[138,139]. To date, there are limited studies using the PDO model to study esophageal cancer. Here, we established EAC PDOs for my doctoral research and we are proud to be one of the first groups in Germany to utilize EAC organoids in translational research[198].

The workflow for establishing EAC PDOs can be found in Figure 14a. Briefly, following surgical resection, tumor tissues from EAC patients were minced and subjected to enzymatic dissociation to obtain single cells. These single cells were then seeded into ECM gel domes and cultured in a specialized EAC PDO medium containing Wnt-3A, R-Spondin1, and human EGF to support tumor cell growth in a 3D dimension. One typical example of organoids formation from single cells was illustrated in Figure 14b.

We further validated EAC PDOs by comparing the morphology and pathological features with paired tissues using Hematoxylin-eosin (H&E) staining and IHC staining. EAC PDOs shared similar expression patterns of epithelial marker Pan-CK and cell proliferation marker Ki67 with paired tissues. We included αSMA, a fibroblast marker, as a negative control showing positive expression in paired tissues but not in PDOs, indicating the absence of contaminating fibroblasts in our tumor organoids (Figure 14c).

Efficient propagation of the EAC PDOs is crucial for subsequent experimental applications. We found that EAC PDOs can be subcultured and cryopreserved with and without single-cell digestion. As shown in Figure 14d, EAC PDOs could be subcultured effectively either with or without single-cell digestion when they reached confluency. Here, as a part of my doctoral research, we introduced a visual protocol to standardize routine maintenance and propagation of EAC PDOs, providing a guide for researchers to choose appropriate methods based

on their specific research interests[198].

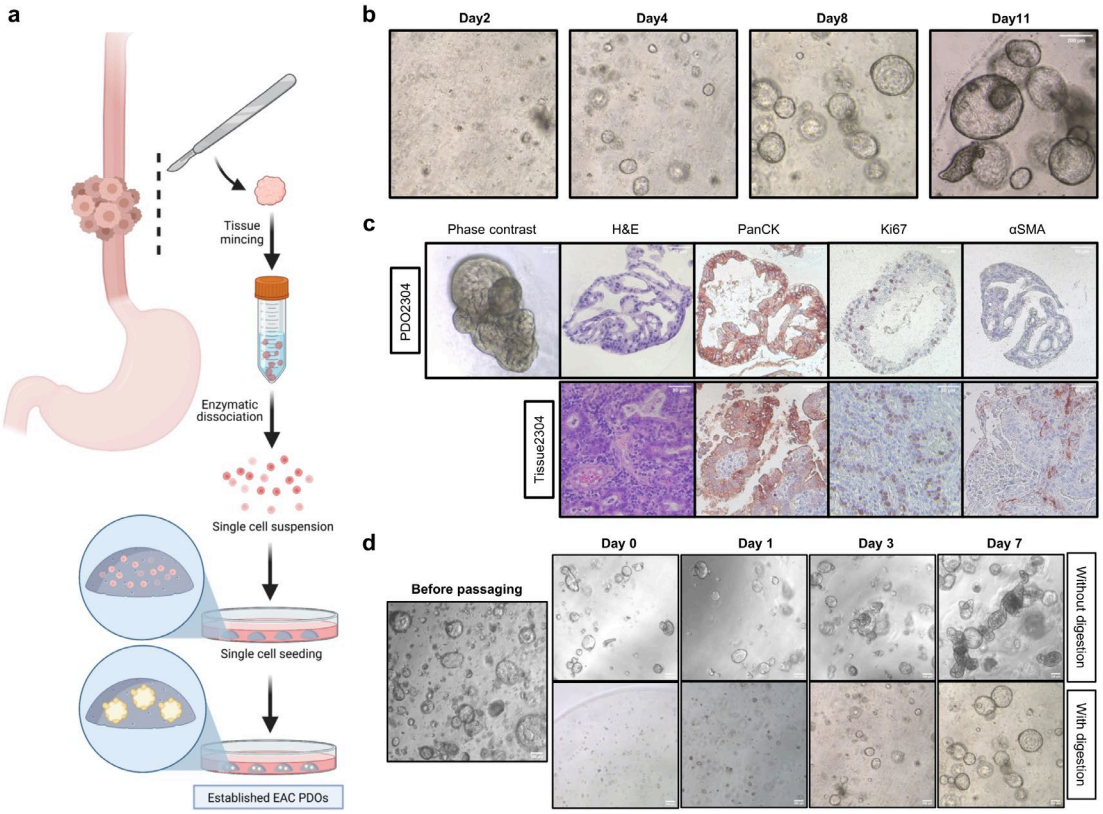

Figure 14. Generation and validation of EAC patient-derived tumor organoids.

a. A workflow of establishing EAC PDOs from EAC patient primary tissues.
b. The phase-contrast images demonstrate the process of EAC organoids formation from single cells over the days. Scale bar: 200μm.
c. Histological comparison of EAC PDOs and paired patient tissues. The figure includes a phase-contrast image of compact PDOs, as well as H&E staining and IHC staining for the epithelial maker Pan-CK, cell proliferation marker Ki67, and fibroblast marker αSMA in both PDOs and tissues. Scale bar: 50μm.
d. The phase-contrast images demonstrate morphological characteristics of EAC PDOs subculture with and without single-cell digestion over the days. It demonstrates that EAC PDOs can be subcultured effectively either with or without single-cell digestion when they reach confluency. Scale bar: 100μm[198].

8. The 3D organoids model confirms the enhanced EAC PDO treatment resistance through paired EAC CAFs co-culture and rGDF15 supplement

To study the tumor-stroma interactions using the EAC PDO model, we have

established EAC PDOs with paired CAFs from the same patient's tissue and performed a dome co-culture system as well as a transwell co-culture system (Figure 15).

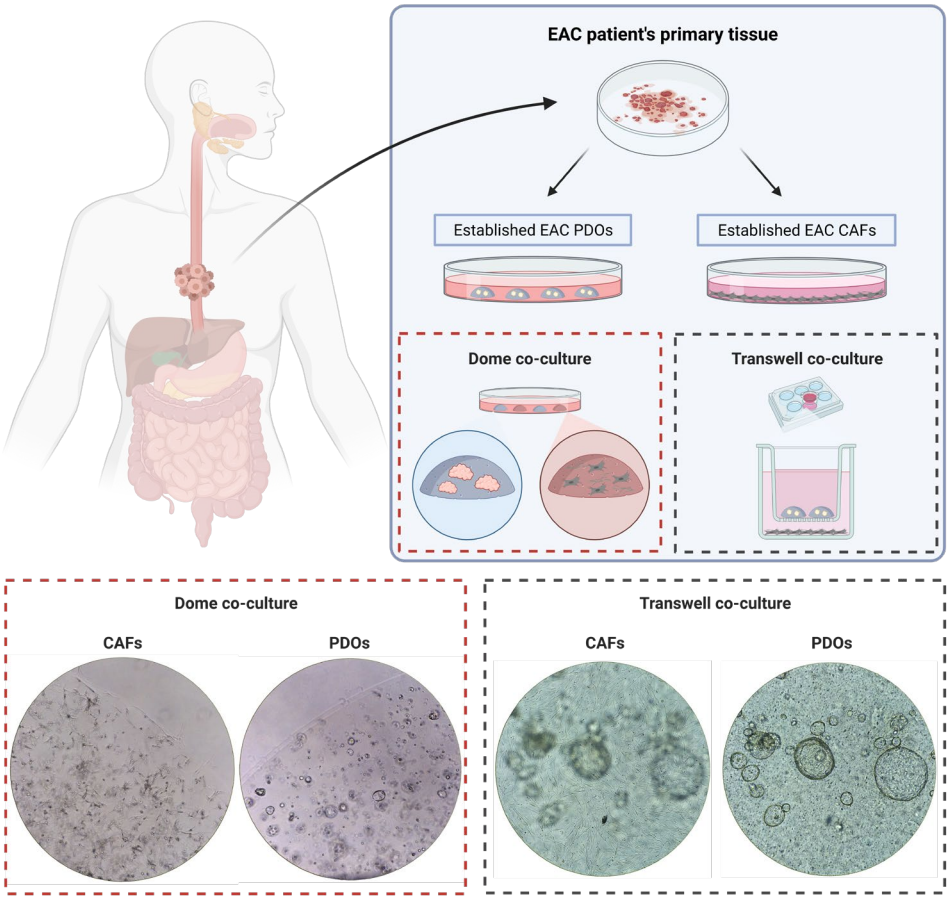

Figure 15. A workflow of establishing EAC PDOs and EAC CAFs from the same patient's tissue for dome-based co-culture and transwell-based co-culture.

In the dome co-culture system, paired EAC CAFs were seeded into separate ECM gel domes within the same plate and grown in the same culture medium as EAC PDOs, which allowed EAC PDOs to be harvested without contamination by CAFs, enabling further experiments to study the organoids. In the transwell co-culture system, following the approach used in 2D cell co-culture, CAFs were seeded on the bottom of the plate, while EAC PDOs were embedded in ECM gels and cultured on the 0.4μm pore size transwell insert. Example images captured under a phase contrast microscope of these two co-

culture systems were shown in Figure 15.

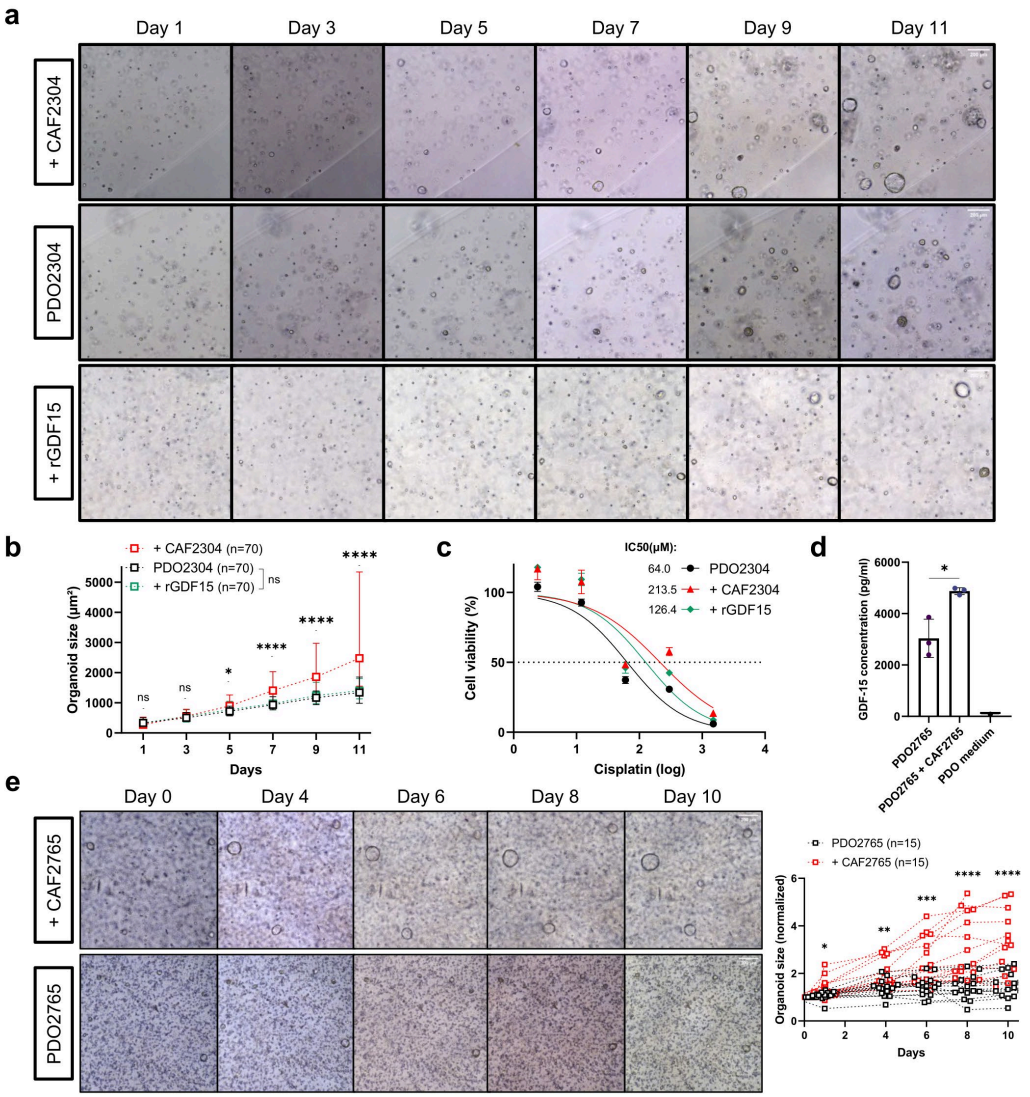

Figure 16. The 3D organoids model confirms the enhanced EAC PDO treatment resistance through paired EAC CAFs co-culture and rGDF15 supplement.

a. Growth kinetics of EAC PDOs with and without dome-based co-culture of paired CAFs and with human rGDF15 protein supplement. PDO sizes are tracked under an ECHO Rebel microscope, and the corresponding areas of PDOs are measured and digitized using ECHO pro (v6.4.1) software. Scale bar: 200μm.

b. Growth kinetics of EAC PDOs with and without dome-based co-culture of paired CAFs and with human rGDF15 protein supplement. The sizes of 70 individual PDOs from each group are measured, revealing a time-dependent increase that is significantly higher in the co-culture group than in the control group. There is no significant difference in size between the rGDF15 and control groups. Data are represented as mean ± SD. Paired t-test, ns: $p>0.05$, *$p<0.05$, ****$p<0.0001$.

c. Cell viability assay reveals that co-culturing EAC PDOs with paired CAFs or culturing

EAC PDOs in the human rGDF15 protein supplement organoids medium results in decreased sensitivity to cisplatin treatment, as compared to the control group.

d. GDF15 concentrations are significantly higher in the co-culture medium as compared to the control medium in the transwell co-culture system of EAC PDOs and paired CAFs. Data are represented as mean ± SD. Unpaired t-test, *p<0.05.
e. Growth kinetics of EAC PDOs with and without the transwell co-culture of paired CAFs. PDO sizes are tracked under an ECHO Rebel microscope, and the corresponding areas of PDOs are measured and digitized using ECHO pro (v6.4.1) software. The sizes of 15 individual PDOs from each group are measured, revealing a time-dependent increase that is significantly higher in the co-culture group than in the control group. Scale bar: 200μm. Data are represented individually. Paired t-test, *p<0.05, **p<0.01, ***p<0.001, ****p<0.0001.

In line with the 2D culture results, paired CAFs promoted EAC PDO cell proliferation in both dome coculture system (Figure 16a, 16b) and transwell co-culture system (Figure 16e). For dome-based coculture, 70 organoids from each co-culture group and control group were measured by size and individually tracked for 11 days. For transwell co-culture, due to the limited space in the transwell chamber, only 15 organoids from each group were monitored. In addition, EAC PDOs showed enhanced cisplatin resistance after being co-cultured with paired CAFs for two weeks in the dome coculture system (Figure 16c). We did not perform the drug sensitivity assay in the transwell co-culture system due to the limited number of PDO cells harvested from the chamber.

We further tested the GDF15 concentration in the transwell co-culture system. The supernatants were collected 72 hours after the co-culture in a total of 4 ml culture medium. Consistently, GDF15 concentrations were significantly higher in the co-culture medium as compared to control (4876.38 ± 133.50 pg/ml vs. 3035.36 ± 747.91 pg/ml, p=0.0137) (Figure 16d). However, the addition of human rGDF15 protein to the PDO culture medium did not enhance PDO cell proliferation (Figure 16a, 16b). As to treatment resistance, PDOs after two weeks of culturing in the medium with rGDF15 supplement showed enhanced cisplatin resistance compared to control (Figure 16c).

Collectively, the 3D PDO model validated the findings from 2D cell line

experiments that EAC CAFs promote EAC cell treatment resistance with the involvement of GDF15 as one of the contributing factors.

9. GDF15 depletion results in impaired mitochondrial function in EAC cells

To explore the molecular mechanisms underlying the effects of GDF15 on EAC cells, we utilized proteomics analysis to investigate the impact of GDF15 knockdown on the EAC cell proteome. Cells from OE33 sh-NT, OE33 sh-GDF15, and OE33 sh-GDF15 with 50 ng/ml rGDF15 treatment for seven days were collected for proteomics analysis.

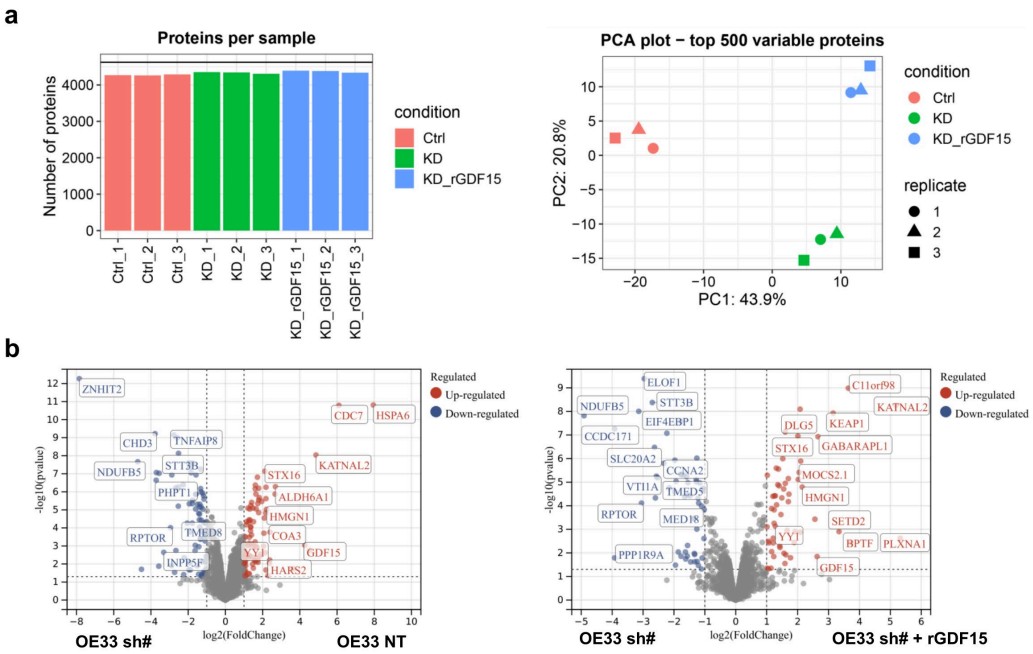

Figure 17. Proteomics analysis of OE33 cells with GDF15 depletion.

a. The quality control of protein omics data. Numbers of proteins of each group with three biological replicants are shown on the left panel and principal component analysis (PCA) is shown on the right panel. More than 4000 proteins are identified in each sample and distinct protein expression profiles are achieved among the experimental groups.

b. Volcano plots showing dysregulated proteins in OE33 sh-NT, OE33 sh-GDF15, and OE33 sh-GDF15 plus 50ng/ml rGDF15 treatment for seven days. The plots display the log2 fold change (x-axis) versus the -log10 *p*-value (y-axis) for each protein. Proteins upregulated and downregulated are denoted in red and blue, respectively, while non-

significant genes are represented in gray. The dashed lines represent the thresholds for statistical significance.

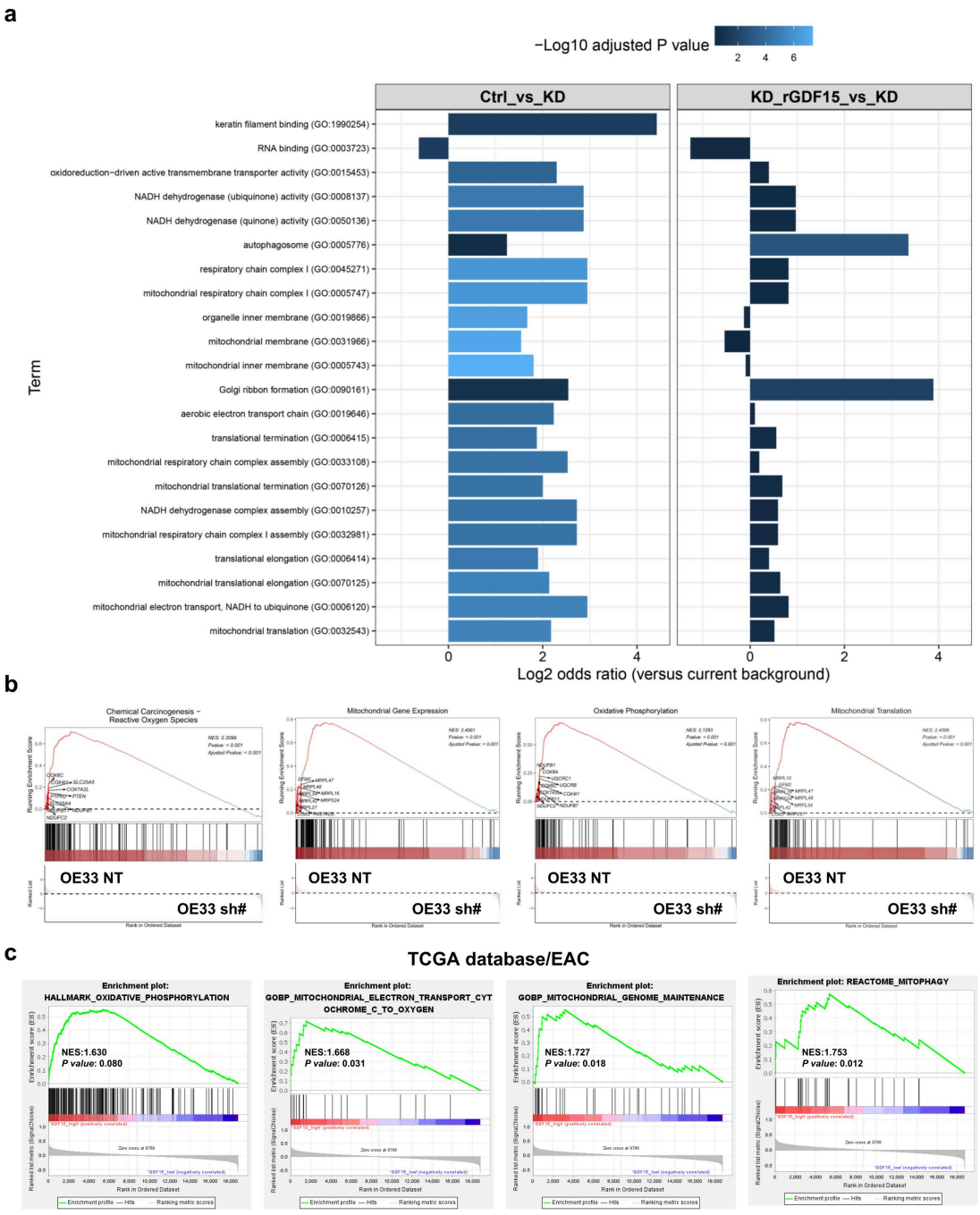

Figure 18. Pathway enrichment analysis links GDF15 to mitochondrial function in EAC cells.

a. Gene Ontology (GO) analysis results of differentially expressed proteins in the OE33 sh-NT group and the OE33 sh-GDF15 + rGDF15 group as compared to the OE33 sh-GDF15 group. Each bar represents a specific pathway, with the length of the bar corresponding to the log2 (odds ratio) for the enrichment when compared with the OE33 sh-GDF15 group. The color of the bar indicates the degree of significance, with

lighter colors indicating higher significance. The most enriched categories in our comparison were related to mitochondrial metabolism, including mitochondrial respiratory chain complex, mitochondrial electron transport, and mitochondrial translation.

b. Gene Set Enrichment Analysis (GSEA) of differently expressed proteins in OE33 sh-NT and OE33 sh-GDF15 groups. The y-axis represents the enrichment score, and the x-axis represents the rank of the genes. The normalized enrichment score (NES) and the corresponding *p*-value are indicated in the upper right corner of the plot. Reactive oxygen species, oxidative phosphorylation, mitochondrial gene expression, and translation were significantly enriched in the OE33 sh-NT group.
c. Gene Set Enrichment Analysis (GSEA) of differently expressed proteins in GDF15 high expression group and GDF15 low expression group in EAC patients from the TCGA database. The y-axis represents the enrichment score, and the x-axis represents the rank of the genes. The NES and the corresponding *p*-value are indicated. Mitochondrial function and mitochondrial homeostasis related pathways are enriched in GDF15 high expression group.

The sample quality control showed that more than 4000 proteins were detected in each measured sample and distinct protein expression profiles were achieved among the experimental groups (Figure 17a). A total of 865 significant differentially expressed proteins were identified in the OE33 sh-GDF15 group as compared to control where 46 proteins showed a fold change greater than two. Additionally, treatment with rGDF15 significantly enriched 459 proteins in OE33 sh-GDF15 cells, of which 31 proteins exhibited a fold change greater than two (Figure 17b).

The Gene Ontology (GO) analysis of differentially enriched proteins in the OE33 sh-NT group and the OE33 sh-GDF15 + rGDF15 group as compared to the OE33 sh-GDF15 group revealed a strong association with mitochondrial metabolism, including mitochondrial respiratory chain complex, mitochondrial electron transport, and mitochondrial translation (Figure 18a). Consistently, Gene Set Enrichment Analysis (GSEA) significantly enriched mitochondrial metabolism-related pathways in the OE33 sh-NT group, including reactive oxygen species, oxidative phosphorylation, mitochondrial gene expression, and translation (Figure 18b). Furthermore, we utilized the TCGA database for external validation and conducted GSEA analysis on the high and low GDF15

expression groups in EAC patients shown in Figure 11e. Consistent with the proteomics analysis, data extracted from the TCGA database showed that the GDF15 high expression group exhibited significant positive correlations with mitochondrial oxidative phosphorylation as well as mitochondrial homeostasis in EAC patients (Figure 18c).

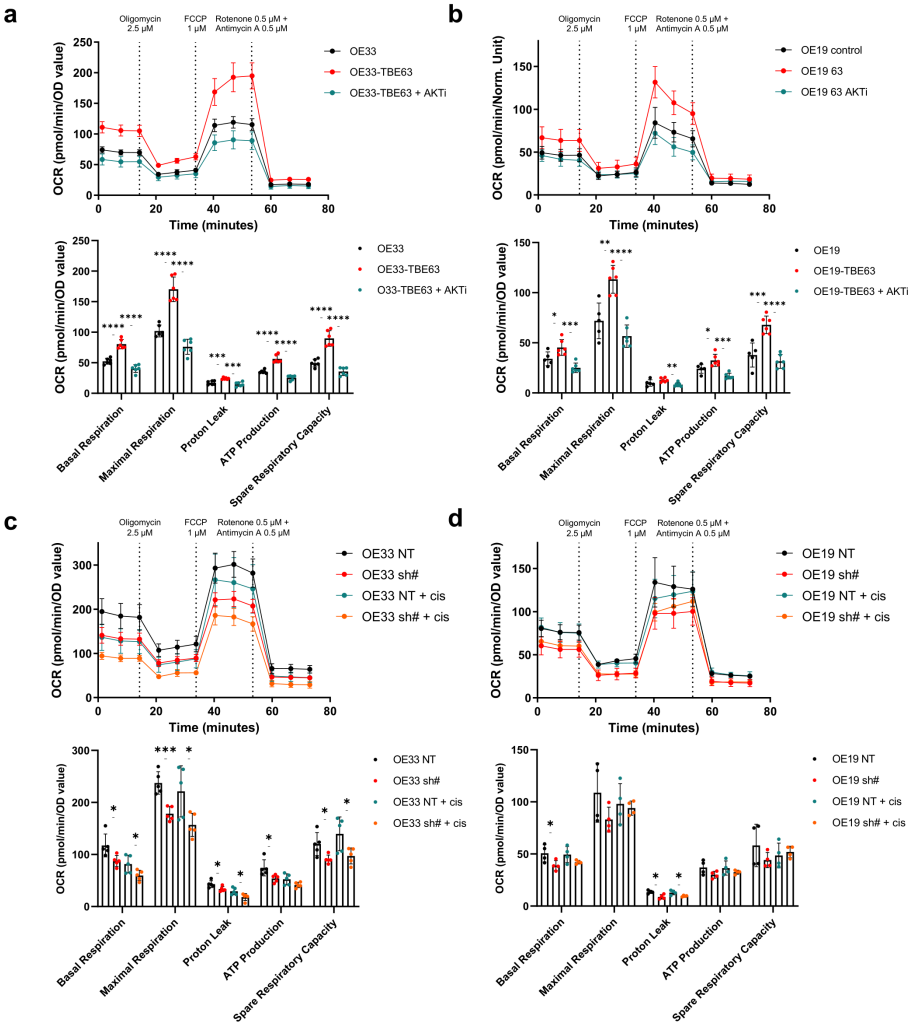

Figure 19. GDF15 depletion results in impaired mitochondrial function in EAC cells.

a. Seahorse XF cell mitochondrial stress test shows the real-time oxygen consumption rate (OCR) of OE33, OE33 after co-culture with TBE63 for seven days and the same OE33-TEB63 co-culture setup with consistently 1μM AKT inhibitor VIII (AKTi) supplement. Cells are sequentially treated with 2.5μM oligomycin, 1μM carbonyl cyanide-p-trifluoromethoxy phenylhydrazone (FCCP), and a combination of 0.5μM rotenone and 0.5μM antimycin A. Data are represented as mean ± SD. Unpaired t-test, ***p<0.001, ****p<0.0001.

b. Seahorse XF cell mitochondrial stress test shows the real-time OCR of OE19, OE19 after co-culture with TBE63 for seven days and the same OE19-TEB63 co-culture

setup with consistently 1μM AKTi supplement. Cells are sequentially treated with 2.5μM oligomycin, 1μM FCCP, and a combination of 0.5μM rotenone and 0.5μM antimycin A. Data are represented as mean ± SD. Unpaired t-test, *p<0.05, **p< 0.01, ***p<0.001, ****p<0.0001.

c. Seahorse XF cell mitochondrial stress test shows the real-time OCR of OE33 sh-NT and OE33 sh-GDF15 groups with and without 3μM cisplatin treatment for 24 hours. Cells are sequentially treated with 2.5μM oligomycin, 1μM FCCP, and a combination of 0.5μM rotenone and 0.5μM antimycin A. Sh-GDF15 groups show significantly decreased OCR than sh-NT groups both in basal conditions and under cisplatin treatment-induced stress. Data are represented as mean ± SD. Unpaired t-test, *p<0.05, ***p<0.001.

d. Seahorse XF cell mitochondrial stress test shows the real-time OCR of OE19 sh-NT and OE19 sh-GDF15 groups with and without 30μM cisplatin treatment for 24 hours. Cells are sequentially treated with 2.5μM oligomycin, 1μM FCCP, and a combination of 0.5μM rotenone and 0.5μM antimycin A. Sh-GDF15 groups shows decreased OCR than sh-NT groups both in basal conditions and under cisplatin treatment-induced stress. Data are represented as mean ± SD. Unpaired t-test, *p<0.05.

Based on the compelling evidence linking GDF15 to mitochondrial function through pathway enrichments, we conducted the Seahorse XF cell mitochondrial stress test, which monitors real-time OCR in live cells.

Following a seven-day co-culture with EAC CAFs, both OE33 and OE19 cell lines exhibited notable improvements in mitochondrial function, as evidenced by significant enhancements in basal respiration, maximal respiration, mitochondrial ATP production, and spare respiratory capacity (Figure 19a, 19b). To assess mitochondrial function in GDF15-depleted cells, we monitored the real-time OCR in OE33 and OE19 sh-NT and sh-GDF15 cells with and without cisplatin treatment for 24 hours. Our findings revealed a significant reduction in basal respiration in the sh-GDF15 groups compared to the sh-NT groups, indicating impaired mitochondrial function (Figure 19c, 19d). Additionally, the sh-GDF15 groups exhibited decreased maximal respiration, mitochondrial ATP production, and spare respiratory capacity, suggesting compromised mitochondrial energy production (Figure 19c, 19d). These observations were consistent after exposing cells to cisplatin treatment for 24 hours, further confirming the detrimental effect of GDF15 depletion on mitochondrial

dysfunction under treatment-induced stress.

Taken together, our findings highlighted the significance of EAC CAFs in promoting mitochondrial function within EAC cells. Notably, the depletion of GDF15 in EAC cells adversely affected mitochondrial function, leading to compromised energy metabolism.

10. GDF15 depletion attenuates AKT pathway activation in EAC cells

To explore the underlying signaling pathways associated with CAF/GDF15-mediated treatment resistance, we conducted the KEGG pathway enrichment analysis using the transcriptomic data previously described (Figure 10a, 10b). Here, several common pathways were enriched in OE33 cells following the co-culture of both TBE60 and TBE63 CAFs, including MAPK signaling pathway, PI3K-AKT signaling pathway, cellular senescence, cell cycle, apoptosis, and TNF signaling pathway (Figure 20a, 20b).

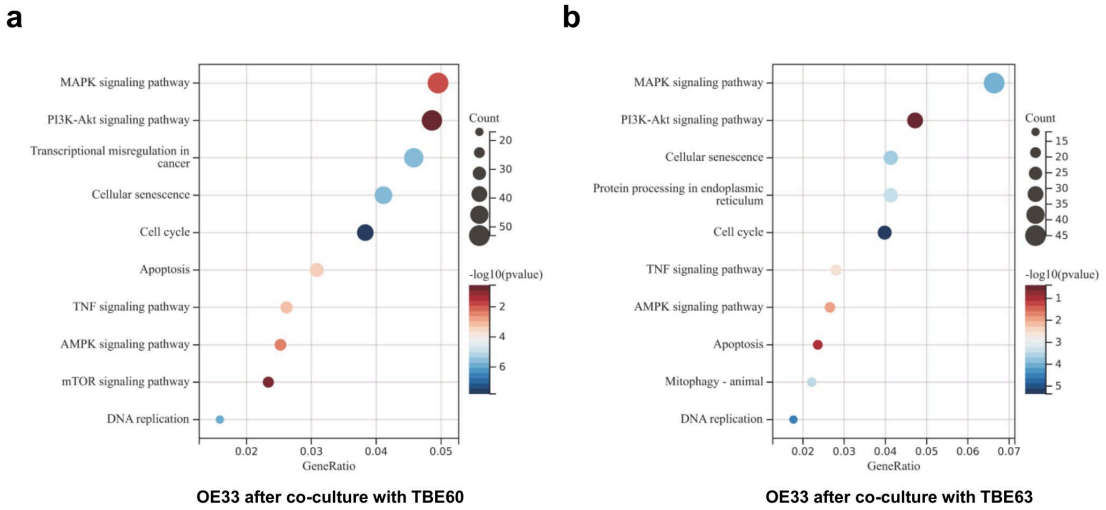

Figure 20. The KEGG pathway enrichment analysis of OE33 after co-cultured with TBE60 and TBE63 CAFs.

a. KEGG pathway enrichment of OE33 after co-cultured with TBE60. Each dot represents a specific pathway, and its position and size indicate the proportion and count of genes associated with a particular pathway. The color of the bar indicates the degree of significance.

b. KEGG pathway enrichment of OE33 after co-cultured with TBE63. Each dot represents a specific pathway, and its position and size indicate the proportion and count of genes associated with a particular pathway. The color of the bar indicates the degree of

significance.

Dysregulation of the AKT pathway has been implicated in various critical cellular processes such as proliferation, survival, apoptosis, metabolism, differentiation, and motility[214]. In cancer cells, AKT activation has been recognized as a key mechanism in mediating treatment resistance, enabling tumor cells to evade the effects of chemotherapy, targeted therapies, and radiation[215,216]. Therefore, we were particularly interested in exploring its potential role in our experimental system. We assessed the activation status of the AKT pathway by analyzing the protein expression levels of phosphorylated AKT (p-AKT) and total AKT using western blotting.

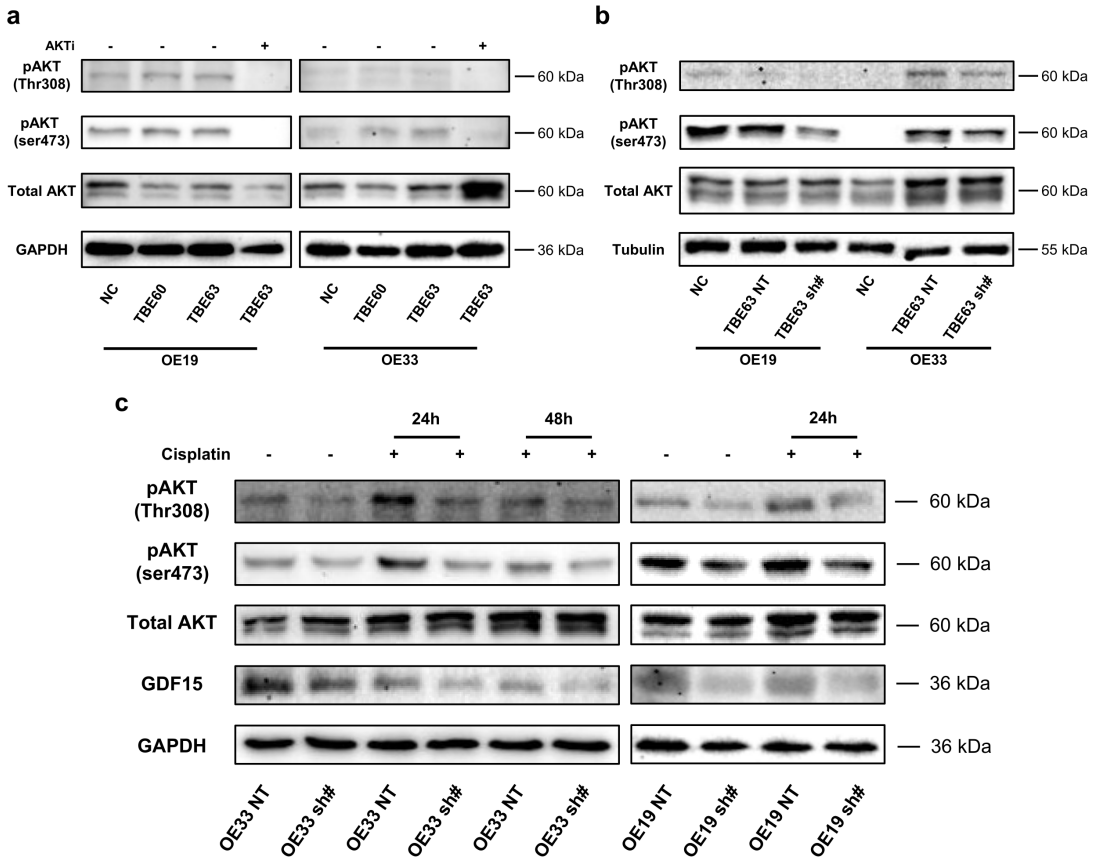

Figure 21. GDF15 depletion attenuates AKT pathway activation in EAC cells.

a. Immunoblot analysis shows the levels of phosphorylated AKT (p-AKT) in OE33 and OE19 cells with and without TBE60 and TBE63 CAFs co-culture. Increased levels of p-AKT are observed in OE33 and OE19 after co-culture with TBE60 and TEB63 CAFs, which can be inhibited by a consistent supplement of 1μM AKT inhibitor VIII (AKTi).

b. Immunoblot analysis shows the levels of p-AKT in OE33 and OE19 cells with TBE63 sh-NT and TBE63 sh-GDF15 co-culture. Decreased levels of p-AKT are observed in OE33 and OE19 after co-culture with TBE63 sh-GDF15 CAFs.
c. Immunoblot analysis shows the levels of p-AKT in OE33 and OE19 cells with and without GDF15 depletion. GDF15 depletion results in reduced p-AKT levels in OE33 and OE19 cells, and this effect is further enhanced upon cisplatin treatment.

The results showed increased levels of p-AKT in both OE33 and OE19 cells after co-culture with TBE60 and TBE63, indicating the activation of the AKT pathway mediated by CAFs (Figure 21a). Besides, we observed decreased p-AKT levels when OE33 and OE19 cells were co-cultured with GDF15-depleted TBE63 CAFs, suggesting that GDF15 played a partial role in CAF-mediated AKT activation (Figure 21b). Moreover, GDF15 depletion in both OE33 and OE19 cells resulted in reduced AKT pathway activation, which was further accentuated upon treatment with cisplatin, suggesting the contribution of GDF15 to the partial activation of the AKT pathway in EAC cells (Figure 21c).
We further investigated the impact of AKT pathway inhibition using a consistent supplement of 1μM AKTi in our co-culture setup. Successful inhibition of the AKT pathway was achieved in both OE33 and OE19 cells upon AKTi treatment (Figure 21a). Notably, deactivation of the AKT pathway resulted in a reduction in the mitochondrial function that had been enhanced by co-culturing with CAFs (Figure 19a, 19b), suggesting that CAFs partially activated mitochondrial functions through the AKT pathway.

11. High serum GDF15 concentration after the CROSS treatment predicts poor overall survival in EAC patients

Following the landmark CROSS trial in 2012[18], the CROSS regimen, consisting of weekly administration of carboplatin and paclitaxel for five weeks and concurrent radiotherapy in a total of 41.4 Gy, has become the standard neoadjuvant chemoradiotherapy strategy in the management of locally advanced esophageal cancer worldwide.

We retrospectively reviewed the surgical biobank from the University Hospital of Cologne and identified a consecutive series of 55 EAC patients who had available serum samples collected before and after undergoing the CROSS treatment between January 2017 and December 2020. These paired serum samples were then selected for GDF15 concentration measurement. The mean serum GDF15 concentration before the CROSS treatment was 938.5 ± 341.7pg/ml. Following the CROSS treatment, a significant increase in GDF15 serum concentration was observed, with a mean value of 1672 ± 742.1pg/ml (p<0.0001, Figure 22a).

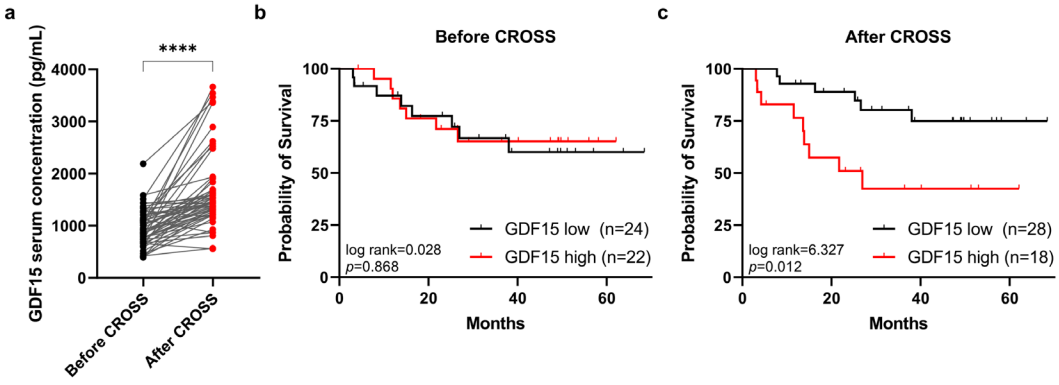

Figure 22. Clinical significance of serum GDF15 concentration in EAC patients.

a. Paired serum GDF15 concentration before and after the CROSS treatment in 55 EAC patients. Serum GDF15 is significantly higher after the CROSS treatment. Paired t-test, ****p<0.0001.
b. Survival analysis of serum GDF15 high group and serum GDF15 low group that are divided according to the GDF15 concentrations before the CROSS treatment. There is no significant difference between the serum GDF15 high group and the serum GDF15 low group regarding overall survival in EAC patients (Log rank=0.028, p=0.868).
c. Survival analysis of serum GDF15 high group and serum GDF15 low group that are divided according to the GDF15 concentrations after the CROSS treatment. High levels of serum GDF15 concentration are significantly associated with reduced overall survival in EAC patients (Log rank=6.327, p=0.012).

Among 55 EAC patients with serum GDF15 concentration measurements, complete clinical and follow-up information were accessible for 46 patients. Based on the GDF15 concentration, patients were divided into GDF15 low and GDF15 high groups before and after undergoing the CROSS treatment. The

detailed patient characteristics were summarized in Table 7. Before the CROSS treatment, there were 24 patients categorized as GDF15 low (Mean ± SD: 708.1 ± 161.0pg/ml) and 22 patients categorized as GDF15 high (Mean ± SD: 1183 ± 183.5pg/ml). After the CROSS treatment, the GDF15 low group consisted of 28 patients (Mean ± SD: 1233.5 ± 285.8pg/ml), while the GDF15 high group comprised 18 patients (Mean ± SD: 2385.4 ± 736.3pg/ml). No significant differences were found between the GDF15 low group and the GDF15 high group regarding age (p=0.220 before CROSS, p=0.980 after CROSS), gender (p=0.702 before CROSS, p=0.917 after CROSS), BMI (p=0.294 before CROSS, p=0.766 after CROSS), ypT stage (p=0.211 before CROSS, p=0.379 after CROSS), and ypN stage (p=0.563 before CROSS, p= 0.280 after CROSS). However, patients with high serum GDF15 concentrations at diagnosis, but not after the CROSS treatment (p=0.221), tended to have minor/partial responses to CROSS treatment compared to the low serum GDF15 group (59.1% vs. 30.4%, p=0.053).

Table 7. Comparison of patient characteristics in serum GDF15 low group and high group before and after the CROSS treatment.

	Before CROSS (n=46)			After CROSS (n=46)		
	GDF15 low (n=24)	GDF15 high (n=22)	*P*	GDF15 low (n=28)	GDF15 high (n=18)	*P*
GDF15 (pg/ml), mean±SD	708.1±161.0	1183±183.5	**<0.0001**	1233.5 ± 285.8	2385.4 ± 736.3	**<0.0001**
Age (years), mean±SD	61.5 ± 8.7	64.7 ± 9.4	0.220	63.1 ± 7.2	63.0 ± 11.7	0.980
Gender, n (%)			0.702			0.917
Male	19 (79.2)	19(86.4)		23 (82.1)	15 (83.3)	
Female	5(20.8)	3(13.6)		5 (17.9)	3 (16.7)	
BMI	26.6 ± 4.8	28.0 ± 4.4	0.294	27.1 ± 4.7	27.5 ± 4.6	0.766
Response*			0.053			0.221
Minor/Partial	7 (30.4)	13 (59.1)		10 (37.0)	10 (55.6)	
Major/Complete	16(69.4)	9 (40.9)		17 (63.0)	8 (44.4)	
ypT, n (%)			0.211			0.379
T0-1	12 (50.0)	7 (31.8)		13 (46.4)	6 (33.3)	
T2-3	12 (50.0)	15 (68.2)		15 (53.6)	12 (66.7)	
ypN, n (%)			0.536			0.280
N0	12 (50.0)	13 (59.1)		17 (60.7)	8 (44.4)	
N1-3	12 (50.0)	9 (40.9)		11 (39.3)	10 (55.6)	

*one missing data. Bold text indicates a significant difference.

Before the CROSS treatment, the 3-year survival rates for the GDF15 low and GDF15 high groups were 66.7% and 65.2%, respectively. There was no significant difference between the GDF15 low and GDF15 high groups on OS (Log rank=0.028, *p*=0.868, Figure 22b). However, following the CROSS treatment, the 3-year survival rates for the GDF15 low and GDF15 high groups were 80.3% and 42.5%, respectively. The high serum concentration of GDF15 was significantly associated with poor OS in EAC patients (Log rank=6.327, *p*=0.012, Figure 22c).

Table 8. Univariate and multivariate Cox regression analyses of prognostic factors for overall survival in EAC patients.

	Univariate analysis HR (95%CI)	*P*	Multivariate analysis HR (95%CI)	*P*
Serum GDF15 before CROSS		0.863		0.426
Low	1			
High	0.914 (0.331-2.523)			
Serum GDF15 after CROSS		**0.018**		
Low	1		1	**0.034**
High	3.506 (1.239-9.921)		3.100 (1.092-8.799)	
Age		0.411		
≤60	1			
>60	0.718 (0.260-1.980)			
Gender		0.663		
Female	1			
Male	1.392 (0.314-6.173)			
BMI	1.007 (0.896-1.133)	0.901		
Response				
Minor/Partial	1	0.103		
Major/Complete	2.405 (0.838-6.901)			
ypT		**0.032**		0.052
T0-1	1		1	
T2-3	4.024 (1.125-14.392)		3.559 (0.991-12.784)	
ypN		**0.022**		0.253
N0	1			
N1-3	3.629 (1.200-10.974)			

Bold text indicates a significant difference.

Similarly, univariate Cox regression analysis revealed that high serum concentration of GDF15 after the CROSS treatment (HR: 3.506, 95% CI: 1.239-

9.921, *p*=0.018), higher ypT stage (HR: 4.024, 95% CI: 1.125-14.392, *p*=0.032), and higher ypN stage (HR: 3.629, 95% CI: 1.200-10.974, *p*=0.022) were significantly associated with worse OS, whereas no significant association was found for GDF15 concentration before the CROSS treatment (HR: 0.914, 95%CI: 0.331-2.523, *p*=0.863) (Table 8). In the multivariate Cox regression analysis, serum GDF15 concentration after the CROSS treatment was an independent risk factor for OS, with high levels of serum GDF15 significantly predicting poor OS in EAC patients (HR: 3.100, 95% CI: 1.092-8.799, *p*=0.034).

Discussion

Compared with traditional meta-analysis, network meta-analysis allows simultaneous comparison of multiple interventions and provides more precise estimates of relative effects by incorporating both direct and indirect evidence from multiple studies[211,217]. When it comes to the neoadjuvant treatments in esophageal cancer, the limited direct comparisons between NCRT and NCT, coupled with several studies comparing NCRT or NCT with surgery alone, make network meta-analysis a powerful tool for robust evaluation by employing surgery alone as a common comparator and synthesizing direct and indirect evidence. Our comprehensive network meta-analysis addressed the importance of NCRT in treating locally advanced esophageal cancer. However, despite the observed effective efficacy of NCRT in treating ESCC patients, with a pathological complete response (pCR) rate of approximately 50%[18,19], EAC patients exhibit higher resistance to NCRT, with an approximate pCR rate of only 20%[18,31]. The persistent emergence of treatment resistance to chemotherapy and radiotherapy remains the main challenge in the management of EAC. Over the last decades, genomic and transcriptomic analyses have provided robust evidence of the genetic complexity of EAC, revealing a high mutational burden and extensive chromosomal instability[218]. To understand the potential genomic alterations after neoadjuvant treatment, Findlay JM et al. compared 30 paired EAC samples before and after neoadjuvant chemotherapy and revealed that patients with higher mutation burden before treatment tended to have a better response to NCT. Additionally, they observed acquired mutations in the tumor samples after NCT treatment [219]. Noorani A et al. compared 10 paired EAC samples before and after NCT and indicated that the differences observed between pre- and pos- NCT treatment samples were reflective of tumor heterogeneity, whereas the overall genomic profile of EAC remained largely similar before and after NCT[220]. As a

highly heterogeneous disease, studies have reported an association between high genomic intratumor heterogeneity and a poor response to neoadjuvant chemotherapy in EAC patients[221]. By analyzing the tumor microenvironment, a key driver for tumor heterogeneity, at the transcriptomic level, Hao D et al. revealed that long survivors from advanced EAC patients exhibited an immune-activated TME[222]. Similarly, Li J et al. demonstrated that a high stromal activity TME was associated with advanced tumor stage and poor prognosis in EAC[223]. Here, instead of solely focusing on the EAC tumor cells, we expand to study EAC treatment resistance from the perspective of the TME, which provides a more comprehensive understanding of the intrinsic heterogeneity of esophageal cancer.

Through the generation of EAC CAFs and conducting CAF-tumor co-culture experiments, we corroborate the existing literature indicating that EAC CAFs indeed promote tumor growth and treatment resistance in EAC cells. Different from the previous reports by Ebbing et al. using EAC CAF-derived conditional medium to culture EAC cells[91], the transwell co-culture as well as the 3D dome co-culture systems used in our study allowed for bidirectional feedback between EAC cells and EAC CAFs. It should be noted that direct CAF-tumor contact theoretically provides a more accurate representation of the TME. Karakasheva TA has identified IL-6 from tumor-stroma interaction by conducting a direct co-culture of EC cells and CAFs and isolating EC cells using a magnetic bead-based method for expression analysis[90]. However, we refrained from using direct co-culture in our study due to concerns about potential cell contamination of CAFs in tumor cells and inadequate tumor cell numbers for further functional assessment. In recent years, the development of single-cell RNA-seq technology has enriched our understanding of the heterogeneity of CAFs within the TME. One recent leading-edge review article provided a comprehensive summary of the latest evidence, primarily derived from studies in pancreatic and breast cancers, and classified CAFs into four

distinct functional groups: iCAFs (inflammatory CAFs), myCAFs (myofibroblastic CAFs), apCAFs (antigen-presenting CAFs), and vCAFs (vascular CAFs)[53]. We acknowledge the presence of heterogeneity among the EAC CAFs used in this study, as evidenced by distinct expression profiles of fibroblast-related markers (Figure 6). According to this subtyping system, TBE60 and TBE63 might be classified as iCAFs, characterized by high expression of IL6 and relatively low expression of αSMA, TBO1657 may belong to myCAFs, showing opposite expression patterns compared to iCAFs. However, more markers are required for better subtyping of CAF2304 and CAF2765. Despite the indirect co-culture approach used in this study and the notable heterogeneity among EAC CAFs, our results consistently demonstrated the promoting effect of different CAFs on the progression of different EAC cells, which was further validated by paired CAFs and EAC PDOs from the same patients. These findings indicate the stability of our co-culture system and underscore the robust CAF-mediated EAC treatment resistance phenotypes in the context of EAC tumor-stroma interaction *in vitro*. Until now, there is still no specific CAF subtyping system in EAC. With a resource of over 30 EAC CAFs established in our research group, and the access to single-cell RNA-seq data from four treatment-naive EAC patients' primary tissues, further investigation in EAC CAFs subtyping and their potential functional heterogeneity on EAC tumors is the next key research focus in our team.

To explore potential factors involved in the EAC CAF-tumor interaction in transcriptomic analysis, our focus was on the dynamically changed genes in the transwell co-culture system, rather than upregulated genes in tumor cells. GDF15 was identified with an opposite expression pattern between EAC CAFs and EAC cells. Known as macrophage inhibitor 1, GDF15 has been predominantly studied in the context of macrophage-related TME across various types of cancer[96]. However, only limited research has been focused on the role of CAF-derived GDF15 in cancer progression. Zhai Y et al. successfully

established CAFs by inducing differentiation of mesenchymal stem cells and they found that knocking down GDF15 in CAFs resulted in a reduction of CAF-mediated resistance to cytarabine treatment in leukemia cells[224]. Bruzzese F et al. performed an overexpression of GDF15 in mouse fibroblasts and observed that prostate cancer cells exhibited enhanced cell proliferation, migration, and invasion abilities when cultured in the GDF15 overexpressed fibroblasts' conditional medium[225]. In our study, the upregulated GDF15 expression in EAC CAFs from transcriptomic analysis suggests that CAFs secrete GDF15 into the TME with the stimulation of EAC cells. This finding was further validated by ELISA showing elevated GDF15 concentration in the co-culture system and decreased GDF15 concentration after knocking down GDF15 in CAFs (Figure 12a, Figure 13b). In a comprehensive analysis of EAC CAF-derived cytokines, Ebbing EA et al. reported that GDF15 was four times higher in EAC CAF-derived conditional medium compared with the control medium[91]. The consistency between our study and external data supports the significance of CAF-derived GDF15 in the EAC tumor-stroma interaction. We found that EAC CAFs promote EAC treatment resistance partly through the secretion of GDF15. Interestingly, GDF15 depletion in EAC tumor cells showed restored sensitivity to chemotherapy as well as radiotherapy *in vitro,* indicating that GDF15 functions in treatment resistance through both the paracrine effect from EAC CAFs and intrinsic tumor regulation. One indication of GDF15's potential involvement in EAC treatment resistance was previously described by Karakasheva et al.[177]. In their study using EAC PDOs to model patients' response to chemotherapy, they observed a common upregulation of GDF15 expression after exposing three different EAC PDOs to cisplatin and paclitaxel treatments. This increased GDF15 expression may suggest a protective role for EAC cells under treatment stress. Additionally, another study reported the protective role of GDF15 against cisplatin treatment in ESCC patients[137]. The authors used rGDF15 to treat ESCC cells and found an increase in cisplatin

resistance following the rGDF15 treatment. Moreover, they identified TGF-β receptor II (TGFBR2) as a GDF15 receptor in ESCC cells[137]. Similarly, Okamoto et al. reported that rGDF15 enhanced ESCC cell proliferation, migration, and invasion through TGFBR2 activation[136]. However, it is essential to approach these results with caution, as there is a possibility that the recombinant GDF15 protein might have been contaminated with TGF-β[226]. Given that TGFBR2 is a TGF-β receptor and several previous studies have indicated that GDF15 does not bind to the TGF-β receptor[227,228], the observed effects in ESCC cells could potentially be attributed to TGF-β rather than GDF15. Therefore, we only used rGDF15 in GDF15-depleted cells as a rescue analysis to double-validate CAF-mediated treatment resistance in this study (Figure 13d). In subsequent pathway analysis, we omitted rGDF15 to avoid potentially biased findings and to ensure a more accurate assessment of the role of GDF15 in the context of EAC treatment resistance. We found that CAFs activated the AKT pathway in EAC cells partly through GDF15 secretion, and depletion of GDF15 in EAC cells decreased AKT activation. This finding was consistent with previous studies reporting that CAFs activated the AKT signaling pathway in ESCC[82,229,230]. However, it is important to note that all the studies demonstrating GDF15-mediated AKT pathway activation in ESCC were based on rGDF15 treatment[115,136,137]. Notably, to date, only one study, which focused on CRC, has reported a correlation between fibroblast-secreted GDF15 and AKT pathway activation[135]. Here, our study provided a novel mechanism underlying CAF-mediated treatment resistance in EAC cells, thereby underscoring the potential therapeutic significance of targeting GDF15 in the EAC tumor microenvironment.

Accumulating evidence suggested that essential mitochondrial functions partly contribute to cancer treatment resistance, with resistant tumor cells exhibiting higher reliance on mitochondrial oxidative phosphorylation (OXPHOS) and respiration but reduced reliance on glycolysis[231,232]. In our study, we found that

CAFs enhanced EAC cells' mitochondrial function partly through activation of the AKT pathway. The association between mitochondrial function and treatment resistance in EAC was previously described by Aichler M et al. in a study involving proteomic analysis of pre-treatment biopsy samples from 23 EAC patients. Their findings indicated that patients with pre-existing defects in mitochondrial respiratory complexes were more sensitive to chemotherapy[233]. Besides, Buckley AM et al. reported enhanced radiosensitivity in EAC cells upon utilizing pyrazinib to inhibit OXPHOS[234]. A recent study performed RNA-seq of six matched tissue samples (two ESCC and four EAC) before and after NCRT and enriched enhanced OXPHOS components in EC patients after NCRT[180]. Additionally, targeting mitochondrial biogenesis in EAC cells increased cell sensitivity to chemotherapy and ionizing iratation[180]. Therefore, CAFs may protect EAC cells against treatment stress partly through enhancing mitochondrial function. In recent years, the role of GDF15 as an important mitokine in response to mitochondrial stress has received increasing attention[235,236]. Khan NA et al. reported that mitochondrial DNA (mtDNA) replication defect activated the mTOR1/ATF4 axis and integrated mitochondrial stress response, leading to the production of fibroblast growth factor (FGF21) and GDF15 [237]. Mitochondrial damage that was induced by TGF-β incubation showed increased GDF15 expression and protein release in normal dermal fibroblasts[238]. In a meta-analysis including seven RCTs with 845 participants, Lin Y et al. demonstrated that GDF15 exhibits potential as a diagnostic marker for predicting patients with mitochondrial disorders, with a sensitivity of 0.83 (95% CI: 0.65-0.92) and specificity of 0.92 (95% CI: 0.84-0.96)[239]. We did not investigate the mitokine role of GDF15 in this study, instead, we observed a positive regulatory effect of GDF15 on EAC mitochondria function, as evidenced by significant enrichment of mitochondrial-related pathways in OE33 sh-NT cells compared to OE33 sh-GDF15 cells, and impaired mitochondrial function in EAC GDF15 knockdown cells. Our findings are consistent with

previous reports suggesting that depletion of GDF15 in human dermal fibroblasts resulted in the accumulation of dysfunctional mitochondria and led to premature senescence[240]. Besides, overexpression of GDF15 in transgenic mice prevented hepatic steatosis by suppressing oxidative stress and mitochondrial damage[241]. To date, there is still no study reported on the association between GDF15 and mitochondrial function in EAC. Therefore, we suggest that future investigations could focus on the underlying mechanisms of GDF15 as both a mitokine and a mitochondrial regulator in the context of CAF-related TME.

Due to the difficulties and ethical concerns associated with establishing orthotopic esophageal cancer mouse models, and the use of subcutaneous mouse models may not fully capture the complex tumor-stroma interactions involving human CAFs[174,175], we turned to using tumor PDOs as a reliable and cost-effective model for studying EAC. The successful utilization of EAC PDOs with paired EAC CAFs for *in vitro* co-culture in this study provided a novel and valuable approach for investigating the CAF-related TME in EAC using patient-derived material. A recent study established a CRC organoid-stroma biobank containing 30 matched PDOs with CAFs and performed comprehensive molecular and functional analyses. They found that organoid-stroma co-cultures provided improved preclinical models for predicting therapy efficiency than organoids monoculture, highlighting the potential of using organoids and paired CAFs as promising translational tools for personalized treatment[242]. Several previous studies have used different indirect and direct co-culture techniques to explore the interaction between CAFs and PDOs. Liu J et al. reported direct co-culture, transwell co-culture, and CAF-derived conditional medium co-culture in their study involving CAFs and liver cancer organoids derived from both mice and human samples. Their results showed the supportive effects of CAFs in liver cancer proliferation and treatment resistance[243]. Schuth S et al. conducted both direct co-culture and transwell co-

culture to explore the interaction of pancreatic stellate cells (PSCs) and pancreatic cancer organoids. Their findings supported the existence of CAF heterogeneity in pancreatic cancer and demonstrated that tumors activated PSCs to CAFs[244]. Direct co-culture of oral squamous cell carcinoma organoids with paired CAFs in the same ECM gel domes showed a notable enhancement in the organoid formation ability compared with control[245]. By using the live image-based drug assay to assess drug sensitivity in the direct CAF-PDO coculture system, Schuth S et al. reported enhanced chemoresistance to various chemotherapeutic drugs in pancreatic cancer organoids when co-cultured with paired CAFs[246]. In addition to transwell co-culture, Luo X et al. introduced a novel indirect co-culture method where CRC organoids were seeded in hyaluronan-gelatin hydrogels, and CAFs were added on top of the hydrogel constructs. They observed enhanced CRC organoid proliferation in the presence of CAFs even in basal medium without growth factors, suggesting a tumor-promoting paracrine effect of CAFs[247]. In our study, we described dome co-culture and transwell co-culture systems in culturing EAC PDOs with paired CAFs. Both co-culture systems are effective and practical. Each system demonstrated its feasibility in detecting CAF-mediated EAC proliferation, with the dome co-culture system offering additional utility in drug sensitivity screening. To the best of our knowledge, this is the first study to utilize matched PDOs and CAFs in studying EC TME. With an expanding collection of EAC PDOs and paired CAFs from our biobank, the potential applications of these valuable models can be further explored and enhanced in future studies.

Corroborating with the literature[117–119], we observed a clinical significance of GDF15 as a potential biomarker for EAC patients, as evidenced by the significant survival differences based on both stratified tissue expression levels and serum concentrations of GDF15. While several studies reported encouraging prognostic role of GDF15 in ESCC patients[114–116], we noted a more promising prognostic value of GDF15 in EAC, supported by data from

public databases showing higher GDF15 expression levels in EAC than ESCC, as well as a significant survival correlation of stratified GDF15 expression in the EAC population, but not in the ESCC population. Besides, unlike previous studies that only detected serum GDF15 concentration at diagnosis, we measured paired serum samples before and after the CROSS treatment, the classic NCRT regimen in treating EC patients, and we found significantly increased GDF15 serum concentration after the CROSS treatment. It is widely proved that GDF15 serves as a stress-response cytokine, with changes observed in both expression and serum levels in response to different stimuli across various disease processes[97,248]. The evaluated serum GDF15 after the CROSS treatment may be a protective reaction for cancer cells in response to chemoradiotherapy treatment. Besides, the GDF15-GFRAL signaling plays a crucial role in cancer cachexia and is implicated in chemotherapy-induced emesis, anorexia, and weight loss observed in cancer patients[122,249,250]. Inhibition of GDF15 activity not only reversed GDF15-induced weight loss but also alleviated chemotherapy-induced side effects[249,250]. Given that malnutrition and cachexia are common symptoms in EC patients, targeting GDF15 may represent a potential strategy to improve the quality of life for EC patients. More interestingly, our data suggested that patients with evaluated serum GDF15 after CROSS treatment, but not at the diagnosis stage, independently predicted a poor prognosis in EAC. Besides, patients with high serum GDF15 at diagnosis, but not after the CROSS treatment, exhibited a tendency toward reduced pathological response to the CROSS treatment in EAC patients (p=0.053). These novel findings addressed the importance of monitoring dynamic changes in serum GDF15 levels along with clinical interventions in EAC patients. Here, we provided a hint for future studies to explore the potential of GDF15 as a biomarker in different treatment processes of EAC patients by conducting large-scale investigations and exploring its predictive value in treatment response and patient outcomes.

We address several limitations in this study. Firstly, in our initial study design, our focus was primarily on the general effect of CAFs on EAC cells, and we did not delve into exploring the CAF heterogeneity and diverse functions of different types of CAFs on EAC. With growing evidence supporting the existence of distinct CAF subtypes exhibiting both tumor-promoting and tumor-suppressing functions in the literature, we are highly motivated to pursue future research focusing on the study of CAF heterogeneity using the valuable patient-derived EAC CAFs from our biobank. Secondly, we did not perform animal experiments in this study. This decision was made due to concerns that the mouse stroma may potentially influence the function of human CAFs in the subcutaneous xenograft mouse model. Instead, we established EAC PDOs with paired CAFs to study the tumor-stroma interaction. The use of PDOs to reduce the reliance on basic animal models has been a prominent topic of discussion in recent years[139,169,170]. Despite the absence of *in vivo* data, the consistent results obtained from our novel matched PDO-CAF co-culture models strengthen the validity of our findings. Thirdly, the lack of utilizing GDF15 neutralization antibodies as well as GDF15 inhibitors limited the translational significance of this study. At the beginning of my doctoral research, there were still rare commercially available GDF15 neutralization antibodies or inhibitors, leading us to resort to GDF15 knockdown in CAFs/EAC cells to study its function. However, with the commercialized GDF15 inhibitor (Ponsegromab) and neutralizing antibody (CTL-002) in the market[251,252], future studies could provide a more comprehensive and clinically relevant investigation of GDF15 as a potential therapeutic target in EAC. In addition, it is important to acknowledge that our study had a relatively small sample size for the clinical evaluation of serum GDF15 as a biomarker for EAC, with survival information available for only 46 patients. Nevertheless, our findings aligned with the existing literature, highlighting the promising role of GDF15 as a potential biomarker in EAC. Besides, we enhanced the reliability of our findings by

performing external validation using the TCGA database. Furthermore, our study uniquely included the measurement of paired serum samples both at diagnosis and after CROSS treatment, providing valuable insights into the dynamic changes of GDF15 as a potential biomarker at different treatment stages. Future studies with larger sample sizes are warranted to validate the role of GDF15 as a biomarker at different clinical management stages of EAC.

Conclusion

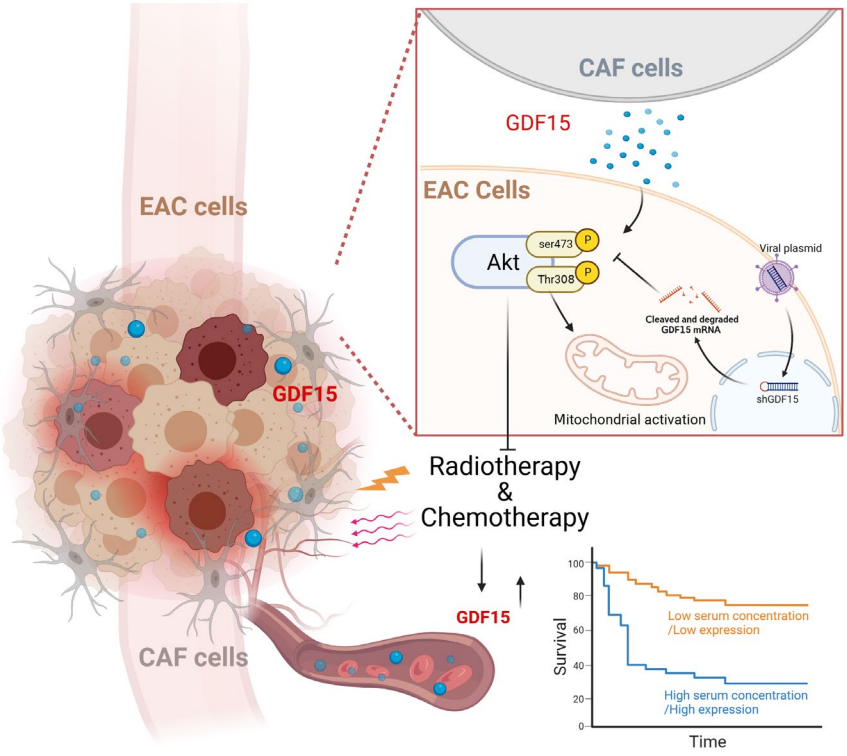

1. We corroborated current guidelines recommending neoadjuvant chemoradiotherapy followed by surgery as the optimal treatment strategy in the management of patients with locally advanced esophageal cancer.
2. Generated from patients' primary tissue, matched EAC CAFs and EAC PDOs offered a feasible approach to studying tumor-stroma interactions *in vitro*.
3. EAC CAFs enhanced EAC cell proliferation and treatment resistance, with the treatment resistance partially attributed to the secretion of GDF15, leading to AKT pathway activation. Besides, the depletion of GDF15 in EAC cells resulted in reduced treatment resistance, highlighting the dual role of GDF15 as both a paracrine factor from EAC CAFs and an intrinsic regulator within the EAC tumor.
4. We found EAC CAFs enhanced EAC cell mitochondrial function partly through the AKT pathway activation. Besides, apart from the function of GDF15 as a mitokine involved in the mitochondrial stress response, the

depletion of GDF15 in tumor cells resulted in impaired mitochondrial function in EAC, suggesting a regulatory role of GDF15 on EAC mitochondria function.

5. We emphasized the significance of monitoring dynamic changes in GDF15 levels during the treatment process in EAC patients as a potential biomarker. We found that high GDF15 serum concentration at diagnosis may indicate reduced neoadjuvant chemoradiotherapy sensitivity, while high GDF15 serum concentration after NCRT (CROSS treatment) independently predicts poor overall survival in EAC patients.

Acknowledgment

We thank the TCGA program that the results in Figure 11 are partly based upon data generated by the TCGA Research Network: https://www.cancer.gov/tcga. We thank the technical assistance from Lisa Raatz, Susanne Neiss, Michaela Heitmann, and Anke Wienand-Dorweiler. I appreciate Guangzhou Elite Scholarship Council (GESC) for the financial support for my doctoral study.

Finally, this marks the end of my doctoral thesis, and at the same time, a flood of memories comes to mind. It has been 12 years since I embarked on my journey in clinical medicine and medical research. First and foremost, I want to thank myself for not giving up and always keeping myself together in the up and down days. Well done, Ningbo! Thank you for keeping fighting even during numerous times of self-doubt. Thank you for starting to find who you are in this overwhelming world. I am so glad that during your doctoral study, you try to confront your shortcomings, accept your failures, learn to talk to yourself and become comfortable with yourself. It was challenging, really, but looking back on this journey now, see, it wasn't as hard as it seemed.

I want to thank my dear mom, Ying Xiang (向英), for her great support and unreserved love all the way along with me. As a single mother, she offers me all the best no matter how many challenges she has struggled with. I am so proud of how wonderful mom she is, and I am so grateful to be her son and her close friend. 谢谢你妈妈，我爱你！

I want to thank my supervisors, Prof. Dr. Christiane Bruns, and Dr. Yue Zhao for the financial support and supervisions during my research. I am sincerely grateful for Prof. Bruns's invaluable guidance unwavering support, and mentorship throughout my research journey. As to Berry, Berry is such an open-minded, empathetic, and super nice mentor. Like a big sister in this family, she always tries her best to support me not only in scientific questions but also in

my life problems. I feel so lucky to get enrolled in this team, where I learned how to enjoy science and developed independent scientific thinking as well as trouble shooting skills. Without Berry's constant supervision and mentorship, this growth would not have been possible. I deeply thank Lisa, for the joy and quality working time we spend together. With Lisa's professional assistance, we generated one of the first EAC PDO case in Cologne and made the utilization of EAC PDOs with paired CAFs in EAC research possible. More importantly, we have learned how to work joyfully in the lab and embrace the beauty of exploring scientific uncertainty. I thank Michaela for professional assistant in my project as well as warmly help in my life in Germany. As a foreigner student in this country, Michy always makes sure that I feel welcomed and supported. She is readily available to help me with any problems I encounter in my life here, offering me a feeling of home. I want to thank Dr. Zhefang Wang for being an exceptional tutor, guiding me through the fundamentals of scientific skills and instilling in me a deep understanding of how to conduct science with efficiency and reliability. I want to sincerely thank Susanne and Anke for their technical assistance and warmly taking care of me in my study and routine life. I extend my heartfelt thanks to PhD program co-supervisors, Prof. Dr. Axel Hillmer and Prof. Dr. Thomas Langer, for their exceptional expertise and patient guidance.

I want to thank all the people supported me in this journey. I am immensely grateful for my master supervisor, Prof. Dr. Peng Lin, who has been a guiding light in my lowest moments. As a compassionate and skilled surgeon, he sets an inspiring example of what it truly means to be a righteous and kind doctor. I feel incredibly fortunate to learn from his actions, as they serve as a valuable guide in my own journey. I want to express my heartfelt gratitude to Weidong Wang, a dear life-long friend, who offered me valuable and constructive advice during several moments of uncertainty in my life. His attentive listening and guidance have been instrumental in helping me navigate important decisions.

Without his unwavering support, I wouldn't be where I am today. I want to extend my thanks to Jiarong Li for being such wonderful company and support during the early days of my new life in Germany. Thank you for being such a good listener and advisor in my difficult times, and always being by my side when I am needed. I truly appreciate the joy and meaningful growth you have brought into my life. Last but not least, I want to express my heartfelt gratitude to Pedro Lino, a wonderful human being who brought light into my life during the most stressful days of my doctoral research. You brought joy, happiness and hope to my life, and you showed me a completely new direction that I had always overlooked. I am incredibly grateful to have you by my side, and I truly believe that we will keep fighting together in the future.

Time to enjoy adult life!

Abbreviation

2D: two-dimensional;

3D: three-dimensional;

5-FU: fluorouracil;

AGEJ: adenocarcinoma of gastroesophageal junction;

ANOVA: one-way analysis of variance;

apCAFs: antigen presenting CAFs;

BE: Barrett's esophagus;

CAA: chloroacetamide;

CAFs: cancer-associated fibroblasts;

CCL5: CC motif chemokine ligand 5;

CI: confidence interval;

CNS: central nervous system;

CRC: colorectal carcinoma;

CrIs: credible intervals;

CROSS: Dutch Chemoradiotherapy for Oesophageal Cancer followed by Surgery Study;

CSCs: cancer stem cells;

DC: dendritic cell;

DFS: disease-free survival;

DTT: dithiothreitol;

EAC: esophageal adenocarcinoma;

EC: esophageal cancer;

ECAR: extracellular acidification rate;

ECM: extracellular matrix;

ELISA: enzyme-linked immunosorbent assay;

EMT: epithelial-mesenchymal transition;

ESCC: esophageal squamous cell carcinoma;

ESCs: embryonic stem cells;

FCCP: Carbonyl cyanide-p-trifluoromethoxy phenylhydrazone;

FGF2: fibroblast growth factor-2;

FGF21: fibroblast growth factor

GC: gastric cancer;

GDF15: growth differentiation factor 15;

GEJ: gastroesophageal junction;

GEO: Gene Expression Omnibus;

GERD: gastroesophageal reflux disease.

GFRAL: glial cell line–derived neurotrophic factor receptor alpha (GFRα)-like;

GI: gastrointestinal;

GO analysis: Gene Ontology analysis;

GSEA: Gene Set Enrichment Analysis;

H&E: Hematoxylin-eosin;

HER2: human epidermal growth factor receptor 2;

HIF1α: hypoxia-inducible factor 1α;

HR: hazard ratio;

HRP: horseradish peroxidase;

iCAFs: inflammatory CAFs;

IF: immunofluorescence;

IHC: immunohistochemistry;

IL-6: interleukin 6;

LFQ: label-free quantification;

Lgr5: leucine-rich repeat-containing G protein-coupled receptor 5;

lncRNA: long noncoding RNAs;

lnHR: natural logarithm of the hazard ratios;

Ln-γ2: laminin γ2;

Lys-C: Lysyl endopeptidase;

MIC-1: macrophage inhibitory cytokine 1;

mtDNA: mitochondrial DNA

myCAFs: myofibroblastic CAFs;

NAG-1: non-steroidal anti-inflammatory drug-activated gene-1;

NCRT: neoadjuvant chemoradiotherapy;

NCT: neoadjuvant chemotherapy;

NES: normalized enrichment score;

NSAIDs: non-steroidal anti-inflammatory drugs;

OCR: oxygen consumption rate;

OS: overall survival;

OXPHOS: mitochondrial oxidative phosphorylation

PAI-1: plasminogen activator inhibitor-1;

p-AKT: phosphorylated AKT;

PCA: principal component analysis;

pCR: pathological complete response;

PD-1: programmed death 1;

PDE5i: phosphodiesterase type 5 inhibitors;

PDOs: patient-derived tumor organoids;

PEI: polyethylenimine;

PFS: progression-free survival;

PSCs: pancreatic stellate cells

pTis: pathological carcinoma in situ;

qPCR: quantitative Real-time PCR;

RCTs: randomized controlled trials.

rGDF15: recombinant GDF15 protein;

RNA-seq: RNA sequencing;

RoB2 tool: risk-of-bias tool;

Rot/AA: rotenone/antimycin A;

SD: standard deviation;

SNVs: single nucleotide variants;

SPRY1: Sprouty RTK signaling antagonist 1;

TAMs: tumor-associated macrophages;

TCGA: The Cancer Genome Atlas;

TEAB: triethylammonium bicarbonate;

TGF-β1: transforming growth factor-β1;

TME: tumor microenvironment;

vCAFs: vascular CAFs;

References

1. Sung H, Ferlay J, Siegel RL, et al. Global Cancer Statistics 2020: GLOBOCAN Estimates of Incidence and Mortality Worldwide for 36 Cancers in 185 Countries. CA Cancer J Clin. 2021;71(3):209-249. doi:10.3322/caac.21660
2. Lagergren J, Smyth E, Cunningham D, Lagergren P. Oesophageal cancer. Lancet. 2017;390(10110):2383-2396. doi:10.1016/S0140-6736(17)31462-9
3. Morgan E, Soerjomataram I, Rumgay H, et al. The Global Landscape of Esophageal Squamous Cell Carcinoma and Esophageal Adenocarcinoma Incidence and Mortality in 2020 and Projections to 2040: New Estimates From GLOBOCAN 2020. Gastroenterology. 2022;163(3):649-658.e2. doi:10.1053/j.gastro.2022.05.054
4. Thrift AP. Global burden and epidemiology of Barrett oesophagus and oesophageal cancer. Nat Rev Gastroenterol Hepatol. 2021;18(6):432-443. doi:10.1038/s41575-021-00419-3
5. Uhlenhopp DJ, Then EO, Sunkara T, Gaduputi V. Epidemiology of esophageal cancer: update in global trends, etiology and risk factors. Clin J Gastroenterol. 2020;13(6):1010-1021. doi:10.1007/s12328-020-01237-x
6. Eluri S, Shaheen NJ. Barrett's Esophagus: Diagnosis and Management. Gastrointest Endosc. 2017;85(5):889-903. doi:10.1016/j.gie.2017.01.007
7. Shaheen NJ, Falk GW, Iyer PG, et al. Diagnosis and Management of Barrett's Esophagus: An Updated ACG Guideline. Am J Gastroenterol. 2022;117(4):559-587. doi:10.14309/ajg.0000000000001680
8. Coleman HG, Xie SH, Lagergren J. The Epidemiology of Esophageal Adenocarcinoma. Gastroenterology. 2018;154(2):390-405. doi:10.1053/j.gastro.2017.07.046
9. Freedman ND, Murray LJ, Kamangar F, et al. Alcohol intake and risk of oesophageal adenocarcinoma: a pooled analysis from the BEACON Consortium. Gut. 2011;60(8):1029-1037. doi:10.1136/gut.2010.233866

10. Anderson LA, Cantwell MM, Watson RGP, et al. The association between alcohol and reflux esophagitis, Barrett's esophagus, and esophageal adenocarcinoma. Gastroenterology. 2009;136(3):799-805. doi:10.1053/j.gastro.2008.12.005

11. Pandeya N, Williams G, Green AC, Webb PM, Whiteman DC, Australian Cancer Study. Alcohol consumption and the risks of adenocarcinoma and squamous cell carcinoma of the esophagus. Gastroenterology. 2009;136(4):1215-1224, e1-2. doi:10.1053/j.gastro.2008.12.052

12. Toh Y, Oki E, Ohgaki K, et al. Alcohol drinking, cigarette smoking, and the development of squamous cell carcinoma of the esophagus: molecular mechanisms of carcinogenesis. Int J Clin Oncol. 2010;15(2):135-144. doi:10.1007/s10147-010-0057-6

13. Abnet CC, Arnold M, Wei WQ. Epidemiology of Esophageal Squamous Cell Carcinoma. Gastroenterology. 2018;154(2):360-373. doi:10.1053/j.gastro.2017.08.023

14. Pandeya N, Williams GM, Sadhegi S, Green AC, Webb PM, Whiteman DC. Associations of duration, intensity, and quantity of smoking with adenocarcinoma and squamous cell carcinoma of the esophagus. Am J Epidemiol. 2008;168(1):105-114. doi:10.1093/aje/kwn091

15. Ajani JA, D'Amico TA, Bentrem DJ, et al. Esophageal and Esophagogastric Junction Cancers, Version 2.2023, NCCN Clinical Practice Guidelines in Oncology. Journal of the National Comprehensive Cancer Network. 2023;21(4):393-422. doi:10.6004/jnccn.2023.0019

16. Ishihara R, Arima M, Iizuka T, et al. Endoscopic submucosal dissection/endoscopic mucosal resection guidelines for esophageal cancer. Dig Endosc. 2020;32(4):452-493. doi:10.1111/den.13654

17. Eyck BM, van Lanschot JJB, Hulshof MCCM, et al. Ten-Year Outcome of Neoadjuvant Chemoradiotherapy Plus Surgery for Esophageal Cancer: The Randomized Controlled CROSS Trial. JCO. 2021;39(18):1995-2004.

doi:10.1200/JCO.20.03614

18. Van Hagen P, Hulshof MCCM, Van Lanschot JJB, et al. Preoperative Chemoradiotherapy for Esophageal or Junctional Cancer. N Engl J Med. 2012;366(22):2074-2084. doi:10.1056/NEJMoa1112088

19. Yang H, Liu H, Chen Y, et al. Neoadjuvant Chemoradiotherapy Followed by Surgery Versus Surgery Alone for Locally Advanced Squamous Cell Carcinoma of the Esophagus (NEOCRTEC5010): A Phase III Multicenter, Randomized, Open-Label Clinical Trial. JCO. 2018;36(27):2796-2803. doi:10.1200/JCO.2018.79.1483

20. Yang H, Liu H, Chen Y, et al. Long-term Efficacy of Neoadjuvant Chemoradiotherapy Plus Surgery for the Treatment of Locally Advanced Esophageal Squamous Cell Carcinoma: The NEOCRTEC5010 Randomized Clinical Trial. JAMA Surgery. 2021;156(8):721-729. doi:10.1001/jamasurg.2021.2373

21. Kitagawa Y, Ishihara R, Ishikawa H, et al. Esophageal cancer practice guidelines 2022 edited by the Japan esophageal society: part 1. Esophagus. 2023;20(3):343-372. doi:10.1007/s10388-023-00993-2

22. Kitagawa Y, Ishihara R, Ishikawa H, et al. Esophageal cancer practice guidelines 2022 edited by the Japan Esophageal Society: part 2. Esophagus. 2023;20(3):373-389. doi:10.1007/s10388-023-00994-1

23. Ando N, Iizuka T, Ide H, et al. Surgery plus chemotherapy compared with surgery alone for localized squamous cell carcinoma of the thoracic esophagus: a Japan Clinical Oncology Group Study--JCOG9204. J Clin Oncol. 2003;21(24):4592-4596. doi:10.1200/JCO.2003.12.095

24. Ando N, Kato H, Igaki H, et al. A randomized trial comparing postoperative adjuvant chemotherapy with cisplatin and 5-fluorouracil versus preoperative chemotherapy for localized advanced squamous cell carcinoma of the thoracic esophagus (JCOG9907). Ann Surg Oncol. 2012;19(1):68-74. doi:10.1245/s10434-011-2049-9

25. Kato K, Ito Y, Daiko H, et al. A randomized controlled phase III trial comparing two chemotherapy regimen and chemoradiotherapy regimen as neoadjuvant treatment for locally advanced esophageal cancer, JCOG1109 NExT study. JCO. 2022;40(4_suppl):238-238. doi:10.1200/JCO.2022.40.4_suppl.238

26. Allum WH, Stenning SP, Bancewicz J, Clark PI, Langley RE. Long-Term Results of a Randomized Trial of Surgery With or Without Preoperative Chemotherapy in Esophageal Cancer. JCO. 2009;27(30):5062-5067. doi:10.1200/JCO.2009.22.2083

27. Smyth EC, Nilsson M, Grabsch HI, van Grieken NC, Lordick F. Gastric cancer. Lancet. 2020;396(10251):635-648. doi:10.1016/S0140-6736(20)31288-5

28. Ychou M, Boige V, Pignon JP, et al. Perioperative Chemotherapy Compared With Surgery Alone for Resectable Gastroesophageal Adenocarcinoma: An FNCLCC and FFCD Multicenter Phase III Trial. JCO. 2011;29(13):1715-1721. doi:10.1200/JCO.2010.33.0597

29. Cunningham D, Allum WH, Stenning SP, et al. Perioperative Chemotherapy versus Surgery Alone for Resectable Gastroesophageal Cancer. New England Journal of Medicine. 2006;355(1):11-20. doi:10.1056/NEJMoa055531

30. Al-Batran SE, Homann N, Pauligk C, et al. Perioperative chemotherapy with fluorouracil plus leucovorin, oxaliplatin, and docetaxel versus fluorouracil or capecitabine plus cisplatin and epirubicin for locally advanced, resectable gastric or gastro-oesophageal junction adenocarcinoma (FLOT4): a randomised, phase 2/3 trial. The Lancet. 2019;393(10184):1948-1957. doi:10.1016/S0140-6736(18)32557-1

31. Gebauer F, Plum PS, Damanakis A, et al. Long-Term Postsurgical Outcomes of Neoadjuvant Chemoradiation (CROSS) Versus Chemotherapy (FLOT) for Multimodal Treatment of Adenocarcinoma of the Esophagus and the

Esophagogastric Junction. Ann Surg Oncol. Published online May 21, 2023. doi:10.1245/s10434-023-13643-9

32. Hoeppner J, Lordick F, Brunner T, et al. ESOPEC: prospective randomized controlled multicenter phase III trial comparing perioperative chemotherapy (FLOT protocol) to neoadjuvant chemoradiation (CROSS protocol) in patients with adenocarcinoma of the esophagus (NCT02509286). BMC Cancer. 2016;16(1):503. doi:10.1186/s12885-016-2564-y

33. Reynolds J, Preston S, O'Neill B, et al. ICORG 10-14: NEOadjuvant trial in Adenocarcinoma of the oEsophagus and oesophagoGastric junction International Study (Neo-AEGIS). BMC Cancer. 2017;17(1):401. doi:10.1186/s12885-017-3386-2

34. Rivera F, Romero C, Jimenez-Fonseca P, et al. Phase II study to evaluate the efficacy of Trastuzumab in combination with Capecitabine and Oxaliplatin in first-line treatment of HER2-positive advanced gastric cancer: HERXO trial. Cancer Chemother Pharmacol. 2019;83(6):1175-1181. doi:10.1007/s00280-019-03820-7

35. Bang YJ, Van Cutsem E, Feyereislova A, et al. Trastuzumab in combination with chemotherapy versus chemotherapy alone for treatment of HER2-positive advanced gastric or gastro-oesophageal junction cancer (ToGA): a phase 3, open-label, randomised controlled trial. Lancet. 2010;376(9742):687-697. doi:10.1016/S0140-6736(10)61121-X

36. Janjigian YY, Shitara K, Moehler M, et al. First-line nivolumab plus chemotherapy versus chemotherapy alone for advanced gastric, gastro-oesophageal junction, and oesophageal adenocarcinoma (CheckMate 649): a randomised, open-label, phase 3 trial. Lancet. 2021;398(10294):27-40. doi:10.1016/S0140-6736(21)00797-2

37. Doki Y, Ajani JA, Kato K, et al. Nivolumab Combination Therapy in Advanced Esophageal Squamous-Cell Carcinoma. N Engl J Med. 2022;386(5):449-462. doi:10.1056/NEJMoa2111380

38. Kato K, Cho BC, Takahashi M, et al. Nivolumab versus chemotherapy in patients with advanced oesophageal squamous cell carcinoma refractory or intolerant to previous chemotherapy (ATTRACTION-3): a multicentre, randomised, open-label, phase 3 trial. The Lancet Oncology. 2019;20(11):1506-1517. doi:10.1016/S1470-2045(19)30626-6

39. Sun JM, Shen L, Shah MA, et al. Pembrolizumab plus chemotherapy versus chemotherapy alone for first-line treatment of advanced oesophageal cancer (KEYNOTE-590): a randomised, placebo-controlled, phase 3 study. Lancet. 2021;398(10302):759-771. doi:10.1016/S0140-6736(21)01234-4

40. Janjigian YY, Kawazoe A, Yañez P, et al. The KEYNOTE-811 trial of dual PD-1 and HER2 blockade in HER2-positive gastric cancer. Nature. 2021;600(7890):727-730. doi:10.1038/s41586-021-04161-3

41. Shah MA, Kojima T, Hochhauser D, et al. Efficacy and Safety of Pembrolizumab for Heavily Pretreated Patients With Advanced, Metastatic Adenocarcinoma or Squamous Cell Carcinoma of the Esophagus: The Phase 2 KEYNOTE-180 Study. JAMA Oncol. 2019;5(4):546-550. doi:10.1001/jamaoncol.2018.5441

42. Kato K, Kojima T, Hochhauser D, et al. Pembrolizumab in previously treated metastatic esophageal cancer: Longer term follow-up from the phase 2 KEYNOTE-180 Study. JCO. 2019;37(15_suppl):4032-4032. doi:10.1200/JCO.2019.37.15_suppl.4032

43. Kojima T, Shah MA, Muro K, et al. Randomized Phase III KEYNOTE-181 Study of Pembrolizumab Versus Chemotherapy in Advanced Esophageal Cancer. J Clin Oncol. 2020;38(35):4138-4148. doi:10.1200/JCO.20.01888

44. Kelly RJ, Ajani JA, Kuzdzal J, et al. Adjuvant Nivolumab in Resected Esophageal or Gastroesophageal Junction Cancer. N Engl J Med. 2021;384(13):1191-1203. doi:10.1056/NEJMoa2032125

45. Paget S. The distribution of secondary growths in cancer of the breast. 1889. Cancer Metastasis Rev. 1989;8(2):98-101.

46. Anderson NM, Simon MC. The tumor microenvironment. Current Biology. 2020;30(16):R921-R925. doi:10.1016/j.cub.2020.06.081

47. de Visser KE, Joyce JA. The evolving tumor microenvironment: From cancer initiation to metastatic outgrowth. Cancer Cell. 2023;41(3):374-403. doi:10.1016/j.ccell.2023.02.016

48. Assaraf YG, Brozovic A, Gonçalves AC, et al. The multi-factorial nature of clinical multidrug resistance in cancer. Drug Resist Updat. 2019;46:100645. doi:10.1016/j.drup.2019.100645

49. Correia AL, Bissell MJ. The tumor microenvironment is a dominant force in multidrug resistance. Drug Resist Updat. 2012;15(1-2):39-49. doi:10.1016/j.drup.2012.01.006

50. Nallasamy P, Nimmakayala RK, Parte S, Are AC, Batra SK, Ponnusamy MP. Tumor microenvironment enriches the stemness features: the architectural event of therapy resistance and metastasis. Mol Cancer. 2022;21(1):225. doi:10.1186/s12943-022-01682-x

51. Chen X, Song E. Turning foes to friends: targeting cancer-associated fibroblasts. Nat Rev Drug Discov. 2019;18(2):99-115. doi:10.1038/s41573-018-0004-1

52. Kobayashi H, Enomoto A, Woods SL, Burt AD, Takahashi M, Worthley DL. Cancer-associated fibroblasts in gastrointestinal cancer. Nat Rev Gastroenterol Hepatol. 2019;16(5):282-295. doi:10.1038/s41575-019-0115-0

53. Chhabra Y, Weeraratna AT. Fibroblasts in cancer: Unity in heterogeneity. Cell. 2023;186(8):1580-1609. doi:10.1016/j.cell.2023.03.016

54. Biffi G, Tuveson DA. Diversity and Biology of Cancer-Associated Fibroblasts. Physiol Rev. 2021;101(1):147-176. doi:10.1152/physrev.00048.2019

55. Galbo PM, Zang X, Zheng D. Molecular Features of Cancer-associated Fibroblast Subtypes and their Implication on Cancer Pathogenesis, Prognosis, and Immunotherapy Resistance. Clin Cancer Res. 2021;27(9):2636-2647.

doi:10.1158/1078-0432.CCR-20-4226

56. Galbo PM, Zang X, Zheng D. Implication of cancer associated fibroblast subtypes on cancer pathogenesis, prognosis, and immunotherapy resistance. Clin Cancer Res. 2021;27(9):2636-2647. doi:10.1158/1078-0432.CCR-20-4226

57. Chen Y, McAndrews KM, Kalluri R. Clinical and therapeutic relevance of cancer-associated fibroblasts. Nat Rev Clin Oncol. 2021;18(12):792-804. doi:10.1038/s41571-021-00546-5

58. Fiori ME, Di Franco S, Villanova L, Bianca P, Stassi G, De Maria R. Cancer-associated fibroblasts as abettors of tumor progression at the crossroads of EMT and therapy resistance. Mol Cancer. 2019;18(1):70. doi:10.1186/s12943-019-0994-2

59. Wu F, Yang J, Liu J, et al. Signaling pathways in cancer-associated fibroblasts and targeted therapy for cancer. Signal Transduct Target Ther. 2021;6(1):218. doi:10.1038/s41392-021-00641-0

60. Hessmann E, Patzak MS, Klein L, et al. Fibroblast drug scavenging increases intratumoural gemcitabine accumulation in murine pancreas cancer. Gut. 2018;67(3):497-507. doi:10.1136/gutjnl-2016-311954

61. Dalin S, Sullivan MR, Lau AN, et al. Deoxycytidine Release from Pancreatic Stellate Cells Promotes Gemcitabine Resistance. Cancer Research. 2019;79(22):5723-5733. doi:10.1158/0008-5472.CAN-19-0960

62. Hesler RA, Huang JJ, Starr MD, et al. TGF-β-induced stromal CYR61 promotes resistance to gemcitabine in pancreatic ductal adenocarcinoma through downregulation of the nucleoside transporters hENT1 and hCNT3. Carcinogenesis. 2016;37(11):1041-1051. doi:10.1093/carcin/bgw093

63. Richards KE, Zeleniak AE, Fishel ML, Wu J, Littlepage LE, Hill R. Cancer-associated fibroblast exosomes regulate survival and proliferation of pancreatic cancer cells. Oncogene. 2017;36(13):1770-1778. doi:10.1038/onc.2016.353

64. Hu C, Xia R, Zhang X, et al. circFARP1 enables cancer-associated

fibroblasts to promote gemcitabine resistance in pancreatic cancer via the LIF/STAT3 axis. Mol Cancer. 2022;21(1):24. doi:10.1186/s12943-022-01501-3

65. McAndrews KM, Chen Y, Darpolor JK, et al. Identification of Functional Heterogeneity of Carcinoma-Associated Fibroblasts with Distinct IL6-Mediated Therapy Resistance in Pancreatic Cancer. Cancer Discov. 2022;12(6):1580-1597. doi:10.1158/2159-8290.CD-20-1484

66. Qi R, Bai Y, Li K, et al. Cancer-associated fibroblasts suppress ferroptosis and induce gemcitabine resistance in pancreatic cancer cells by secreting exosome-derived ACSL4-targeting miRNAs. Drug Resist Updat. 2023;68:100960. doi:10.1016/j.drup.2023.100960

67. Cui Zhou D, Jayasinghe RG, Chen S, et al. Spatially restricted drivers and transitional cell populations cooperate with the microenvironment in untreated and chemo-resistant pancreatic cancer. Nat Genet. 2022;54(9):1390-1405. doi:10.1038/s41588-022-01157-1

68. Nallasamy P, Nimmakayala RK, Karmakar S, et al. Pancreatic Tumor Microenvironment Factor Promotes Cancer Stemness via SPP1-CD44 Axis. Gastroenterology. 2021;161(6):1998-2013.e7. doi:10.1053/j.gastro.2021.08.023

69. Garcia Garcia CJ, Huang Y, Fuentes NR, et al. Stromal HIF2 Regulates Immune Suppression in the Pancreatic Cancer Microenvironment. Gastroenterology. 2022;162(7):2018-2031. doi:10.1053/j.gastro.2022.02.024

70. Ham IH, Oh HJ, Jin H, et al. Targeting interleukin-6 as a strategy to overcome stroma-induced resistance to chemotherapy in gastric cancer. Mol Cancer. 2019;18(1):68. doi:10.1186/s12943-019-0972-8

71. Jin Z, Lu Y, Wu X, et al. The cross-talk between tumor cells and activated fibroblasts mediated by lactate/BDNF/TrkB signaling promotes acquired resistance to anlotinib in human gastric cancer. Redox Biol. 2021;46:102076. doi:10.1016/j.redox.2021.102076

72. Qu X, Liu B, Wang L, et al. Loss of cancer-associated fibroblast-derived

exosomal DACT3-AS1 promotes malignant transformation and ferroptosis-mediated oxaliplatin resistance in gastric cancer. Drug Resist Updat. 2023;68:100936. doi:10.1016/j.drup.2023.100936

73. Huang TX, Tan XY, Huang HS, et al. Targeting cancer-associated fibroblast-secreted WNT2 restores dendritic cell-mediated antitumour immunity. Gut. Published online March 9, 2021. doi:10.1136/gutjnl-2020-322924

74. Chen X, Liu J, Zhang Q, et al. Exosome-mediated transfer of miR-93-5p from cancer-associated fibroblasts confer radioresistance in colorectal cancer cells by downregulating FOXA1 and upregulating TGFB3. J Exp Clin Cancer Res. 2020;39(1):65. doi:10.1186/s13046-019-1507-2

75. Qiu L, Yue J, Ding L, Yin Z, Zhang K, Zhang H. Cancer-associated fibroblasts: An emerging target against esophageal squamous cell carcinoma. Cancer Letters. 2022;546:215860. doi:10.1016/j.canlet.2022.215860

76. McShane R, Arya S, Stewart AJ, Caie PD, Bates M. Prognostic features of the tumour microenvironment in oesophageal adenocarcinoma. Biochim Biophys Acta Rev Cancer. 2021;1876(2):188598. doi:10.1016/j.bbcan.2021.188598

77. Chen Y, Zhu S, Liu T, et al. Epithelial cells activate fibroblasts to promote esophageal cancer development. Cancer Cell. 2023;41(5):903-918.e8. doi:10.1016/j.ccell.2023.03.001

78. Lavon H, Scherz-Shouval R. Insights into the co-evolution of epithelial cells and fibroblasts in the esophageal tumor microenvironment. Cancer Cell. 2023;41(5):826-828. doi:10.1016/j.ccell.2023.03.020

79. Qiu H, Zhang X, Qi J, et al. Identification and characterization of FGFR2+ hematopoietic stem cell-derived fibrocytes as precursors of cancer-associated fibroblasts induced by esophageal squamous cell carcinoma. J Exp Clin Cancer Res. 2022;41(1):240. doi:10.1186/s13046-022-02435-w

80. Dunbar KJ, Karakasheva TA, Tang Q, et al. Tumor-derived CCL5 recruits cancer-associated fibroblasts and promotes tumor cell proliferation in

esophageal squamous cell carcinoma. Mol Cancer Res. Published online April 7, 2023:MCR-22-0872. doi:10.1158/1541-7786.MCR-22-0872

81. Tong Y, Yang L, Yu C, et al. Tumor-Secreted Exosomal lncRNA POU3F3 Promotes Cisplatin Resistance in ESCC by Inducing Fibroblast Differentiation into CAFs. Molecular Therapy - Oncolytics. 2020;18:1-13. doi:10.1016/j.omto.2020.05.014

82. Che Y, Wang J, Li Y, et al. Cisplatin-activated PAI-1 secretion in the cancer-associated fibroblasts with paracrine effects promoting esophageal squamous cell carcinoma progression and causing chemoresistance. Cell Death Dis. 2018;9(7):759. doi:10.1038/s41419-018-0808-2

83. Zhao Q, Huang L, Qin G, et al. Cancer-associated fibroblasts induce monocytic myeloid-derived suppressor cell generation via IL-6/exosomal miR-21-activated STAT3 signaling to promote cisplatin resistance in esophageal squamous cell carcinoma. Cancer Letters. 2021;518:35-48. doi:10.1016/j.canlet.2021.06.009

84. Zhang H, Xie C, Yue J, et al. Cancer-associated fibroblasts mediated chemoresistance by a FOXO1/TGFβ1 signaling loop in esophageal squamous cell carcinoma. Mol Carcinog. 2017;56(3):1150-1163. doi:10.1002/mc.22581

85. Zhang H, Yue J, Jiang Z, et al. CAF-secreted CXCL1 conferred radioresistance by regulating DNA damage response in a ROS-dependent manner in esophageal squamous cell carcinoma. Cell Death Dis. 2017;8(5):e2790. doi:10.1038/cddis.2017.180

86. Zhang H, Hua Y, Jiang Z, et al. Cancer-associated Fibroblast-promoted LncRNA DNM3OS Confers Radioresistance by Regulating DNA Damage Response in Esophageal Squamous Cell Carcinoma. Clin Cancer Res. 2019;25(6):1989-2000. doi:10.1158/1078-0432.CCR-18-0773

87. Chen QY, Li YN, Wang XY, et al. Tumor Fibroblast-Derived FGF2 Regulates Expression of SPRY1 in Esophageal Tumor-Infiltrating T Cells and Plays a Role in T-cell Exhaustion. Cancer Res. 2020;80(24):5583-5596.

doi:10.1158/0008-5472.CAN-20-1542

88. Li L, Wei JR, Dong J, et al. Laminin γ2-mediating T cell exclusion attenuates response to anti-PD-1 therapy. Sci Adv. 2021;7(6):eabc8346. doi:10.1126/sciadv.abc8346

89. Huang TX, Tan XY, Huang HS, et al. Targeting cancer-associated fibroblast-secreted WNT2 restores dendritic cell-mediated antitumour immunity. Gut. 2022;71(2):333-344. doi:10.1136/gutjnl-2020-322924

90. Karakasheva TA, Lin EW, Tang Q, et al. IL-6 Mediates Cross-Talk between Tumor Cells and Activated Fibroblasts in the Tumor Microenvironment. Cancer Res. 2018;78(17):4957-4970. doi:10.1158/0008-5472.CAN-17-2268

91. Ebbing EA, van der Zalm AP, Steins A, et al. Stromal-derived interleukin 6 drives epithelial-to-mesenchymal transition and therapy resistance in esophageal adenocarcinoma. Proc Natl Acad Sci U S A. 2019;116(6):2237-2242. doi:10.1073/pnas.1820459116

92. Sharpe BP, Hayden A, Manousopoulou A, et al. Phosphodiesterase type 5 inhibitors enhance chemotherapy in preclinical models of esophageal adenocarcinoma by targeting cancer-associated fibroblasts. Cell Rep Med. 2022;3(6):100541. doi:10.1016/j.xcrm.2022.100541

93. Bootcov MR, Bauskin AR, Valenzuela SM, et al. MIC-1, a novel macrophage inhibitory cytokine, is a divergent member of the TGF-β superfamily. Proc Natl Acad Sci U S A. 1997;94(21):11514-11519.

94. Kim KS, Baek SJ, Flake GP, Loftin CD, Calvo BF, Eling TE. Expression and regulation of nonsteroidal anti-inflammatory drug-activated gene (NAG-1) in human and mouse tissue. Gastroenterology. 2002;122(5):1388-1398. doi:10.1053/gast.2002.32972

95. Baek SJ, Eling T. Growth differentiation factor 15 (GDF15): A survival protein with therapeutic potential in metabolic diseases. Pharmacol Ther. 2019;198:46-58. doi:10.1016/j.pharmthera.2019.02.008

96. Siddiqui JA, Pothuraju R, Khan P, et al. Pathophysiological role of Growth

Differentiation factor (GDF15) in Obesity, Cancer, and Cachexia. Cytokine Growth Factor Rev. 2022;64:71-83. doi:10.1016/j.cytogfr.2021.11.002

97. Breit SN, Brown DA, Tsai VWW. The GDF15-GFRAL Pathway in Health and Metabolic Disease: Friend or Foe? Annual Review of Physiology. 2021;83(1):127-151. doi:10.1146/annurev-physiol-022020-045449

98. Tsai VWW, Husaini Y, Sainsbury A, Brown DA, Breit SN. The MIC-1/GDF15-GFRAL Pathway in Energy Homeostasis: Implications for Obesity, Cachexia, and Other Associated Diseases. Cell Metab. 2018;28(3):353-368. doi:10.1016/j.cmet.2018.07.018

99. Suriben R, Chen M, Higbee J, et al. Antibody-mediated inhibition of GDF15-GFRAL activity reverses cancer cachexia in mice. Nat Med. 2020;26(8):1264-1270. doi:10.1038/s41591-020-0945-x

100. Benichou O, Coskun T, Gonciarz MD, et al. Discovery, development, and clinical proof of mechanism of LY3463251, a long-acting GDF15 receptor agonist. Cell Metab. 2023;35(2):274-286.e10. doi:10.1016/j.cmet.2022.12.011

101. Wiklund FE, Bennet AM, Magnusson PKE, et al. Macrophage inhibitory cytokine-1 (MIC-1/GDF15): a new marker of all-cause mortality. Aging Cell. 2010;9(6):1057-1064. doi:10.1111/j.1474-9726.2010.00629.x

102. Arfsten H, Cho A, Freitag C, et al. GDF-15 in solid vs non-solid treatment-naïve malignancies. Eur J Clin Invest. 2019;49(11):e13168. doi:10.1111/eci.13168

103. Wang Y, Jiang T, Jiang M, Gu S. Appraising growth differentiation factor 15 as a promising biomarker in digestive system tumors: a meta-analysis. BMC Cancer. 2019;19(1):177. doi:10.1186/s12885-019-5385-y

104. Liu JY, Dong XX, Lu JN, et al. Utility of GDF-15 as a diagnostic biomarker in gastric cancer: an investigation combining GEO, TCGA and meta-analysis. FEBS Open Bio. 2019;9(1):35-42. doi:10.1002/2211-5463.12537

105. Ge X, Zhang X, Ma Y, Chen S, Chen Z, Li M. Diagnostic value of macrophage inhibitory cytokine 1 as a novel prognostic biomarkers for early

gastric cancer screening. J Clin Lab Anal. 2021;35(1):e23568. doi:10.1002/jcla.23568

106. Mehta RS, Song M, Bezawada N, et al. A prospective study of macrophage inhibitory cytokine-1 (MIC-1/GDF15) and risk of colorectal cancer. J Natl Cancer Inst. 2014;106(4):dju016. doi:10.1093/jnci/dju016

107. Danta M, Barber DA, Zhang HP, et al. Macrophage inhibitory cytokine-1/growth differentiation factor-15 as a predictor of colonic neoplasia. Aliment Pharmacol Ther. 2017;46(3):347-354. doi:10.1111/apt.14156

108. Brown DA, Ward RL, Buckhaults P, et al. MIC-1 Serum Level and Genotype: Associations with Progress and Prognosis of Colorectal Carcinoma1. Clinical Cancer Research. 2003;9(7):2642-2650.

109. Li C, Wang X, Casal I, et al. Growth differentiation factor 15 is a promising diagnostic and prognostic biomarker in colorectal cancer. J Cell Mol Med. 2016;20(8):1420-1426. doi:10.1111/jcmm.12830

110. Mehta RS, Chong DQ, Song M, et al. Association Between Plasma Levels of Macrophage Inhibitory Cytokine-1 Before Diagnosis of Colorectal Cancer and Mortality. Gastroenterology. 2015;149(3):614-622. doi:10.1053/j.gastro.2015.05.038

111. Wallin U, Glimelius B, Jirström K, et al. Growth differentiation factor 15: a prognostic marker for recurrence in colorectal cancer. Br J Cancer. 2011;104(10):1619-1627. doi:10.1038/bjc.2011.112

112. Barderas R, Mendes M, Torres S, et al. In-depth characterization of the secretome of colorectal cancer metastatic cells identifies key proteins in cell adhesion, migration, and invasion. Mol Cell Proteomics. 2013;12(6):1602-1620. doi:10.1074/mcp.M112.022848

113. Brown DA, Hance KW, Rogers CJ, et al. Serum macrophage inhibitory cytokine-1 (MIC-1/GDF15): a potential screening tool for the prevention of colon cancer? Cancer Epidemiol Biomarkers Prev. 2012;21(2):337-346. doi:10.1158/1055-9965.EPI-11-0786

114. Wang XB, Jiang XR, Yu XY, et al. Macrophage inhibitory factor 1 acts as a potential biomarker in patients with esophageal squamous cell carcinoma and is a target for antibody-based therapy. Cancer Sci. 2014;105(2):176-185. doi:10.1111/cas.12331

115. Urakawa N, Utsunomiya S, Nishio M, et al. GDF15 derived from both tumor-associated macrophages and esophageal squamous cell carcinomas contributes to tumor progression via Akt and Erk pathways. Lab Invest. 2015;95(5):491-503. doi:10.1038/labinvest.2015.36

116. Lu ZH, Yang L, Yu JW, et al. Weight loss correlates with macrophage inhibitory cytokine-1 expression and might influence outcome in patients with advanced esophageal squamous cell carcinoma. Asian Pac J Cancer Prev. 2014;15(15):6047-6052. doi:10.7314/apjcp.2014.15.15.6047

117. Fisher OM, Levert-Mignon AJ, Lord SJ, et al. MIC-1/GDF15 in Barrett's oesophagus and oesophageal adenocarcinoma. Br J Cancer. 2015;112(8):1384-1391. doi:10.1038/bjc.2015.100

118. Fisher OM, Levert-Mignon AJ, Lord SJ, et al. MIC-1/GDF15 in Barrett's oesophagus and oesophageal adenocarcinoma. British Journal of Cancer. 2015;112(8):1384-1391. doi:10.1038/bjc.2015.100

119. Skipworth RJE, Deans D a. C, Tan BHL, et al. Plasma MIC-1 correlates with systemic inflammation but is not an independent determinant of nutritional status or survival in oesophago-gastric cancer. Br J Cancer. 2010;102(4):665-672. doi:10.1038/sj.bjc.6605532

120. Spanopoulou A, Gkretsi V. Growth differentiation factor 15 (GDF15) in cancer cell metastasis: from the cells to the patients. Clin Exp Metastasis. 2020;37(4):451-464. doi:10.1007/s10585-020-10041-3

121. Rochette L, Méloux A, Zeller M, Cottin Y, Vergely C. Functional roles of GDF15 in modulating microenvironment to promote carcinogenesis. Biochim Biophys Acta Mol Basis Dis. 2020;1866(8):165798. doi:10.1016/j.bbadis.2020.165798

122. Modi A, Dwivedi S, Roy D, et al. Growth differentiation factor 15 and its role in carcinogenesis: an update. Growth Factors. 2019;37(3-4):190-207. doi:10.1080/08977194.2019.1685988

123. Jang TJ, Kim NI, Lee CH. Proapoptotic activity of NAG-1 is cell type specific and not related to COX-2 expression. Apoptosis. 2006;11(7):1131-1138. doi:10.1007/s10495-006-8160-x

124. Jang TJ, Kang HJ, Kim JR, Yang CH. Non-steroidal anti-inflammatory drug activated gene (NAG-1) expression is closely related to death receptor-4 and -5 induction, which may explain sulindac sulfide induced gastric cancer cell apoptosis. Carcinogenesis. 2004;25(10):1853-1858. doi:10.1093/carcin/bgh199

125. Pang RP, Zhou JG, Zeng ZR, et al. Celecoxib induces apoptosis in COX-2 deficient human gastric cancer cells through Akt/GSK3beta/NAG-1 pathway. Cancer Lett. 2007;251(2):268-277. doi:10.1016/j.canlet.2006.11.032

126. Kim KK, Lee JJ, Yang Y, You KH, Lee JH. Macrophage inhibitory cytokine-1 activates AKT and ERK-1/2 via the transactivation of ErbB2 in human breast and gastric cancer cells. Carcinogenesis. 2008;29(4):704-712. doi:10.1093/carcin/bgn031

127. Joo M, Kim D, Lee MW, Lee HJ, Kim JM. GDF15 Promotes Cell Growth, Migration, and Invasion in Gastric Cancer by Inducing STAT3 Activation. Int J Mol Sci. 2023;24(3):2925. doi:10.3390/ijms24032925

128. Lee DH, Yang Y, Lee SJ, et al. Macrophage Inhibitory Cytokine-1 Induces the Invasiveness of Gastric Cancer Cells by Up-Regulating the Urokinase-type Plasminogen Activator System1. Cancer Research. 2003;63(15):4648-4655.

129. Guo J, Bian Y, Wang Y, Chen L, Yu A, Sun X. S100A4 influences cancer stem cell-like properties of MGC803 gastric cancer cells by regulating GDF15 expression. Int J Oncol. 2016;49(2):559-568. doi:10.3892/ijo.2016.3556

130. Yu S, Li Q, Yu Y, et al. Activated HIF1α of tumor cells promotes chemoresistance development via recruiting GDF15-producing tumor-associated macrophages in gastric cancer. Cancer Immunol Immunother. 2020;69(10):1973-1987. doi:10.1007/s00262-020-02598-5

131. Shimizu D, Ishikawa T, Ichikawa Y, et al. Prediction of chemosensitivity of colorectal cancer to 5-fluorouracil by gene expression profiling with cDNA microarrays. Int J Oncol. 2005;27(2):371-376.

132. Proutski I, Stevenson L, Allen WL, et al. Prostate-derived factor—a novel inhibitor of drug-induced cell death in colon cancer cells. Molecular Cancer Therapeutics. 2009;8(9):2566-2574. doi:10.1158/1535-7163.MCT-09-0158

133. Ding Y, Hao K, Li Z, et al. c-Fos separation from Lamin A/C by GDF15 promotes colon cancer invasion and metastasis in inflammatory microenvironment. J Cell Physiol. 2020;235(5):4407-4421. doi:10.1002/jcp.29317

134. Ishige T, Nishimura M, Satoh M, et al. Combined Secretomics and Transcriptomics Revealed Cancer-Derived GDF15 is Involved in Diffuse-Type Gastric Cancer Progression and Fibroblast Activation. Sci Rep. 2016;6:21681. doi:10.1038/srep21681

135. Guo Y, Ayers JL, Carter KT, et al. Senescence-associated tissue microenvironment promotes colon cancer formation through the secretory factor GDF15. Aging Cell. 2019;18(6):e13013. doi:10.1111/acel.13013

136. Okamoto M, Koma YI, Kodama T, Nishio M, Shigeoka M, Yokozaki H. Growth Differentiation Factor 15 Promotes Progression of Esophageal Squamous Cell Carcinoma via TGF-β Type II Receptor Activation. Pathobiology. 2020;87(2):100-113. doi:10.1159/000504394

137. Du Y, Ma Y, Zhu Q, et al. GDF15 negatively regulates chemosensitivity via TGFBR2-AKT pathway-dependent metabolism in esophageal squamous cell carcinoma. Front Med. 2023;17(1):119-131. doi:10.1007/s11684-022-

0949-7

138. Hofer M, Lutolf MP. Engineering organoids. Nat Rev Mater. 2021;6(5):402-420. doi:10.1038/s41578-021-00279-y

139. LeSavage BL, Suhar RA, Broguiere N, Lutolf MP, Heilshorn SC. Next-generation cancer organoids. Nat Mater. 2022;21(2):143-159. doi:10.1038/s41563-021-01057-5

140. Wilson HV. A New Method by Which Sponges May Be Artificially Reared. Science. 1907;25(649):912-915. doi:10.1126/science.25.649.912

141. Harrison RG. Observations on the living developing nerve fiber. Proceedings of the Society for Experimental Biology and Medicine. 1906;4(1):140-143. doi:10.3181/00379727-4-98

142. Eiraku M, Watanabe K, Matsuo-Takasaki M, et al. Self-Organized Formation of Polarized Cortical Tissues from ESCs and Its Active Manipulation by Extrinsic Signals. Cell Stem Cell. 2008;3(5):519-532. doi:10.1016/j.stem.2008.09.002

143. Sato T, Vries RG, Snippert HJ, et al. Single Lgr5 stem cells build crypt-villus structures in vitro without a mesenchymal niche. Nature. 2009;459(7244):262-265. doi:10.1038/nature07935

144. Corrò C, Novellasdemunt L, Li VSW. A brief history of organoids. American Journal of Physiology-Cell Physiology. 2020;319(1):C151-C165. doi:10.1152/ajpcell.00120.2020

145. Simian M, Bissell MJ. Organoids: A historical perspective of thinking in three dimensions. J Cell Biol. 2017;216(1):31-40. doi:10.1083/jcb.201610056

146. Perrone F, Zilbauer M. Biobanking of human gut organoids for translational research. Exp Mol Med. 2021;53(10):1451-1458. doi:10.1038/s12276-021-00606-x

147. Nikolaev M, Mitrofanova O, Broguiere N, et al. Homeostatic mini-intestines through scaffold-guided organoid morphogenesis. Nature. 2020;585(7826):574-578. doi:10.1038/s41586-020-2724-8

148. Li VSW. Modelling intestinal inflammation and infection using “mini-gut” organoids. Nat Rev Gastroenterol Hepatol. 2021;18(2):89-90. doi:10.1038/s41575-020-00391-4

149. Seidlitz T, Merker SR, Rothe A, et al. Human gastric cancer modelling using organoids. Gut. 2019;68(2):207-217. doi:10.1136/gutjnl-2017-314549

150. Vlachogiannis G, Hedayat S, Vatsiou A, et al. Patient-derived organoids model treatment response of metastatic gastrointestinal cancers. Science. 2018;359(6378):920-926. doi:10.1126/science.aao2774

151. Huang L, Desai R, Conrad DN, et al. Commitment and oncogene-induced plasticity of human stem cell-derived pancreatic acinar and ductal organoids. Cell Stem Cell. 2021;28(6):1090-1104.e6. doi:10.1016/j.stem.2021.03.022

152. Breunig M, Merkle J, Wagner M, et al. Modeling plasticity and dysplasia of pancreatic ductal organoids derived from human pluripotent stem cells. Cell Stem Cell. 2021;28(6):1105-1124.e19. doi:10.1016/j.stem.2021.03.005

153. Marsee A, Roos FJM, Verstegen MMA, et al. Building consensus on definition and nomenclature of hepatic, pancreatic, and biliary organoids. Cell Stem Cell. 2021;28(5):816-832. doi:10.1016/j.stem.2021.04.005

154. Prior N, Inacio P, Huch M. Liver organoids: from basic research to therapeutic applications. Gut. 2019;68(12):2228-2237. doi:10.1136/gutjnl-2019-319256

155. Little MH, Combes AN. Kidney organoids: accurate models or fortunate accidents. Genes Dev. 2019;33(19-20):1319-1345. doi:10.1101/gad.329573.119

156. Nishinakamura R. Human kidney organoids: progress and remaining challenges. Nat Rev Nephrol. 2019;15(10):613-624. doi:10.1038/s41581-019-0176-x

157. Sachs N, de Ligt J, Kopper O, et al. A Living Biobank of Breast Cancer Organoids Captures Disease Heterogeneity. Cell. 2018;172(1-2):373-386.e10.

doi:10.1016/j.cell.2017.11.010

158. Chen P, Zhang X, Ding R, et al. Patient-Derived Organoids Can Guide Personalized-Therapies for Patients with Advanced Breast Cancer. Adv Sci (Weinh). 2021;8(22):e2101176. doi:10.1002/advs.202101176

159. Sachs N, Papaspyropoulos A, Zomer‐van Ommen DD, et al. Long‐term expanding human airway organoids for disease modeling. EMBO J. 2019;38(4):e100300. doi:10.15252/embj.2018100300

160. Miller AJ, Dye BR, Ferrer-Torres D, et al. Generation of lung organoids from human pluripotent stem cells in vitro. Nat Protoc. 2019;14(2):518-540. doi:10.1038/s41596-018-0104-8

161. Kim M, Mun H, Sung CO, et al. Patient-derived lung cancer organoids as in vitro cancer models for therapeutic screening. Nat Commun. 2019;10(1):3991. doi:10.1038/s41467-019-11867-6

162. van der Vaart J, Bosmans L, Sijbesma SF, et al. Adult mouse and human organoids derived from thyroid follicular cells and modeling of Graves' hyperthyroidism. Proc Natl Acad Sci U S A. 2021;118(51):e2117017118. doi:10.1073/pnas.2117017118

163. Liang J, Qian J, Yang L, et al. Modeling Human Thyroid Development by Fetal Tissue-Derived Organoid Culture. Adv Sci (Weinh). 2022;9(9):e2105568. doi:10.1002/advs.202105568

164. Tan HY, Cho H, Lee LP. Human mini-brain models. Nat Biomed Eng. 2021;5(1):11-25. doi:10.1038/s41551-020-00643-3

165. Cakir B, Xiang Y, Tanaka Y, et al. Engineering of human brain organoids with a functional vascular-like system. Nat Methods. 2019;16(11):1169-1175. doi:10.1038/s41592-019-0586-5

166. Zhao H, Cheng Y, Kalra A, et al. Generation and multiomic profiling of a TP53/CDKN2A double-knockout gastroesophageal junction organoid model. Sci Transl Med. 2022;14(673):eabq6146. doi:10.1126/scitranslmed.abq6146

167. Karakasheva TA, Kijima T, Shimonosono M, et al. Generation and

Characterization of Patient‐Derived Head and Neck, Oral, and Esophageal Cancer Organoids. Current Protocols in Stem Cell Biology. 2020;53(1). doi:10.1002/cpsc.109

168. Trisno SL, Philo KED, McCracken KW, et al. Esophageal Organoids from Human Pluripotent Stem Cells Delineate Sox2 Functions during Esophageal Specification. Cell Stem Cell. 2018;23(4):501-515.e7. doi:10.1016/j.stem.2018.08.008

169. Clevers H. Modeling Development and Disease with Organoids. Cell. 2016;165(7):1586-1597. doi:10.1016/j.cell.2016.05.082

170. Kim J, Koo BK, Knoblich JA. Human organoids: model systems for human biology and medicine. Nat Rev Mol Cell Biol. 2020;21(10):571-584. doi:10.1038/s41580-020-0259-3

171. Tosca EM, Ronchi D, Facciolo D, Magni P. Replacement, Reduction, and Refinement of Animal Experiments in Anticancer Drug Development: The Contribution of 3D In Vitro Cancer Models in the Drug Efficacy Assessment. Biomedicines. 2023;11(4):1058. doi:10.3390/biomedicines11041058

172. Li W, Zhou Z, Zhou X, et al. 3D Biomimetic Models to Reconstitute Tumor Microenvironment In Vitro: Spheroids, Organoids, and Tumor-on-a-Chip. Adv Healthc Mater. Published online March 14, 2023:e2202609. doi:10.1002/adhm.202202609

173. Zanoni M, Cortesi M, Zamagni A, Arienti C, Pignatta S, Tesei A. Modeling neoplastic disease with spheroids and organoids. J Hematol Oncol. 2020;13(1):97. doi:10.1186/s13045-020-00931-0

174. Lee NP, Chan CM, Tung LN, Wang HK, Law S. Tumor xenograft animal models for esophageal squamous cell carcinoma. J Biomed Sci. 2018;25(1):66. doi:10.1186/s12929-018-0468-7

175. Saito T, Ohashi S, Mizumoto A, Muto M. Patient-derived tumor models of esophageal cancer. Enzymes. 2019;46:97-111. doi:10.1016/bs.enz.2019.10.003

176. Liu H, Wang X. Esophageal organoids: applications and future prospects. J Mol Med (Berl). Published online June 29, 2023. doi:10.1007/s00109-023-02340-5

177. Karakasheva TA, Gabre JT, Sachdeva UM, et al. Patient-derived organoids as a platform for modeling a patient's response to chemoradiotherapy in esophageal cancer. Sci Rep. 2021;11:21304. doi:10.1038/s41598-021-00706-8

178. Derouet MF, Allen J, Wilson GW, et al. Towards personalized induction therapy for esophageal adenocarcinoma: organoids derived from endoscopic biopsy recapitulate the pre-treatment tumor. Sci Rep. 2020;10(1):14514. doi:10.1038/s41598-020-71589-4

179. Li X, Francies HE, Secrier M, et al. Organoid cultures recapitulate esophageal adenocarcinoma heterogeneity providing a model for clonality studies and precision therapeutics. Nat Commun. 2018;9(1):2983. doi:10.1038/s41467-018-05190-9

180. Dings MPG, van der Zalm AP, Bootsma S, et al. Estrogen-related receptor alpha drives mitochondrial biogenesis and resistance to neoadjuvant chemoradiation in esophageal cancer. Cell Rep Med. 2022;3(11):100802. doi:10.1016/j.xcrm.2022.100802

181. Scott SJ, Li X, Jammula S, et al. Evidence that polyploidy in esophageal adenocarcinoma originates from mitotic slippage caused by defective chromosome attachments. Cell Death Differ. 2021;28(7):2179-2193. doi:10.1038/s41418-021-00745-8

182. Kijima T, Nakagawa H, Shimonosono M, et al. Three-Dimensional Organoids Reveal Therapy Resistance of Esophageal and Oropharyngeal Squamous Cell Carcinoma Cells. Cellular and Molecular Gastroenterology and Hepatology. 2019;7(1):73-91. doi:10.1016/j.jcmgh.2018.09.003

183. Shimonosono M, Tanaka K, Flashner S, et al. Alcohol Metabolism Enriches Squamous Cell Carcinoma Cancer Stem Cells That Survive Oxidative

Stress via Autophagy. Biomolecules. 2021;11(10):1479. doi:10.3390/biom11101479

184. Kasagi Y, Chandramouleeswaran PM, Whelan KA, et al. The Esophageal Organoid System Reveals Functional Interplay Between Notch and Cytokines in Reactive Epithelial Changes. Cell Mol Gastroenterol Hepatol. 2018;5(3):333-352. doi:10.1016/j.jcmgh.2017.12.013

185. Ko KP, Huang Y, Zhang S, et al. Key Genetic Determinants Driving Esophageal Squamous Cell Carcinoma Initiation and Immune Evasion. Gastroenterology. Published online May 29, 2023:S0016-5085(23)00803-X. doi:10.1053/j.gastro.2023.05.030

186. Zheng B, Ko KP, Fang X, et al. A new murine esophageal organoid culture method and organoid-based model of esophageal squamous cell neoplasia. iScience. 2021;24(12):103440. doi:10.1016/j.isci.2021.103440

187. Nowicki-Osuch K, Zhuang L, Jammula S, et al. Molecular phenotyping reveals the identity of Barrett's esophagus and its malignant transition. Science. 2021;373(6556):760-767. doi:10.1126/science.abd1449

188. De A, Zhou J, Liu P, et al. Forkhead box F1 induces columnar phenotype and epithelial-to-mesenchymal transition in esophageal squamous cells to initiate Barrett's like metaplasia. Lab Invest. 2021;101(6):745-759. doi:10.1038/s41374-021-00534-4

189. Zhang Q, Agoston AT, Pham TH, et al. Acidic Bile Salts Induce Epithelial to Mesenchymal Transition via VEGF Signaling in Non-Neoplastic Barrett's Cells. Gastroenterology. 2019;156(1):130-144.e10. doi:10.1053/j.gastro.2018.09.046

190. Zhang Q, Bansal A, Dunbar KB, et al. A human Barrett's esophagus organoid system reveals epithelial-mesenchymal plasticity induced by acid and bile salts. Am J Physiol Gastrointest Liver Physiol. 2022;322(6):G598-G614. doi:10.1152/ajpgi.00017.2022

191. Zhang Y, Yang Y, Jiang M, et al. 3D Modeling of Esophageal

Development using Human PSC-Derived Basal Progenitors Reveals a Critical Role for Notch Signaling. Cell Stem Cell. 2018;23(4):516-529.e5. doi:10.1016/j.stem.2018.08.009

192. Hutton B, Salanti G, Caldwell DM, et al. The PRISMA extension statement for reporting of systematic reviews incorporating network meta-analyses of health care interventions: checklist and explanations. Ann Intern Med. 2015;162(11):777-784. doi:10.7326/M14-2385

193. Fan N, Wang Z, Zhou C, et al. Comparison of outcomes between neoadjuvant chemoradiotherapy and neoadjuvant chemotherapy in patients with locally advanced esophageal cancer: A network meta-analysis. eClinicalMedicine. 2021;42. doi:10.1016/j.eclinm.2021.101183

194. Sterne JAC, Savović J, Page MJ, et al. RoB 2: a revised tool for assessing risk of bias in randomised trials. BMJ. 2019;366:l4898. doi:10.1136/bmj.l4898

195. Tierney JF, Stewart LA, Ghersi D, Burdett S, Sydes MR. Practical methods for incorporating summary time-to-event data into meta-analysis. Trials. 2007;8(1):16. doi:10.1186/1745-6215-8-16

196. Higgins JPT, Thompson SG, Deeks JJ, Altman DG. Measuring inconsistency in meta-analyses. BMJ. 2003;327(7414):557-560.

197. Valkenhoef G van. GeMTC R package. Published online June 15, 2020. https://github.com/gertvv/gemtc

198. Fan N, Raatz L, Chon SH, Quaas A, Bruns C, Zhao Y. Subculture and Cryopreservation of Esophageal Adenocarcinoma Organoids: Pros and Cons for Single Cell Digestion. JoVE (Journal of Visualized Experiments). 2022;(185):e63281. doi:10.3791/63281

199. Krämer M, Plum PS, Velazquez Camacho O, et al. Cell type-specific transcriptomics of esophageal adenocarcinoma as a scalable alternative for single cell transcriptomics. Mol Oncol. 2020;14(6):1170-1184. doi:10.1002/1878-0261.12680

200. Dobin A, Davis CA, Schlesinger F, et al. STAR: ultrafast universal RNA-seq aligner. Bioinformatics. 2013;29(1):15-21. doi:10.1093/bioinformatics/bts635

201. Love MI, Huber W, Anders S. Moderated estimation of fold change and dispersion for RNA-seq data with DESeq2. Genome Biol. 2014;15(12):550. doi:10.1186/s13059-014-0550-8

202. Tyanova S, Temu T, Cox J. The MaxQuant computational platform for mass spectrometry-based shotgun proteomics. Nat Protoc. 2016;11(12):2301-2319. doi:10.1038/nprot.2016.136

203. Cerami E, Gao J, Dogrusoz U, et al. The cBio Cancer Genomics Portal: An Open Platform for Exploring Multidimensional Cancer Genomics Data. Cancer Discovery. 2012;2(5):401-404. doi:10.1158/2159-8290.CD-12-0095

204. Barrett T, Wilhite SE, Ledoux P, et al. NCBI GEO: archive for functional genomics data sets—update. Nucleic Acids Research. 2013;41(D1):D991-D995. doi:10.1093/nar/gks1193

205. Wang Q, Ma C, Kemmner W. Wdr66 is a novel marker for risk stratification and involved in epithelial-mesenchymal transition of esophageal squamous cell carcinoma. BMC Cancer. 2013;13:137. doi:10.1186/1471-2407-13-137

206. Kitagawa Y, Uno T, Oyama T, et al. Esophageal cancer practice guidelines 2017 edited by the Japan esophageal society: part 2. Esophagus. 2019;16(1):25-43. doi:10.1007/s10388-018-0642-8

207. von Döbeln GA, Klevebro F, Jacobsen AB, et al. Neoadjuvant chemotherapy versus neoadjuvant chemoradiotherapy for cancer of the esophagus or gastroesophageal junction: long-term results of a randomized clinical trial. Diseases of the Esophagus. 2019;32(2). doi:10.1093/dote/doy078

208. Stahl M, Walz MK, Riera-Knorrenschild J, et al. Preoperative chemotherapy versus chemoradiotherapy in locally advanced adenocarcinomas of the oesophagogastric junction (POET): Long-term results

of a controlled randomised trial. European Journal of Cancer. 2017;81:183-190. doi:10.1016/j.ejca.2017.04.027

209. Burmeister BH, Thomas JM, Burmeister EA, et al. Is concurrent radiation therapy required in patients receiving preoperative chemotherapy for adenocarcinoma of the oesophagus? A randomised phase II trial. European Journal of Cancer. 2011;47(3):354-360. doi:10.1016/j.ejca.2010.09.009

210. Nygaard K, Hagen S, Hansen HS, et al. Pre-operative radiotherapy prolongs survival in operable esophageal carcinoma: A randomized, multicenter study of pre-operative radiotherapy and chemotherapy. The second scandinavian trial in esophageal cancer. World J Surg. 1992;16(6):1104-1109. doi:10.1007/BF02067069

211. Rouse B, Chaimani A, Li T. Network meta-analysis: an introduction for clinicians. Intern Emerg Med. 2017;12(1):103-111. doi:10.1007/s11739-016-1583-7

212. Chen X, Song E. Turning foes to friends: targeting cancer-associated fibroblasts. Nature Reviews Drug Discovery. 2019;18(2):99-115. doi:10.1038/s41573-018-0004-1

213. Lin EW, Karakasheva TA, Hicks PD, Bass AJ, Rustgi AK. The tumor microenvironment in esophageal cancer. Oncogene. 2016;35(41):5337-5349. doi:10.1038/onc.2016.34

214. Sugiyama MG, Fairn GD, Antonescu CN. Akt-ing Up Just About Everywhere: Compartment-Specific Akt Activation and Function in Receptor Tyrosine Kinase Signaling. Front Cell Dev Biol. 2019;7:70. doi:10.3389/fcell.2019.00070

215. Hua H, Zhang H, Chen J, Wang J, Liu J, Jiang Y. Targeting Akt in cancer for precision therapy. J Hematol Oncol. 2021;14:128. doi:10.1186/s13045-021-01137-8

216. Yu L, Wei J, Liu P. Attacking the PI3K/Akt/mTOR signaling pathway for targeted therapeutic treatment in human cancer. Semin Cancer Biol.

2022;85:69-94. doi:10.1016/j.semcancer.2021.06.019

217. Laws A, Tao R, Wang S, Padhiar A, Goring S. A Comparison of National Guidelines for Network Meta-Analysis. Value Health. 2019;22(10):1178-1186. doi:10.1016/j.jval.2019.05.013

218. Hoppe S, Jonas C, Wenzel MC, et al. Genomic and Transcriptomic Characteristics of Esophageal Adenocarcinoma. Cancers (Basel). 2021;13(17):4300. doi:10.3390/cancers13174300

219. Findlay JM, Castro-Giner F, Makino S, et al. Differential clonal evolution in oesophageal cancers in response to neo-adjuvant chemotherapy. Nat Commun. 2016;7:11111. doi:10.1038/ncomms11111

220. Noorani A, Bornschein J, Lynch AG, et al. A comparative analysis of whole genome sequencing of esophageal adenocarcinoma pre- and post-chemotherapy. Genome Res. 2017;27(6):902-912. doi:10.1101/gr.214296.116

221. Murugaesu N, Wilson GA, Birkbak NJ, et al. Tracking the genomic evolution of esophageal adenocarcinoma through neoadjuvant chemotherapy. Cancer Discov. 2015;5(8):821-831. doi:10.1158/2159-8290.CD-15-0412

222. Hao D, He S, Harada K, et al. Integrated genomic profiling and modelling for risk stratification in patients with advanced oesophagogastric adenocarcinoma. Gut. 2021;70(11):2055-2065. doi:10.1136/gutjnl-2020-322707

223. Li J, Zeng Z, Jiang X, et al. Stromal microenvironment promoted infiltration in esophageal adenocarcinoma and squamous cell carcinoma: a multi-cohort gene-based analysis. Sci Rep. 2020;10(1):18589. doi:10.1038/s41598-020-75541-4

224. Zhai Y, Zhang J, Wang H, et al. Growth differentiation factor 15 contributes to cancer-associated fibroblasts-mediated chemo-protection of AML cells. J Exp Clin Cancer Res. 2016;35(1):147. doi:10.1186/s13046-016-0405-0

225. Bruzzese F, Hägglöf C, Leone A, et al. Local and Systemic

Protumorigenic Effects of Cancer-Associated Fibroblast-Derived GDF15. Cancer Research. 2014;74(13):3408-3417. doi:10.1158/0008-5472.CAN-13-2259

226. Olsen OE, Skjærvik A, Størdal BF, Sundan A, Holien T. TGF-β contamination of purified recombinant GDF15. PLoS One. 2017;12(11):e0187349. doi:10.1371/journal.pone.0187349

227. Mullican SE, Lin-Schmidt X, Chin CN, et al. GFRAL is the receptor for GDF15 and the ligand promotes weight loss in mice and nonhuman primates. Nat Med. 2017;23(10):1150-1157. doi:10.1038/nm.4392

228. Yang L, Chang CC, Sun Z, et al. GFRAL is the receptor for GDF15 and is required for the anti-obesity effects of the ligand. Nat Med. 2017;23(10):1158-1166. doi:10.1038/nm.4394

229. Jin Y, Meng Q, Zhang B, et al. Cancer-associated fibroblasts-derived exosomal miR-3656 promotes the development and progression of esophageal squamous cell carcinoma via the ACAP2/PI3K-AKT signaling pathway. Int J Biol Sci. 2021;17(14):3689-3701. doi:10.7150/ijbs.62571

230. Sakamoto H, Koma YI, Higashino N, et al. PAI-1 derived from cancer-associated fibroblasts in esophageal squamous cell carcinoma promotes the invasion of cancer cells and the migration of macrophages. Lab Invest. 2021;101(3):353-368. doi:10.1038/s41374-020-00512-2

231. Bosc C, Selak MA, Sarry JE. Resistance Is Futile: Targeting Mitochondrial Energetics and Metabolism to Overcome Drug Resistance in Cancer Treatment. Cell Metabolism. 2017;26(5):705-707. doi:10.1016/j.cmet.2017.10.013

232. Cocetta V, Ragazzi E, Montopoli M. Mitochondrial Involvement in Cisplatin Resistance. Int J Mol Sci. 2019;20(14):3384. doi:10.3390/ijms20143384

233. Aichler M, Elsner M, Ludyga N, et al. Clinical response to chemotherapy in oesophageal adenocarcinoma patients is linked to defects in mitochondria. J

Pathol. 2013;230(4):410-419. doi:10.1002/path.4199

234. Buckley AM, Dunne MR, Lynam-Lennon N, et al. Pyrazinib (P3), [(E)-2-(2-Pyrazin-2-yl-vinyl)-phenol], a small molecule pyrazine compound enhances radiosensitivity in oesophageal adenocarcinoma. Cancer Lett. 2019;447:115-129. doi:10.1016/j.canlet.2019.01.009

235. Conte M, Martucci M, Chiariello A, Franceschi C, Salvioli S. Mitochondria, immunosenescence and inflammaging: a role for mitokines? Semin Immunopathol. 2020;42(5):607-617. doi:10.1007/s00281-020-00813-0

236. Klaus S, Igual Gil C, Ost M. Regulation of diurnal energy balance by mitokines. Cell Mol Life Sci. 2021;78(7):3369-3384. doi:10.1007/s00018-020-03748-9

237. Khan NA, Nikkanen J, Yatsuga S, et al. mTORC1 Regulates Mitochondrial Integrated Stress Response and Mitochondrial Myopathy Progression. Cell Metab. 2017;26(2):419-428.e5. doi:10.1016/j.cmet.2017.07.007

238. Zhou X, Trinh-Minh T, Tran-Manh C, et al. Impaired Mitochondrial Transcription Factor A Expression Promotes Mitochondrial Damage to Drive Fibroblast Activation and Fibrosis in Systemic Sclerosis. Arthritis Rheumatol. 2022;74(5):871-881. doi:10.1002/art.42033

239. Lin Y, Ji K, Ma X, et al. Accuracy of FGF-21 and GDF-15 for the diagnosis of mitochondrial disorders: A meta-analysis. Ann Clin Transl Neurol. 2020;7(7):1204-1213. doi:10.1002/acn3.51104

240. Wedel S, Martic I, Guerrero Navarro L, et al. Depletion of growth differentiation factor 15 (GDF15) leads to mitochondrial dysfunction and premature senescence in human dermal fibroblasts. Aging Cell. 2023;22(1):e13752. doi:10.1111/acel.13752

241. Wang Y, Chen C, Chen J, et al. Overexpression of NAG-1/GDF15 prevents hepatic steatosis through inhibiting oxidative stress-mediated dsDNA release and AIM2 inflammasome activation. Redox Biol. 2022;52:102322.

doi:10.1016/j.redox.2022.102322

242. Farin HF, Mosa MH, Ndreshkjana B, et al. Colorectal cancer organoid-stroma biobank allows subtype-specific assessment of individualized therapy responses. Cancer Discov. Published online July 25, 2023:CD-23-0050. doi:10.1158/2159-8290.CD-23-0050

243. Liu J, Li P, Wang L, et al. Cancer-Associated Fibroblasts Provide a Stromal Niche for Liver Cancer Organoids That Confers Trophic Effects and Therapy Resistance. Cell Mol Gastroenterol Hepatol. 2021;11(2):407-431. doi:10.1016/j.jcmgh.2020.09.003

244. Öhlund D, Handly-Santana A, Biffi G, et al. Distinct populations of inflammatory fibroblasts and myofibroblasts in pancreatic cancer. J Exp Med. 2017;214(3):579-596. doi:10.1084/jem.20162024

245. Zhao H, Jiang E, Shang Z. 3D Co-culture of Cancer-Associated Fibroblast with Oral Cancer Organoids. J Dent Res. 2021;100(2):201-208. doi:10.1177/0022034520956614

246. Schuth S, Le Blanc S, Krieger TG, et al. Patient-specific modeling of stroma-mediated chemoresistance of pancreatic cancer using a three-dimensional organoid-fibroblast co-culture system. J Exp Clin Cancer Res. 2022;41(1):312. doi:10.1186/s13046-022-02519-7

247. Luo X, Fong ELS, Zhu C, et al. Hydrogel-based colorectal cancer organoid co-culture models. Acta Biomaterialia. 2021;132:461-472. doi:10.1016/j.actbio.2020.12.037

248. Tsai VWW, Husaini Y, Sainsbury A, Brown DA, Breit SN. The MIC-1/GDF15-GFRAL Pathway in Energy Homeostasis: Implications for Obesity, Cachexia, and Other Associated Diseases. Cell Metabolism. 2018;28(3):353-368. doi:10.1016/j.cmet.2018.07.018

249. Breen DM, Kim H, Bennett D, et al. GDF-15 Neutralization Alleviates Platinum-Based Chemotherapy-Induced Emesis, Anorexia, and Weight Loss in Mice and Nonhuman Primates. Cell Metab. 2020;32(6):938-950.e6.

doi:10.1016/j.cmet.2020.10.023

250. Suriben R, Chen M, Higbee J, et al. Antibody-mediated inhibition of GDF15–GFRAL activity reverses cancer cachexia in mice. Nat Med. 2020;26(8):1264-1270. doi:10.1038/s41591-020-0945-x

251. Crawford J, Calle RA, Collins SM, et al. Abstract CT108: First-in-patient study of the GDF-15 inhibitor ponsegromab in patients with cancer and cachexia: Safety, tolerability, and exploratory measures of efficacy. Cancer Research. 2023;83(8_Supplement):CT108. doi:10.1158/1538-7445.AM2023-CT108

252. Melero I, Calvo E, Goebeler ME, et al. 504 A phase I, first-in-human clinical trial of the GDF-15 neutralizing antibody CTL-002 in subjects with advanced stage solid tumors (Acronym: GDFATHER). J Immunother Cancer. 2021;9(Suppl 2). doi:10.1136/jitc-2021-SITC2021.504

Ich versichere, dass ich die von mir vorgelegte Dissertation selbstständig angefertigt, die benutzten Quellen und Hilfsmittel vollständig angegeben und die Stellen der Arbeit -einschließlich Tabellen, Karten und Abbildungen -, die anderen Werken im Wortlaut oder dem Sinn nach entnommen sind, in jedem Einzelfall als Entlehnung kenntlich gemacht habe; dass diese Dissertation noch keiner anderen Fakultät oder Universität zur Prüfung vorgelegen hat; dass sie - abgesehen von unten angegebenen Teilpublikationen -noch nicht veröffentlicht worden ist sowie, dass ich eine solche Veröffentlichung vor Abschluss des Promotionsverfahrens nicht vornehmen werde. Die Bestimmungen dieser Promotionsordnung sind mir bekannt. Die von mir vorgelegte Dissertation ist von Prof. Dr. Christiane J. Bruns und Dr. Yue Zhao betreut worden.

Übersicht der Publikationen (bei Bedarf Seite anfügen):

1. **Fan N**, Wang Z, Zhou C, Bludau M, Contino G, Zhao Y, Bruns C. Comparison of outcomes between neoadjuvant chemoradiotherapy and neoadjuvant chemotherapy in patients with locally advanced esophageal cancer: A network meta-analysis. EClinicalMedicine. 2021 Nov 6;42:101183. doi: 10.1016/j.eclinm.2021.101183.
2. **Fan N**, Raatz L, Chon S, Quaas A, Bruns C, Zhao Y. “Subculture and Cryopreservation of Esophageal Adenocarcinoma Organoids: Pros and Cons for Single Cell Digestion.” JoVE (Journal of Visualized Experiments), no. 185 (July 6, 2022): e63281.

Ich versichere, dass ich alle Angaben wahrheitsgemäß nach bestem Wissen und Gewissen gemacht habe und verpflichte mich, jedmögliche, die obigen Angaben betreffenden Veränderungen, dem Promotionsausschuss unverzüglich mitzuteilen.

10.01.2024 ..... Ningbo 樊 .....

Datum Unterschrift